ANALYSIS OF ATOM ARRANGEMENT IN III-V ALLOY SEMICONDUCTORS(Dissertation_全文)

AUTHOR(S):

Ichimura, Masaya

ANALYSIS OF ATOM ARRANGEMENT IN Ⅲ-Ⅴ ALLOY SEMICONDUCTORS

MASAYA ICHIMURA

JANUARY 1988

DEPARTMENT OF ELECTRICAL ENGINEERING
KYOTO UNIVERSITY
KYOTO, JAPAN

ANALYSIS OF ATOM ARRANGEMENT IN Ⅲ-Ⅴ ALLOY SEMICONDUCTORS

MASAYA ICHIMURA

JANUARY 1988

DEPARTMENT OF ELECTRICAL ENGINEERING
KYOTO UNIVERSITY
KYOTO, JAPAN

ABSTRACT

Atom arrangements in III-V alloy semiconductors are theoretically investigated and analyzed by a thermodynamic approach. For ternary alloys, e.g., $In_{1-x}Ga_xAs$ and quaternary alloys of (ABC)D type, e.g., $In_{1-x-y}Ga_xAl_yAs$, the bond strain energy is considered as a dominant interaction among constituent compounds. In these alloys, atoms of different sizes tend to be neighbours, but neighbour pairs of similar size atoms are not favorable. This indicates the preference for unlike-neighbour-pair for the ternary alloys, but not necessarily for the quaternary alloys of (ABC)D type.

For quaternary alloys of (AB)(CD) type, e.g., $In_{1-x}Ga_xAs_{1-y}P_y$, the cohesive energy change depending on the relative numbers of bonds is considered in addition to the strain energy. When the heavier group V atom is assigned to C^V, $In\text{-}D^V$ and $Ga\text{-}C^V$ bonds increase in $In_{1-x}Ga_xC^V_{1-y}D^V_y$, and $Ga\text{-}C^V$ and $Al\text{-}D^V$ bonds increase in $Ga_{1-x}Al_xC^V_{1-y}D^V_y$ at the thermal equilibrium states compared with the case of random atom arrangement. The bond statistics are nearly equal to those of the random case for $In_{1-x}Al_xC^V_{1-y}D^V_y$.

For calculating the strain energy, bond lengths and angles must be known. In the analysis, strain of each bond is calculated in all types of tetrahedron cells. By taking weighted average, the average bond lengths are obtained, and their relation with the atom arrangement is discussed. The results agree fairly well with data from extended-X-ray-absorption fine-structure measurements.

The influences of atom arrangement are studied for some material properties. It is shown for ternary alloys that the alloy scattering mobility and the hardness are influenced by the nonrandomness in the atom arrangement. The stability of superlattices is also studied. The monolayer structure on (100) or (110) surface can be stable, but other structures are not stable at any temperature.

ACKNOWLEDGEMENTS

I would like to express my deep gratitude to Professor Akio Sasaki for his advices and continuous support throughout this work. I am grateful to Professors Hiroyuki Matsunami and Shigeo Fujita for their useful comments on the manuscript. I am very indebted to Dr. Yoshikazu Takeda for his useful and stimulating discussions. I am grateful to Mr. Shizuo Fujita for his useful discussions and Mr. Toyotsugu Ishibashi for his supports.

I would like to thank Professor Kozo Osamura, Department of Metallurgy, Kyoto University, for his stimulating discussions. I am grateful to many researchers for stimulating discussions in "Symposium on Alloy Semiconductor Physics and Electronics" and in other meetings. Useful and enjoyable discussions with my colleagues are also appreciated.

This work was partly supported by the Scientific Research Grant-in-Aid for Special Project Research on "Alloy Semiconductor Physics and Electronics" from the Ministry of Education, Science and Culture, and also by Hattori Hokokai Foundation.

Finally, I would like to thank my wife and my parents for their encouragements and supports.

CONTENTS

I. INTRODUCTION

This study deals with solid solutions of semiconductors which have zincblende structure with group III and group V sublattices and are composed of more than two kinds of elements, i.e., one or more of Al, Ga, and In and one or more of P, As, and Sb. Examples are $Al_{1-x}Ga_xAs$, $In_{1-x}Ga_xAs_{1-y}P_y$, and $In_{1-x-y}Ga_xAl_yAs$. Although they can be called "III-V solid solutions" or "III-V mixed crystals", they are referred to as "III-V alloy semiconductors" or more simply "III-V alloys" in this study.

According to the number of constituent elements, III-V alloys are classified into the following groups: i) ternary or pseudobinary alloys, e.g., $Al_{1-x}Ga_xAs$ and $GaAs_{1-x}P_x$, ii) quaternary or pseudoternary alloys, e.g., $In_{1-x-y}Ga_xAl_yAs$ and $GaSb_{1-x-y}As_xP_y$, iii) quaternary alloys composed of two group III and two group V elements, e.g., $In_{1-x}Ga_xAs_{1-y}P_y$, iv) pentanary alloys, e.g., $In_{1-x-y}Ga_xAl_yAs_{1-z}P_z$, and v) alloy composed of six elements, i.e., $In_{1-x-y}Ga_xAl_ySb_{1-z-w}As_zP_w$. The groups iv) and v) are not dealed with here, since they have not been widely used for devices so far and one is able to know to some extent the results for them from those for other types of alloys. Through this study, the group i) is referred to as ternary alloys, ii) quaternary alloys of (ABC)D type, and iii) quaternary alloys of (AB)(CD) type.

Their importance comes from the flexibility to design material properties. Under the condition of stoichiometry, the relative content of two (or more) kinds of group III or V atoms, i.e., the composition of alloys, can be varied continuously, at least in the composition range outside of miscibility gap, and consequently the material properties can be changed.[1)] Then, for example, one can get the alloy for radiation of a required wavelength by designing the energy band gap. Most of advanced semiconductor technology would not have been evolved without this designability of alloy semiconductors. For example, semiconductor lasers had

not been developed without double heterostructure of a good quality, which cannot be easily constructed by any semiconductor except for alloy semiconductors.[2)]

At present, material properties of many III-V alloys have become known by necessity in device applications.[3)] However, understanding of their properties seems still empirical and phenomenological. In general, properties of an alloy are much harder to understand than those of an element or a compound semiconductor. The band structure would be a good example. At present, very sophisticated methods have been developed for calculating band structures.[4)] However, they cannot be directly applied to alloys because of the lack of periodicity in the atom arrangement: composition disorder exists in alloy semiconductors. In addition, microscopic structural disorder, e.g., change in the nearest-neighbour distances, also influences band structure.[5-7)] These disorders make it difficult to understand or predict not only band structure but also other properties, e.g., electrical, elastic, and thermodynamic properties. Thus, so far, properties of alloys have been understood on the basis of various approximations or macroscopic models.

The simplest model of an alloy is the virtual crystal approximation, VCA. This model assumes an atom with properties linearly varying with the composition of an alloy. For example, each of the group III lattice sites in $In_{1-x}Ga_xAs$ alloy is assumed to be occupied by such hypothetical atom. The crystal structure is assumed to be an undistorted zincblende lattice. It is an useful model: some material parameters, e.g., lattice constant, depend linearly on the composition, i.e., follow the Vegard law, and such linear dependence on composition could be understood on the basis of VCA. However, VCA is obviously insufficient; especially, randomness in the atom arrangement is not considered in the model, and thus, for example, alloy scattering of carriers cannot be explained by VCA. In addition, the results of recent extended-

X-ray-absorption fine-structure measurements show that the III-V ternary and quaternary alloy crystals largely deviate from the structure of VCA.[8-11] VCA is sometimes used by considering nonlinear variation of atom properties with composition. However, so long as the hypothetical atom is assumed, the model has the same shortcomings as mentioned above.

Next, as more advanced models, an ordered alloy model and a completely random alloy model can be considered. In the ordered alloy model, the atom arrangement is assumed to be perfectly ordered, and only a single type of unit cell is considered.[5,12-15] Then, analyses become very easy owing to periodicity. By simulating the alloy of a certain composition by such ordered alloy, one can discuss some phenomena peculiar to alloys, e.g., lattice relaxation. The analysis described in Subsec. 5-3-1 in this study is based on the ordered alloy model. However, such approach is not realistic because the atom arrangement of III-V alloys is, at least somewhat, random.

The random alloy model, where alloy atoms are assumed to be distributed completely at random, has been extensively used. For example, most of the calculations of alloy scattering mobility are based on the assumption of completely random arrangement of atoms.[16] The coherent potential approximation, which is used for calculating electronic or phonon properties of alloys, is usually based on the assumption of random atom arrangement.[17] The regular or simple solution model used in thermodynamic analyses is also a random alloy model.[18] These calculations seem very successful in phenomenological understanding of alloy properties. However, the assumption of random arrangement has not been verified, yet. In addition, ordered arrangement was recently observed by transmission electron microscope in some III-V ternary alloys, e.g., $In_{1-x}Ga_xAs$,[19-21] $Al_{1-x}Ga_xAs$,[22] and $GaAs_{1-x}Sb_x$[23]. Thus, the assumption of random atom arrangement should be reconsidered.

For a more realistic picture of III-V alloys, one must take into account the fact that the atom arrangement is neither completely random nor perfectly ordered. First of all, it is necessary to determine the atom arrangement or degree of order, and then, on the basis of the results, various properties will become possible to discuss, such as alloy scattering mobility, and energy band gap.

Atom arrangement has been extensively investigated for metal alloys: nonrandomness in the arrangement has been observed by, for example, X-ray scattering measurement,[24] and many calculations have been carried out on the basis of thermodynamic theories.[25] However, there are only few studies for atom arrangement in III-V alloys,[26-31] in spite of the fact that they are no less important than those for metal alloys.

The basis of analyses for III-V alloys will be different from that for metal alloys, since III-V compounds are constructed by covalent bondings,[32,33] quite different from metallic cohesion. In Chap. II, basic consideration is given for energetical interactions in III-V alloys. Atom arrangement and bond lengths are quantitatively discussed in Chap. III, IV, and V for III-V ternary, quaternary of (ABC)D, and quaternary alloys of (AB)(CD) type, respectively. The bond length is closely related to atom arrangement, because bond strain energy is a dominant portion of energetical interaction in most III-V alloys, as being shown in Chap. II. In Chap. VI, influences of atom arrangement on material properties are discussed, and the importance of investigating atom arrangement is described. Finally, conclusions and suggestions for possible extensions of the study are given in Chap. VII.

REFERENCES

1) For example, A. Sasaki, M. Nishiuma, and Y. Takeda, Jpn. J. Appl. Phys., 19 (1980)1695.

2) As review, H. C. Casey, Jr. and M. B. Panish, "Heterostructure Lasers" (Academic Press, New York, 1978).

3) For example, S. Adachi, J. Appl. Phys., 58 (1984) R1.

4) For example, J. Ihm and J. D. Joannopoulos, Phys. Rev. B, 24 (1981) 4191.

5) A. Zunger and J. E. Jaffe, Phys. Rev. Lett., 51 (1983) 662.

6) K. C. Hess, R. J. Lempert, and H. Ehrenreich, Phys. Rev. Lett., 52 (1983) 77.

7) A. A. Mbaye, Solid St. Commun., 55 (1985) 183.

8) J. Bellessa, C. Gors, P. Launois, M. Quillec, and H. Launois, "10th Int. Symp. GaAs and Related Compounds, Albuquerque, 1982, Inst. Phys. Conf. Ser. 24" (Inst. Phys., London, 1983), p.529.

9) J. C. Mikkelsen, Jr. and J. B. Boyce, Phys. Rev. Lett., 49 (1982) 1412.

10) T. Sasaki, T. Onda, R. Ito, and N. Ogasawara, Jpn. J. Appl. Phys., 25 (1986) 231.

11) H. Oyanagi, Y. Takeda, T. Matsushita, T. Ishiguro, and A. Sasaki, "12th Int. Symp. GaAs and Related Compounds, Karuizawa, 1985, Inst. Phys. Conf. Ser. 79" (Adams Hilger, 1986), p. 295

12) T. Fukui, Jpn. J. Appl. Phys., 23 (1984) L208, and J. Appl. Phys., 57 (1985) 5188.

13) P. Boguslawski and A. Baldereschi, "Proc. 17th Conf. the Physics of Semiconductors, 1984" (North-Holland, Amsterdam, 1985), p.939

14) U. Pietsch, Phys. Stat. Sol. (b), 133 (1986) 483, and ibid., 134 (1986) 21.

15) T. Ito, Phys. Stat. Sol. (b), 135 (1986) 493.

16) For example, Y. Takeda, "GaInAsP Alloy Semiconductors", edited by T. P. Pearsall (Wiely, Chichester, 1982), Chap. 9, and references therein.

17) For example, A. B. Chen and A. Sher, Phys. Rev. B, 19 (1979) 3057, and ibid, 23 (1981) 5360.

18) As review, Chap. 6 of Ref. 2).

19) H. Nakayama and H. Fujita, "12th Int. Symp. GaAs and Related Compounds, Karuizawa, 1985, Inst. Phys. Conf. Ser. 79" (Adams Hilger, 1986), p.289.

20) M. A. Shahid, S. Mahajan, D. E. Laughlin, and H. M. Cox, Phys. Rev. Lett., 58 (1987) 2567.

21) T. S. Kuan, W. I. Wang, and E. L. Wilkie, Appl. Phys. Lett., 51 (1987) 51.

22) T. S. Kuan, T. F. Kuech, W. I. Wang, and E. L. Wilkie, Phys. Rev. Lett., 54 (1985) 201.

23) H. R. Jen, M. J. Cherng, and G. B. Stringfellow, Appl. Phys. Lett., 48 (1986) 1603.

24) As a review, L. Guttman, "Solid State Physics" edited by F. Seitz and D. Turnbull (Academic, New York, 1956), Vol.3, p. 145.

25) As a review, T. Muto and Y. Takagi, "Solid State Physics" edited by F. Seitz and D. Turnbull (Academic, New York, 1955), Vol.1, p. 193.

26) K. A. Jones, W. Porod, and D. K. Ferry, J. Phys. Chem. Solids, 44 (1983) 107.

27) S. Yamazaki, M. Kishi, and T. Katoda, Phys. Stat. Sol. (b), 113 (1982) 421.

28) K. Onabe, J. Phys. Chem. Solids, 43 (1982) 1071.

29) A. A. Mbaye, L. G. Ferreira, and A. Zunger, Phys. Rev. Lett., 58 (1987) 49.

30) A. Sher, M. Schilfgaarde, A. B. Chen, and W. Chen, Phys. Rev. B, 36 (1987) 4279.

31) M. T. Czyzyk, M. Podgorny, A. Balzarotti, P. Lelardi, N. Motta, A. Kisiel, and M. Z-Slarnawska, Z. Phys. B, 62 (1986) 153.

32) J. C. Phillips, "Bonds and Bands in Semiconductors" (Academic, New York, 1973).

33) W. A. Harrison, "Electronic Structure and the Properties of Solids" (W. H. Freeman, San Francisco, 1980).

II. ENERGETICAL INTERACTIONS IN III-V ALLOY SEMICONDUCTORS

2-1. INTRODUCTION

In thermodynamic analysis, i) calculation of enthalpy and ii) calculation of entropy are generally required. For solid phases, enthalpy is usually assumed to correspond to internal energy. Total enthalpy H can be formally expressed by

$$H = H_o + H_m \quad , \tag{2-1}$$

where H_o is the part varying linearly with composition and H_m the excess part, i.e., mixing enthalpy. Since H_o is uniquely determined from composition and independent of atom arrangement, the atom arrangement is not influenced by H_o. The H_m is caused by interaction among constituent elements in an alloy and influenced by the atom arrangement. It also affects other thermodynamic properties, e.g., range of miscibility gap. In this chapter, the basis for calculating H_m is given.

2-2. SECOND-NEAREST-NEIGHBOUR INTERACTION AND STRAIN ENERGY

In this section, a model previously used is critically reviewed, and the importance of strain energy is described.

The pairwise interaction model (PIM) has been widely used in thermodynamic analysis of metal alloys.[1] According to PIM, the enthalpy H of an alloy $A_{1-x}B_x$ is expressed by

$$H = n_{AA}h_{AA}+n_{BB}h_{BB}+n_{AB}h_{AB} \quad , \tag{2-2}$$

where n_{pq} denotes the number of p-q pair and h_{pq} the enthalpy due to cohesion of p-q pair. Here, h_{pq} has been considered independent of composition x in the PIM.

The PIM has been also applied to III-V alloys not only for

phenomenological description of thermodynamic behavior[2-4], but also for discussing atom arrangement.[5,6]

First, PIM is reviewed and criticized for III-V ternary alloys. The number of nearest-neighbour pairs in a III-V ternary alloy is uniquely determined from atomic composition and varies linearly with composition; for example, the relative numbers of In-As and Ga-As pairs are 1-x and x, respectively for $In_{1-x}Ga_xAs$ alloy. Thus, the nearest-neighbour interaction does not contribute to the mixing enthalpy H_m. On the other hand, it is known that H_m is non-zero (positive) for most III-V ternary alloys.[7] Accoring to PIM, the origin of H_m is the interaction between the second-nearest-neighbour atoms.[2,4] Then, the fact that $H_m>0$ indicates

$$h_{AB} > \frac{1}{2}(h_{AA}+h_{BB}) \quad . \tag{2-3}$$

Here, a larger negative h implies that the stability of the pair is increased, since h is enthalpy. Thus, Eq.(2-3) indicates that A-B pair is unstable compared with like-pairs A-A and B-B. Then, increase of like-pair or clustering of like atoms becomes able to occur.[5]

However, it has not verified that the second nearest-neighbour interaction is dominant in III-V alloys: cohesion of III-V compounds is mostly due to covalent bonding between the nearest-neighbour atoms,[8] and the second nearest-neighbour interaction is expected to have only minor effect. Moreover, it is considered inappropriate to neglect the change in the nearest-neighbour interaction energy.[9] It will be easy to see that lengths or angles of bonds must deviate from their original values when compounds with different lattice constants are mixed and constitute a single crystal of an alloy. Besides, the change in bond length is confirmed by extended X-ray absorption fine-structure measurement.[10-13] The length or angle deviation causes a change in the cohesive energy of bonds. Such energy change is known as strain

energy and has been calculated by some researchers.[14-19] All of their calculations show that the strain energy is comparable to the mixing enthalpy detemined from thermodynamic experiments. Thus, a theory which does not take strain energy into account is not appropriate for III-V alloys. According to a recent pseudopotential calculation, the participation of strain energy to H_m is more than one order greater than those of other energies.[19] This also indicates that PIM is not appropriate for III-V alloys.

Strain energy is very small in $Al_{1-x}Ga_xC^V$ (C^V=P, As, Sb) since the lattice constants of their constituent compounds are almost equal, and then PIM could be valid for these alloys. However, their H_m's are known to be very small,[7] i.e., the second nearest-neighbour interaction energy would be still negligible.

PIM has been applied to quaternary alloys, too.[6] However, the strain energy in quaternary alloys is also shown to be no less than H_m determined experimentally.[20] The domination of strain energy is attributed to covalent character of bonding and thus would hold for most III-V alloys. Thus, PIM is not adopted in this study.

2-2. VALENCE-FORCE-FIELD MODEL

The strain energy is an energy change accompanying changes in atomic spacings: it would involve not only a change in the nearest-neighbour interaction (bond) but also changes in other interactions. However, for covalent bonding crystals where the nearest-neighbour interaction is dominant, an elastic model based on the nearest interaction has been developed. This model is called the valence-force-field (VFF) model and successfully applied to element and compound semiconductors.[21] In this work, the VFF model developed by Martin[22] is adopted; it is extended from the model by Keating[23] and applicable to zincblende structure crystals. In this model, strain energy, ε, involved in a crystal is

calculated in terms of bond length deviations and bond angle distortions:[22,23]

$$\varepsilon = \frac{1}{2}\sum_{j}\frac{3}{4}\alpha_j\frac{[\Delta(d_j^1\cdot d_j^1)]^2}{d_j^{0\,2}} + \frac{1}{2}\sum_{s}\sum_{j,k}\frac{3}{4}\beta_{jk}\frac{[\Delta(d_j^s\cdot d_k^s)]^2}{d_j^0 d_k^0} \quad , \quad (2\text{-}4)$$

where s=1 and 2 denote group III and group V atoms, respectively. The bonds around each atom are denoted by j,k=1~4, and d_j^s and d_k^s are the bond vectors around s atom. d_j^0 is the equilibrium length of bond j. α_j is the force constant of length distortion of bond j, and β_{jk} the force constant of angle distortion between bond j and k.

The elastic constants α and β of III-V compounds are listed in Table 2-I with equilibrium length of each bond.[22] Although elastic constants of AlAs and AlP are not known, they are assumed to be the same as those of GaAs and GaP, respectively; there is a linear relation between elastic and lattice constants of III-V compounds,[24] and lattice constants of AlAs and AlP are almost equal to those of GaAs and GaP, respectively.

Elastic constants of a certain bond in an alloy would be different from those of the corresponding pure compound. However,

MATERIAL	d (Å)	α (10^3 dyn/cm)	β
AlP	2.365	(47.32)	(10.44)
AlAs	2.451	(41.19)	(8.95)
AlSb	2.657	35.35	6.77
GaP	2.360	47.32	10.44
GaAs	2.448	41.19	8.95
GaSb	2.640	33.16	7.22
InP	2.541	43.04	6.24
InAs	2.623	35.18	5.50
InSb	2.806	29.61	4.77

Table 2-I. Bond length d, length distortion elastic constant α, and angle distortion elastic constant β for nine III-V binary compounds.[22]

they can be approximated equal, since the elastic model used in this study is based on the nearest interaction and does not take the influence from the second-nearest interaction.

The values of elastic constants listed in Table 2-I are those at room temperature (RT). The temperature dependence is neglected in the analyses because it is not known except for a few compounds. For GaAs, the elastic constants at 800 K are smaller by about 10 % than those at RT. Thus, the neglect of the temperature dependence will lead to slight overestimation of strain energy at temperatures higher than RT. The temperature dependence of bond length is also neglected in the analyses. If the thermal expansion coefficient is equal for all constituent compounds, the neglect of thermal expansion does not cause any influencial error in estimating strain energy. In fact, there is a difference in thermal expansion coefficients, but it is very small (less than 2×10^{-6} 1/K). Thus, it can be safely neglected.

2-3. LATTICE RELAXATION

In order to calculate the bond strain energy by the VFF model, one need know lengths and angles of bonds. The simplest approach is based on the assumption that the lengths of bonds are all equal to the length of the virtual crystal approximation (VCA), and bond angles are undistorted. However, the resultant strain energy becomes about four times greater than experimentally determined mixing enthalpy.[15] The results of the recent EXAFS measurements show that the bond length in an alloy tends to preserve that in the corresponding binary compound.[10-13] Thus, the above assumption is not a good approximation for bonds in III-V alloys: the lattice relaxes for the reduction in the strain energy of bonds. According to a approach based on the VFF model, the lattice relaxation occurs for equilibrium of length change and angle distortions,[17] and the angles are largely distorted com-

pared with lengths, since the elastic constant of angle distortion β is smaller than that of length deviation α, as can be seen from Table 2-I.

In this study, the lattice relaxation is taken into account in calculating the strain energy on the basis of the VFF model. However, some assumptions are made, i.e., the relaxation is considered under a certain restriction so that the thermodynamic analysis can be carried out analytically. Different assumption is made for a different type of alloy, as will be described in later chapters.

2-4. LATTICE COHERENCY

In estimating the strain energy, it is assumed that lattice coherency is retained in a whole crystal. This assumption is crucial for the discussion about the effect of the strain energy. In order to explain this, the following two cases are considered here.

In the first case, a ternary alloy crystal of composition $x=0.5$ is assumed to decompose into two separate crystals of constiuent binary compounds, apart from each other. Here, the ternary alloy is assumed to have considerable strain energy due to difference in lattice constant between two constituent compounds. After the decomposition, the total strain energy becomes null, since a binary compound crystal has no strain. It should be noted that in this case the lattice constants of the binary compound crystals are their own equilibrium values. In the second case, a small crystal (N atom cluster) of the constituent compound is considered to be inserted to a space for N atoms in a large crystal of $x=0.5$. If they are bonded at the interface, the small crystals are distorted by the surrounding alloy crystal because of lattice mismatch between the alloy and the compound. Then, the strain energy per unit volume of the small crystal is no longer

null and will be even larger than that of the alloy of x=0.5.

From the first case, one could conclude that a cluster of binary compound is energetically preferable to a uniform alloy, but from the second case one could conclude it is not. This difference arises from the fact that lattice coherency is not retained in the first case but in the second case: the strain energy acts on the atom arrangement differently depending on whether the lattice coherency is retained or not.

The next problem is under what condition the lattice coherency is broken. Strained-layer superlattice (SLS) is illustrative of this point. SLS is a periodic multilayer structure composed of two (or more) crystals with different lattice constants.[25] If each layer is sufficiently thick, dislocations generate at the interfaces, and the stress due to misfit between layers is relaxed.[25] Although dislocation itself causes some strain, it exists only in vicinity of each interface and the rest of the crystal becomes strain-free. However, on the contrary, if each layer is sufficiently thin, the generation of dislocations is no more preferable: the strain-free region diminishes, and the strain energy caused by dislocations overcomes the reduction in the misfit strain energy.[25] Then, each layer becomes dislocation-free and is strained coherently. These facts can be generalized as follows. Suppose two or more regions with different lattice constants coexist in a crystal. If the size of each region is sufficiently large, the lattice coherency will be necessarily broken. If not, it can be retained. A conventional thermodynamic theory of phase separation neglects the strain caused by coexistence of two or more different composition regions:[26] it is assumed that the lattice constants of the regions are independent, determined by their respective compositions. This approach is appropriate for macroscopic separation where the lattice coherency is not retained. On the other hand, it is necessary to take into account the lattice coherency for single

phase crystals, i.e., crystals without macroscopic composition fluctuation. The coherency will be retained almost completely for a high quality crystal used for devices or a layer epitaxially grown on a certain substrate: the lattice constant averaged within a certain volume scarcely deviates from the value determined from the global composition. The purpose of this study is to discuss microscopic arrangement of atoms in a single phase alloy, and thus the lattice coherency is assumed to be completely retained.

REFERENCES

1) As review, R. A. Swalin, "Thermodynamics of Solids", 2nd ed. (Wiely, New York, 1972).

2) For an example of the calculation based on regular solution model, A. S. Jordan and M. Ilegems, J. Phys. Chem. Solids, 36 (1975) 329.

3) G. B. Stringfellow and P. E. Greene, J. Phys. Chem. Solids, 30 (1969) 1779.

4) R. Kikuchi, Physica, 103B (1981) 41.

5) K. A. Jones, W. Porod, and D. K. Ferry, J. Phys. Chem. Solids, 44 (1983) 107.

6) K. Onabe, J. Phys. Chem. Solids, 43 (1982) 1071.

7) M. B. Panish and M. Ilegems, "Progress in Solid State Chemistry", edited by H. Reiss and J. O. McCaldin (Pergamon, New York, 1972), Vol.7, p. 39.

8) J. C. Phillips, "Bonds and Bands in Semiconductors" (Academic, New York, 1973).

9) T. Onda, R. Ito, and N. Ogasawara, Jpn. J. Appl. Phys., 25 (1986) 82.

10) J. Bellessa, C. Gors, P. Launois, M. Quillec, and H. Launois, "10th Int. Symp. GaAs and Related Compounds, Albuquerque, 1982, Inst. Phys. Conf. Ser. 24" (Inst. Phys., London, 1983), p.529.

11) J. C. Mikkelsen, Jr. and J. B. Boyce, Phys. Rev. Lett., 49 (1982) 1412.

12) T. Sasaki, T. Onda, R. Ito, and N. Ogasawara, Jpn. J. Appl. Phys., 25 (1986) 231.

13) H. Oyanagi, Y. Takeda, T. Matsushita, T. Ishiguro, and A. Sasaki, "12th Int. Symp. GaAs and Related Compounds, Karuizawa, 1985, Inst. Phys. Conf. Ser. 79" (Adams Hilger, 1986), p. 295.

14) K. Osamura, K. Nakajima, and Y. Murakami, J. Jpn. Soc. Metall., 36 (1972) 744.

15) P. A. Fedders and M. W. Muller, J. Phys. Chem. Solids, 45 (1984) 685.

16) J. C. Mikkelsen, Jr., J. Electrochem. Soc., 132 (1985) 500.

17) T. Fukui, J. Appl. Phys., 57 (1985) 5188.

18) M. Ichimura and A. Sasaki, J. Appl. Phys., 60 (1986) 3850.

19) T. Ito, Jpn. J. Appl. Phys., 26 (1987) 256.

20) H. Sonomura, J. Appl. Phys., 59 (1986) 739.

21) As review, W. A. Harrison, "Electronic Structure and the Properties of Solids" (W. H. Freeman, San Francisco, 1980), Chap. 8.

22) R. M. Martin, Phys. Rev. B, 1 (1970) 4005.

23) P. N. Keating, Phys. Rev. 145 (1966) 637.

24) S. Adachi, J. Appl. Phys., 58 (1984) R1.

25) For example, J. W. Matthews and A. E. Blackslee, J. Cryst. Growth, 27 (1974) 118.

26) For example, K. Onabe, Jpn. J. Appl. Phys., 21 (1982) L323, and ibid., 22 (1983) 201.

III. ATOM ARRANGEMENT IN TERNARY ALLOY SEMICONDUCTORS

3-1. INTRODUCTION

Composition of a III-V ternary alloy semiconductor is expressed by a single variable x, as in $In_{1-x}Ga_xAs$: this type of alloy is often referred to as a pseudobinary or quasibinary alloy. The composition x is usually chosen so that the alloy has required energy band gap, or so that its lattice constant is equal to that of a certain binary compound, i.e., the alloy is lattice-matched to a certain substrate. For example, x of $GaAs_{1-x}P_x$ used for light-emitting diodes is selected so as to obtain radiation with required photon energy,[1] and x of $In_{1-x}Ga_xAs$ is usually 0.47 for lattice-matching when it is grown on an InP substrate.[2]

In this chapter, the atom arrangement and the bond lengths are discussed on the basis of a thermodynanic analysis for III-V ternary alloy semiconductors. The bond length is closely related to the atom arrangement: As described in the last chapter, the bond strain energy is the dominant portion of the mixing enthalpy for most III-V ternary alloys. Then, nonrandomness is induced in the atom arrangement for reduction in the strain energy (mixing enthalpy): the strain energy causes nonrandomness in the atom arrangement. Conversely, it means that the strain of bonds is expected to be reduced by the nonrandomness on an average. Thus, in this work, the bond length is calculated by considering the nonrandomness.

There are 18 different III-V ternary alloys, and they can be classified into following two groups according to the group of mixed elements: $A^{III}_{1-x}B^{III}_{x}C^{V}$ and $C^{III}A^{V}_{1-x}B^{V}_{x}$, where superscripts III and V represent group III and group V elements, respectively. The analysis is applied to all 18 ternary alloys, and the results show that there is a preference for short-range order in most of them.

3-2. STATISTICS OF TETRAHEDRON CELLS

3-2-1. Formalism of Free Energy

A. Basic figure and entropy

In a thermodynamic analysis, a free energy is calculated as a function of the numbers of basic figures, and then the most probable set of their relative numbers is determined. In general, the enthalpy can be estimated more accurately as a larger basic figure is adopted. However, estimation of the entropy becomes more difficult for a larger basic figure. Here, a tetrahedron cell shown in Fig. 3-1 is chosen as a basic figure: the lattice relaxation can be taken into account,[3] and the entropy can be explicitly expressed as a function of the relative numbers of them, as shown in this section.

In this approach, all of nearest-neighbour bonds are considered for calculating the strain of a certain bond.[4] In a zincblende structure, there are six nearest-neighbour bonds to a certain bond. Three of them share a group III atom and the other three share a group V atom. Then, for example, three of the nearest neighbours of an A-C bond in $A^{III}_{1-x}B^{III}_{x}C^{V}$ alloy are all A-C bonds: they share the A atom with each other. The other three nearest bonds, which share the C atom, are not uniquely determined: they constitute one of five tetrahedra shown in Fig. 3-1.

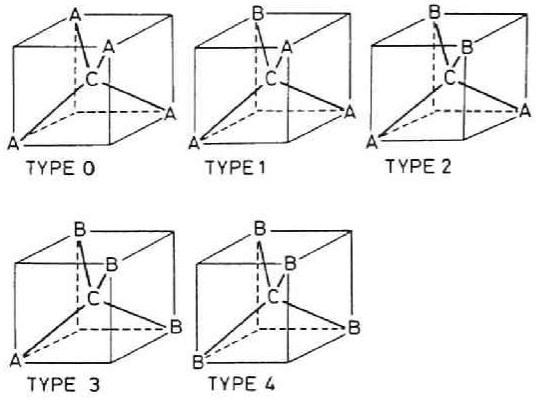

Fig.3-1 Tetrahedron cells in a ternary alloy semiconductor $A^{III}_{1-x}B^{III}_{x}C^{V}$ or $C^{III}A^{V}_{1-x}B^{V}_{x}$.

Thus, types of the tetrahedra shown in Fig. 3-1 involve what the nearest bonds are.[4)]

In calculating entropy as a function of the numbers of tetrahedra, one should note the fact that tetrahedra is not independent entities: Each atom is shared by four tetrahedra and it is impossible, for example, that type-0 and -4 cells be neighbours. In order to obtain an approximate entropy, the method developed by Kikuchi is adopted.[5)] Number of type-i cell is expressed by Ng_iq_i, where q_i is the probability of appearance of a certain configuration of type-i cell and g_i is the degenerecy factor, i.e., the number of different configuration having the same cell composition and given by the combination value of ${}_4C_i$. Since q_i's are relative numbers,

$$\sum g_i q_i = 1 \quad . \tag{3-1}$$

They are related to the composition of B atom, x, as

$$\sum \frac{i}{4} g_i q_i = x \quad . \tag{3-2}$$

The entropy of the face-centered cubic (fcc) lattice was derived by Kikuchi[5)], but the entropy of a ternary zincblende alloy is not the same as that of the fcc lattice. In the zincblende structure, there are two kinds of tetrahedra: one includes an atom of the other group at the central position, and thus four nearest-neighbour pairs (bonds) and six second-nearest pairs (nearest cation-cation or anion-anion pairs) exist, as shown in Fig. 3-1. The other kind of tetrahedron does not include any bonds and constitutes a tetrahedral interstitial site. Since only the nearest-neighbour interaction is taken into the analysis, the distribution of the latter tetrahedron can be excluded when we consider the entropy of ternary alloys. Applying the procedure[5)] to derive the entropy to ternary zincblende alloys,[6)] one obtains

$$S = k_B N \left[3\{x\ln x + (1-x)\ln(1-x)\} - \sum g_i q_i \ln q_i\right] \quad , \qquad (3\text{-}3)$$

where, x denotes the composition of B atom, k_B is the Boltzmann constant, and N the number of atoms in the mixed sublattice. S becomes maximum when atoms are distributed completely at random, i.e., $q_i = x^i(1-x)^{4-i}$. Then, Eq.(3-3) is reduced to

$$S = -k_B N[x\ln x + (1-x)\ln(1-x)] \quad . \qquad (3\text{-}4)$$

This is the entropy of the regular solution model.[7)]

B. Enthalpy: strain energy

For ternary alloys, it is assumed that the mixing enthalpy is the bond strain energy: The relative numbers of bonds are uniquely determined from atomic composition and does not depend on atom arrangement, and thus the strain energy, i.e., the change in cohesive energy of bonds is considered to be a dominant factor determining the atom arrangement.

In calculating the strain energy for each tetrahedron cell, the following assumption is made:

• The mixed sublattice, e.g., the group III sublattice in $In_{1-x}Ga_xAs$ remains an undistored fcc lattice, whereas the sublattice of the common element is distorted.

This assumption is supported by experimental data from extended-X-ray-absorption fine-structure (EXAFS) measurement which show that the nearest cation-cation distances in $In_{1-x}Ga_xAs$ are rather close to the values of the virtual crystal approximation (VCA).[8)] It can be understood from the fact that an atom on the mixed sublattice is surrounded by four identical atoms, whereas the common element atom is surrounded by two different kinds of atoms. Thus, atoms on the mixed sublattice tend to remain at the central position among four identical atoms as in a binary compound;

however the common element atoms shift their position, because the symmetry is broken around them (see also Subsec. 5-3-1).

Because of this assumption, the strain in various types of tetrahedra can be calculated independent of what are the neighbours: the size of each cell is all equal, determined from the global composition or by VCA. However, in reality, their sizes will depend on surrounding local environments, i.e., the mixed sublattice will also deviate from an undistorted fcc lattice. The error caused by the assumption will be discussed in Sec. 3-4.

In calculating the strain energy of a cell, the position of the C atom is found numerically so that the cell strain energy becomes minimum. The lengths of the four bonds within it are simultaneously determined and used for calculating average bond lengths, as will be described in the next section. The Vegard law is assumed for lattice constant of alloys: the VCA atomic spacings vary linearly with composition.

The total strain energy is expressed by

$$H_m = \sum g_i q_i \varepsilon_i \quad , \tag{3-5}$$

where ε_i is the strain energy of type-i cell.

C. Free energy and equilibrium State

The mixing free energy, F_m, is given by $F_m = H_m - TS$ where H_m is the mixing enthalpy and T is the absolute temperature. From Eqs. (3-3) and (3-5), F_m is obtained as

$$F_m = N\sum g_i q_i \varepsilon_i - Nk_B T[3\{x\ln x + (1-x)\ln(1-x)\} - \sum g_i q_i \ln q_i] \quad . \tag{3-6}$$

The values of q_i's at the thermal equilibrium state are obtained from the condition for a minimum free energy:

$$\sum \frac{\partial F}{\partial q_i} \delta q_i = 0 \quad , \tag{3-7}$$

$$\sum g_i \delta q_i = 0 \quad , \tag{3-8}$$

$$\sum \frac{i}{4} g_i \delta q_i = 0 \quad . \tag{3-9}$$

The second and the third equations are the derivatives of Eqs. (3-1) and (3-2), respectively. The conditions are rewritten by using the Lagrange multipliers, λ_1 and λ_2, as

$$\frac{\partial F}{\partial q_i} + \lambda_1 g_i + \lambda_2 \frac{i}{4} g_i = 0 \qquad (i=0\sim4) \quad , \tag{3-10}$$

The equilibrium values, q_i^o's, can be calculated with the conditions of Eqs. (3-1) and (3-2). They are

$$q_i^o = c\, \eta_i \Lambda^{4-i} \qquad (c^{-1} = \sum g_i \eta_i \Lambda^{4-i}) \quad , \tag{3-11}$$

where $\eta_i = \exp(-\varepsilon_i / k_B T)$, and Λ is $\exp(-\lambda_1 / 4k_B T)$ and satisfies the equation:

$$(1-x)\eta_0 \Lambda^4 + (3-4x)\eta_1 \Lambda^3 + (3-6x)\eta_2 \Lambda^2 + (1-4x)\eta_3 \Lambda - x\eta_4 = 0 \quad . \tag{3-12}$$

For expressing the degree of the short-range order quantitatively, the short-range order parameter, σ, is used; it is defined as[9]

$$\sigma = 1 - \frac{P_{AB}}{x} \quad , \tag{3-13}$$

where P_{AB} is the probability that a B atom occupies the second-nearest neighbour site of an A atom. The second-nearest pair in the zincblende structure corresponds to the first-nearest pair on the fcc sublattice; the order parameter which has been used for a binary alloy $A_x B_{1-x}$ can be applied to the mixed fcc sublattice of a zincblende structure of ternary alloy $A_x^{III} B_{1-x}^{III} C^{V}$ or $C^{III} A_x^{V} B_{1-x}^{V}$. The values of σ is negative when atoms tend to order, i.e., there is a preference for unlike second-nearest neighbour pair, whereas

it becomes positive when like atoms tend to cluster.

The order parameter is used in calculating alloy scattering mobility as being described in Chap. VI. It can be used for comparison with experimental data of the X-ray diffuse scattering measurement, since the experimental results are usually expressed in terms of the short-range order parameters.[9)]

The relation between σ and q_i's can be obtained by counting the number of A-B pairs in each tetrahedron:

$$\sigma = 1 - \frac{(q_1+2q_2+q_3)}{x(1-x)} \quad . \tag{3-14}$$

It can be proved by considering the number of A-B pairs in the tetrahedra that the lower limit of σ is -1/3 for ternary zincblende alloys.

3-2-2. Numerical Results

A. Strain energy of tetrahedron cell

The strain energies of five types of tetrahedron cells are shown in Fig. 3-2 and 3-3 for 18 III-V ternary alloy semiconductors. The composition dependence of the strain energy of a certain type of cell has almost the same features for all of 18 kinds of alloys, although the amount of the energy is quite different among alloys. At a given global or average composition, the strain energy is minimum for the cell whose composition is closest to the average composition. For example, in $In_{1-x}Ga_xC^V$ alloy, type-2 (In_2Ga_2) and -3 (In_1Ga_3) cells have the lowest strain energy among five cells for the average composition x=0.5 and x=0.75, respectively. For a given cell, its strain energy is a minimum when its composition is equal to the global composition, e.g., x=0.5 for a type-2 cell. This is because a tetrahedron cell is distorted by its surrounding crystal lattice if there is a difference between the cell composition and the

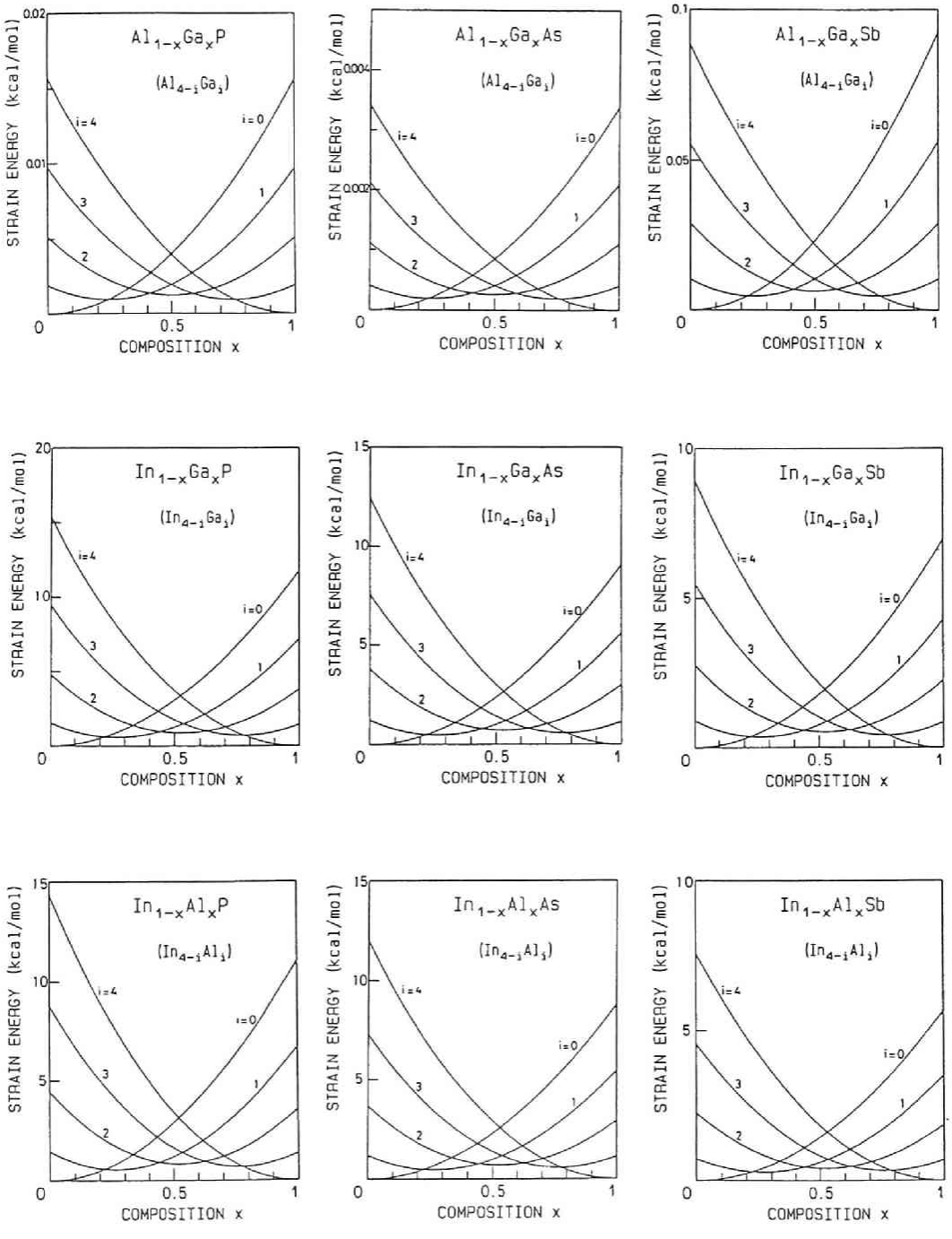

Fig.3-2 Strain energies of tetrahedron cells in ternary alloy semiconductors of $A^{III}_{1-x}B^{III}_{x}C^{V}$ group.

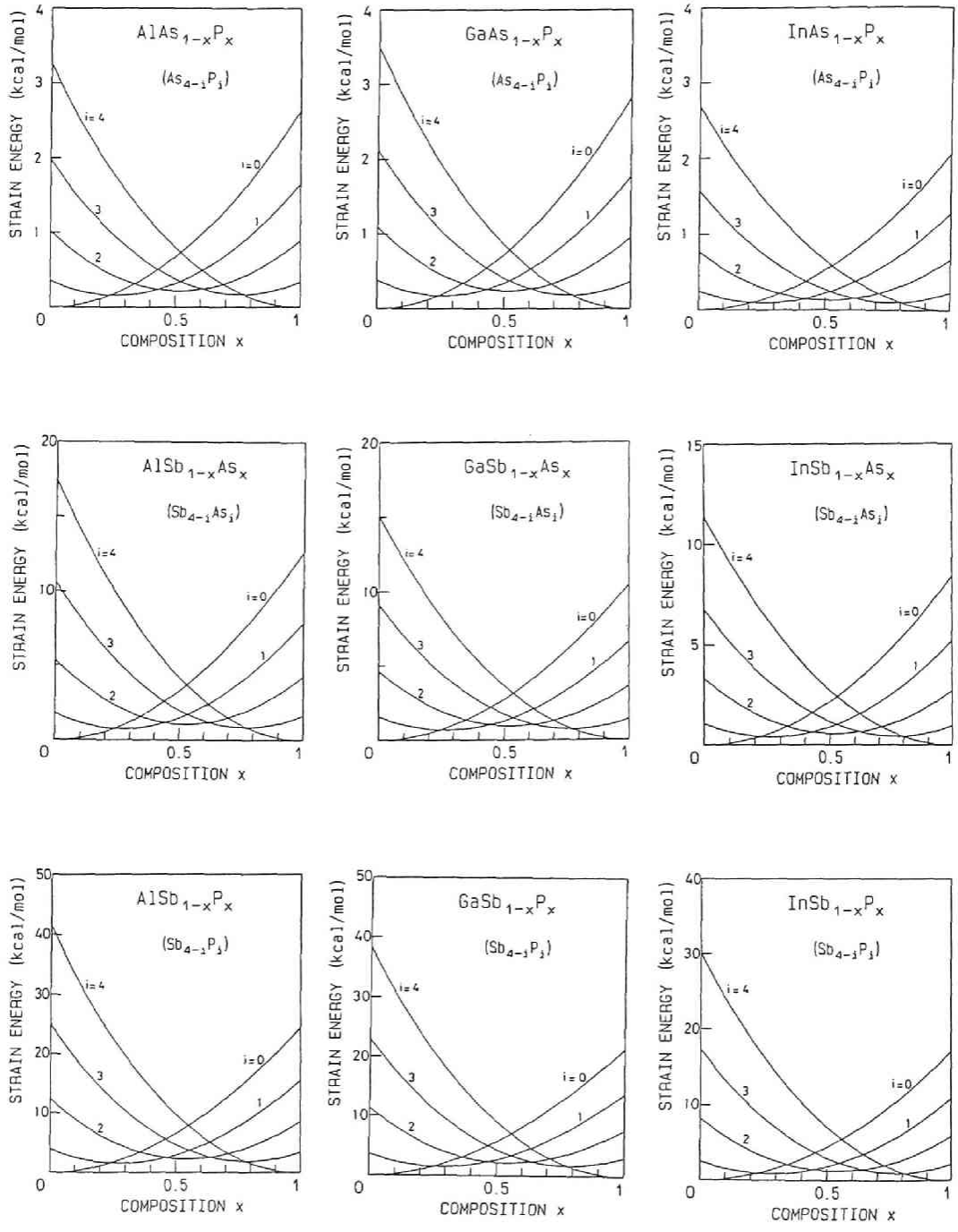

Fig.3-3 Strain energies of tetrahedron cells in ternary alloy semiconductors of $C^{III}A^{V}_{1-x}B^{V}_{x}$ group.

global composition. Figures are not exactly symmetric about x=0.5 because of the difference in elastic constants between constituent binary compounds.

The value of the strain energy is large for alloy systems where there is a large difference in lattice constant between constituent compounds, e.g., $C^{III}Sb_{1-x}P_x$, whereas it is very small for closely lattice-matched alloys, i.e., $Al_{1-x}Ga_xC^V$. For $In_{1-x}Ga_xC^V$ group alloys, for example, amount of the lattice-mismatch is nearly equal, but the strain energy becomes smaller in the following order: $In_{1-x}Ga_xP$ > $In_{1-x}Ga_xAs$ > $In_{1-x}Ga_xSb$. This is due to the difference in elastic constants: elastic constants tend to decrease as the constituent element becomes heavier.

B. Statistics of tetrahedron cells

Figures 3-4 and 3-5 show relative numbers of five types of cells for $A^{III}_{1-x}B^{III}_xC^V$ and $C^{III}A^V_{1-x}B^V_x$ alloys, respectively. The broken lines represent a cell distribution in a random arrangement and the solid lines at the thermal equilibrium state. Temperature of 1000 K, near which usual epitaxial growth is done, is adopted except for alloys involving InSb, for which 800 K is adopted: the melting point of InSb is about 800 K, and the analysis for a solid phase should be carried out for temperatures lower than it. Since the diffusivity of atoms in III-V compounds is very small, the atom arrangement at growth temperature will be preserved at temperatures below.

As it is shown in the figures, the number of the cell whose composition is closest to the global composition increases from the number for the random arrangement. For example, at x=0.5, type-2 cell increases, while type-0 and -4 cells decrease from the random case. By comparing Figs. 3-2, 3-3 and Figs. 3-4, 3-5, we can easily see that a cell with larger energy decreases at the thermal equilibrium state.

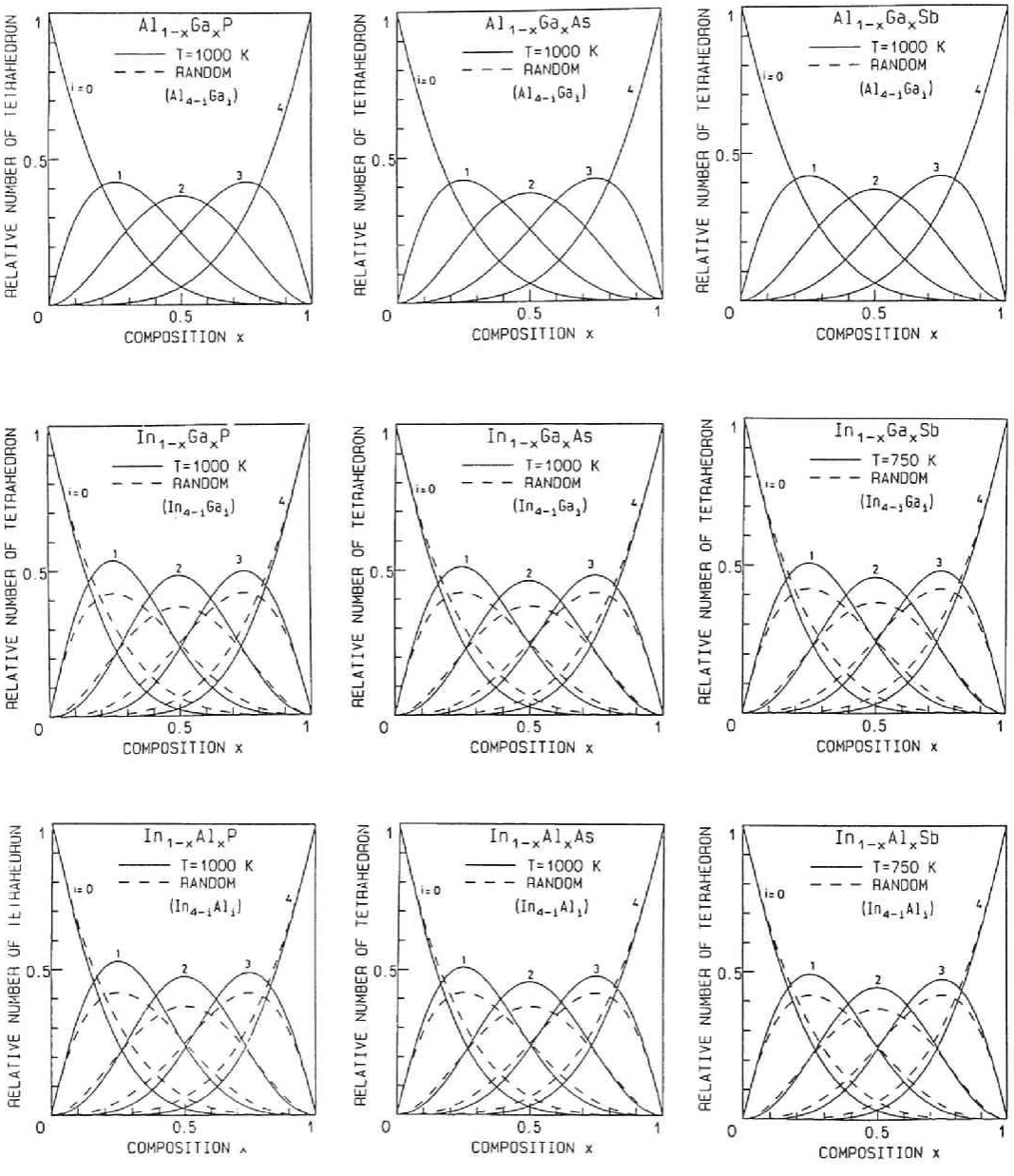

Fig.3-4 Relative numbers or statistics of tetrahedron cells in ternary alloy semiconductors of $A^{III}_{1-x}B^{III}_{x}C^{V}$ group. Broken lines represent completely random arrangement. The relative numbers at 1000 K is little different from those of random mixing in the alloy system of $(Al_{1-x}Ga_x)C^{V}$, and thus the solid and the broken lines are superimposed.

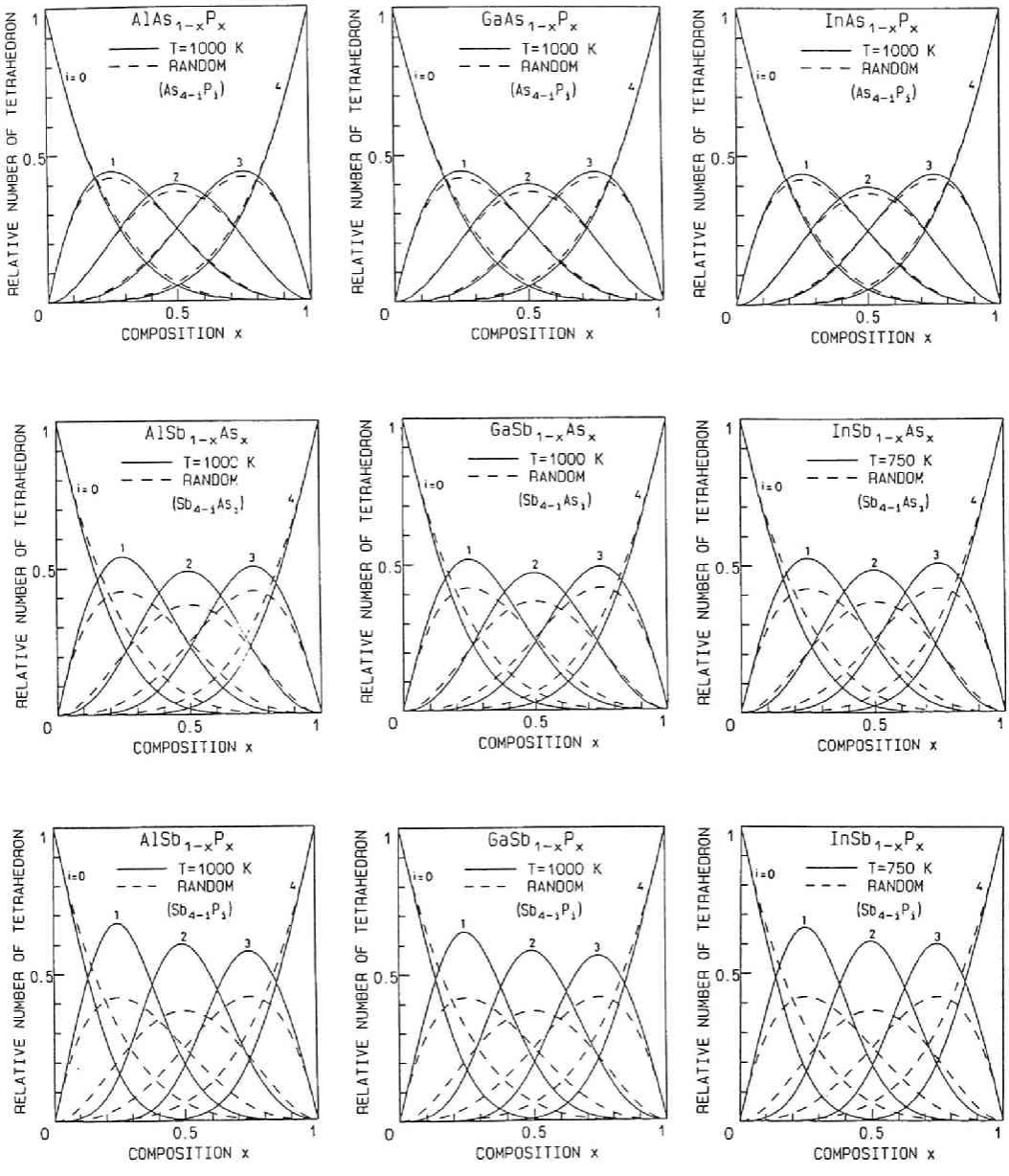

Fig.3-5 Relative numbers or statistics of tetrahedron cells in ternary alloy semiconductors of $C^{III}A^{V}_{1-x}B_{x}^{V}$ group. Broken lines represent completely random arrangement.

As the energy difference among cells increases, the deviation from random arrangement increases. The statistics of tetrahedron cells in $Al_{1-x}Ga_xC^V$ alloys are close to random arrangement, because the strain-energy difference is much smaller than the thermal energy at 1000 K. The results for $In_{1-x}Ga_xC^V$ are almost the same as those for $In_{1-x}Al_xC^V$, since the length of $Ga-C^V$ bond is nearly equal to that of $Al-C^V$ bond.

The figures are in general asymmetric with respect to the line of x=0.5. This is due to the asymmetry of Fig. 3-2 and 3-3, i.e., due to the difference in elastic constants. For an example of $GaSb_{1-x}P_x$, the number of Sb_3P_1 cell at x=0.25 is greater than that of Sb_1P_3 cell at x=0.75, because Ga-Sb has smaller elastic constants than Ga-P as shown in Table 2-I: Sb_3P_1 cell has smaller strain energy than Sb_1P_3 for a certain amount of mismatch between the cell and the surrounding crystal.

The composition dependence of the short-range order parameter is shown in Fig.3-6 for $In_{1-x}Ga_xAs$ alloy. At any global composition, the parameter is negative, which indicates that short-range ordering is more probable than clustering. The parameter is calculated for some other ternary alloys at x=0.5, T=1000 K and listed in Table 3-I with the lattice-mismatch between constituent compounds. The value of $|\sigma|$ increases with the lattice-mismatch.

In Fig. 3-7, temperature dependence of the short-range order parameter and the numbers of cells are shown for $In_{0.5}Ga_{0.5}As$. In the temperature range below 100K, the entropy term, TS, is negligible compared with H_m, and thus there is almost perfect order in the atom arrangement. In the temperature range between 10^2 and 10^4 K, the order parameter decreases logarithmically with temperature. The calculated results show little order at the temperature above 10^4K because of domination of the entropy over H_m, although $In_{0.5}Ga_{0.5}As$ is no longer solid in this temperature range.

MATERIAL	σ T=1000 K x=0.5 (10^{-2})	$\Delta a / \bar{a}$ (%)
(AlGa)As	0	0.20
(AlGa)Sb	-0.10	0.64
(InGa)P	-11.6	7.39
(InGa)As	-9.72	6.92
(InGa)Sb	-7.56	6.11
Ga(AsP)	-3.23	3.64
In(AsP)	-2.73	3.17
Ga(AsSb)	-10.8	7.52
In(AsSb)	-9.36	6.72
Ga(PSb)	-18.8	11.15
In(PSb)	-17.0	9.88

Table 3-I. The short-range order parameter σ at x=0.5, T=1000K and the relative difference in lattice constant $\Delta a/\bar{a}$ between two constituent binary compounds.

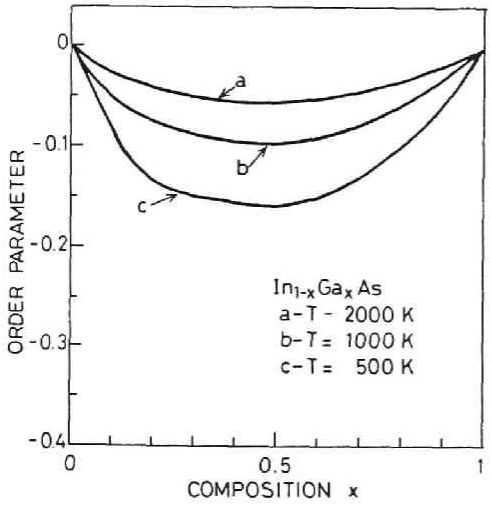

Fig.3-6 Composition dependence of the short-range order parameter σ for $In_{1-x}Ga_xAs$.

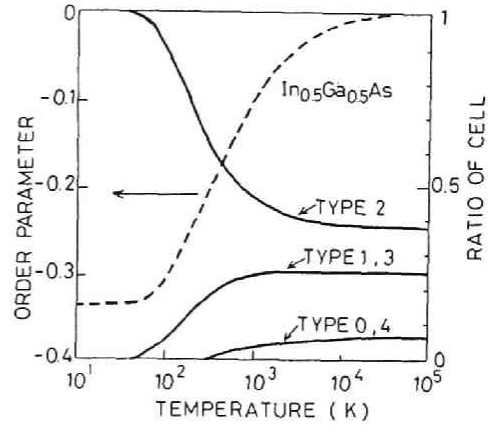

Fig.3-7 Temperature dependence of short-range order parameter σ and relative numbers of tetrahedron cells for $In_{0.5}Ga_{0.5}As$.

C. Total strain energy

Figure 3-8 shows the total strain energy of $In_{1-x}Ga_xAs$ alloy as a function of composition x. The broken line represents the value for the random case and the solid line for the short-range ordering at T=1000 K. Because of ordering, the cell having relatively high strain energy decreases compared with the random case, and therefore the total strain decreases.

It should be noted that, in Fig. 3-8, the total strain energy or the mixing enthalpy is nearly proportional to x(1-x). The relation of $H_m \propto x(1-x)$ has been used to explain the thermodynamic properties of binary or pseudobinary alloys including III-V ternary alloys,[7,10] and the interaction parameter defined by $\Omega = H_m/x(1-x)$ has been determined from the experiments.[10] When the pairwise-interaction model is employed, it has been shown theoretically that $H_m \propto x(1-x)$ for a binary or pseudobinary alloy.[7] The

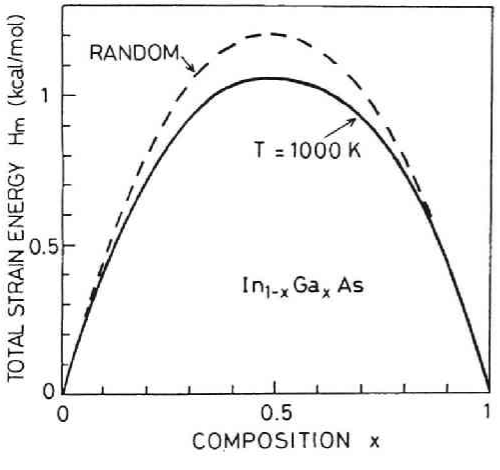

Fig.3-8 Composition dependence of the total strain energy (mixing enthalpy) for $In_{1-x}Ga_xAs$. Broken line: random arrangement. Solid line: at T=1000K.

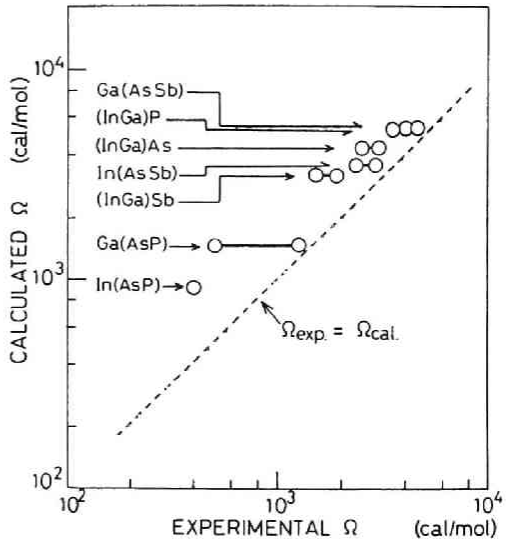

Fig.3-9 Experimental values of interaction parameter, Ω_{exp} versus theoretical values of Ω_{cal} calculated from Eq.(3-15). The values of Ω_{exp} are taken from Refs. 10 and 11.

strain energy is also shown to be proportional to x(1-x) when the macroscopic elastic models are used.[11,12] In the analysis described in the last subsection, the relation $H_m \propto x(1-x)$ does not appear explicitly in the equation, but the total strain energy shown in Fig. 3-8 follows this dependence of H_m on x. Similar composition dependence of H_m is also obtained for other alloys. However, in a highly ordered state, the composition dependence of H_m possesses minimum values at x=0.25, 0.5, and 0.75, and becomes asymmetric about x=0.5. Below but near the melting temperature, the relation $H_m \propto x(1-x)$ is almost satisfied. Because the melting temperatures of most of the alloys listed in Table 3-I are around 1000 °C, we determine the interaction parameter from the present strain energy calculation by using

$$\Omega_{cal} = 4 \cdot H_m(T=1000\ ^\circ C, x=0.5) \ . \qquad (3\text{-}15)$$

The values of Ω_{cal} are plotted against experimentally determined Ω, Ω_{exp}, in Fig. 3-9. Both agree qualitatively, which indicates that the mixing enthalpy is mainly the strain energy. However, Ω_{cal} are larger than Ω_{exp}. This discrepancy would be due to the assumption that the atoms of mixed sublattice are at VCA positions. The neglect of the temperature dependence of elastic constants would also lead to overestimation of the strain energy.

3-3. AVERAGE BOND LENGTH

3-3-1. Calculational Procedure

In $A_{1-x}B_xC$ alloy, an A-C bond appears in the type-0,1,2,and 3 tetrahedra as shown in Fig. 3-1, and the bond length would be different when involved in a different cell. Since the atom arrangement is at least somewhat random, i.e, the alloy is composed of various types of cells, a certain kind of bond is surrounded by various configurations of the nearest bonds. Then,

the bond length is not of a single value, but there are four different lengths for each kind of bond such as the A-C bond lengths in type-0,1,2,3 of tetrahedra and the B-C bond lengths in type-1,2,3,4 of tetrahedra. However, in reality, the second-nearest bonds and further could affect the strain of the bond: each bond length does not possess four discrete values but some additional broadening due to the composition fluctuation outside the tetrahedron. This effect will not be taken into account in the analysis.

The average values of bond lengths can be obtained from the relative numbers of tetrahedra and each bond length. Then, for example, the average A-C bond length $\bar{d}_{AC}$ is calculated by

$$\bar{d}_{AC} = \frac{\sum(4-i)g_i q_i d_{AC}^i}{\sum(4-i)g_i q_i} \qquad (3\text{-}16)$$

where d_{AC}^i and 4-i are the length and the number of A-C bond within type-i tetrahedron, respectively. d_{AC}^i and d_{BC}^i are obtained by minimizing the strain energy of that tetrahedron, while q_i's are by minimizing the total free energy of the alloy crystal, as described in the last section.

3-3-2. Numerical Results

The average bond lengths at room temperature are calculated from Eq.(3-16) taking the short-range order at 1000 K into account, except for the alloys including InSb, for which 800 K is chosen; as stated earlier, the atom arrangement at the growth temperature will be preserved even at room temperature owing to small diffusivity of atoms in solids. The results are given in Figs. 3-10 and 3-11, where bold lines denote the average bond lengths $\bar{d}_{AC}$ and $\bar{d}_{BC}$, broken lines the bond lengths in each cell d_{AC}^i and d_{BC}^i, and solid lines the VCA bond lengths $\bar{d}$. Because of assumption described in the last section, the bond length averaged

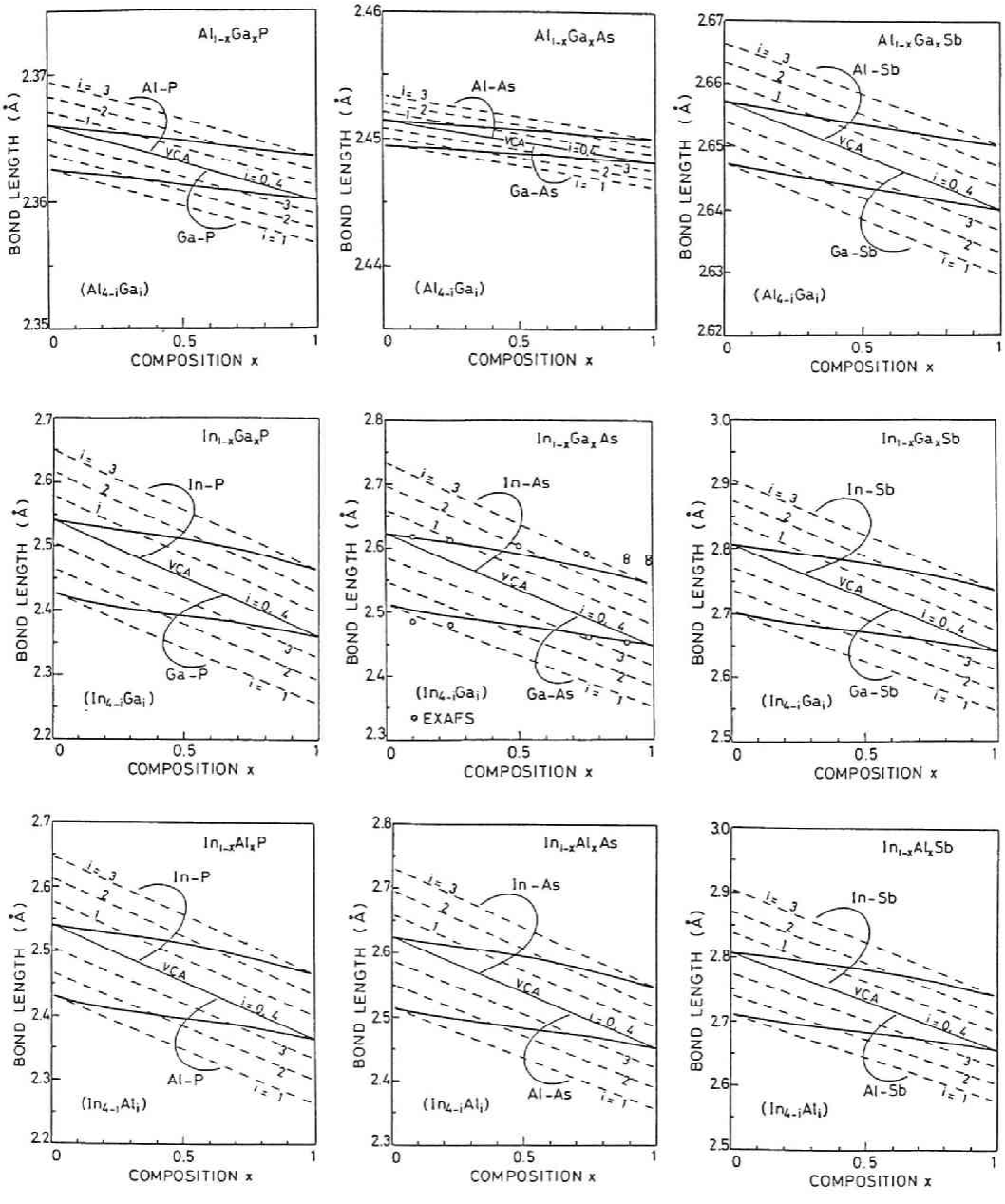

Fig.3-10 Bond length variations in ternary alloy semiconductors of $A^{III}_{1-x}B^{III}_{x}C^{V}$ group with respect to the composition. The solid line with VCA is for the bond length calculated from the virtual crystal approximation, and two bold lines are for the average bond lengths. The broken lines are for the bond lengths in tetrahedron cell of the type-i. Short-range order is taken into account in calculating the average bond lengths.

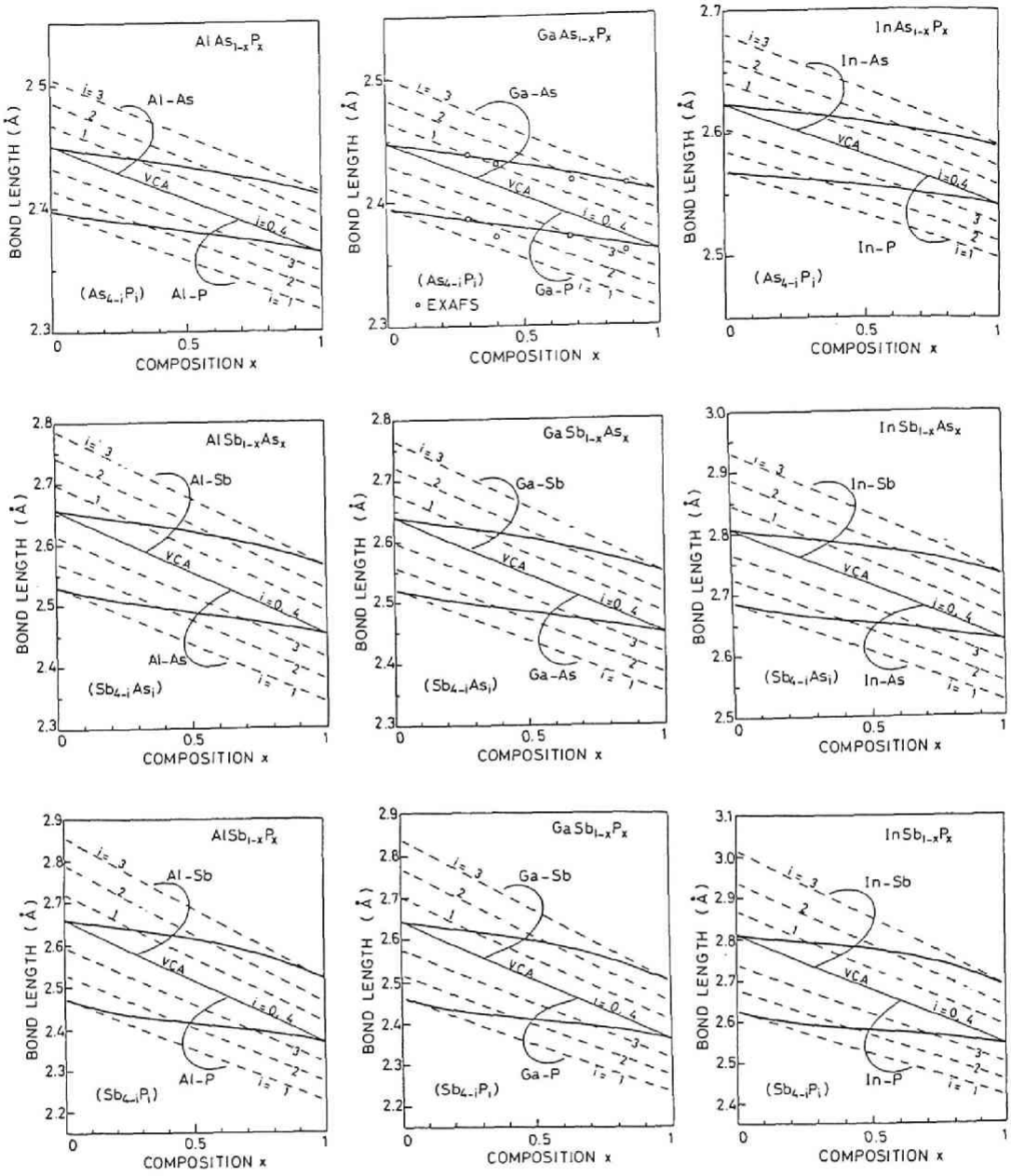

Fig.3-11 Bond length variations in ternary alloy semiconductors of $C^{III}A^{V}_{1-x}B^{V}_{x}$ group with respect to the composition. The solid line with VCA is for the bond length calculated from the virtual crystal approximation, and two bold lines are for the average bond lengths. The broken lines are for the bond lengths in tetrahedron cell of the type-i. Short-range order is taken into account in calculating the average bond lengths.

within a cell is equal to the VCA value $\bar{d}$, i.e., $(4-i)d^{i}_{AC}+id^{i}_{BC}=4\bar{d}$. Thus, bond lengths in type-0 and -4 cells are equal to the VCA value in this model.

The experimental data of bond length by EXAFS measurements are available for $In_{1-x}Ga_xAs$[8] and $GaAs_{1-x}P_x$.[13] The agreements between the experimental and the theoretical values are fairly good for both alloys. However, some discrepancy is seen particularly for $In_{1-x}Ga_xAs$: the bond length deviation from that in the corresponding binary compound is larger for the theoretical values. This difference would be due to the assumption of the model and/or the insufficient validity of the material parameters used here. Some error could not be avoided in the EXAFS measurements and data analyses.

For comparison, the average bond lengths for the complete random arrangement are calculated for $In_{1-x}Ga_xAs$ and plotted by dash-dott lines in Fig. 3-12. Although the difference due to the short-range order is rather small, the average bond lengths in the completely random case deviate from that in the binary compound more largely than those in the equilibrium state do: the bond length deviation is decreased by the short-range order. This can

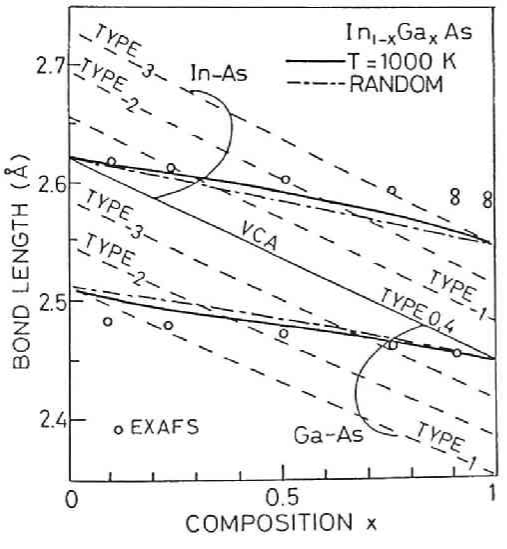

Fig. 3-12 Bond lengths in $In_{1-x}Ga_xAs$. Both bold and dash-dot lines represent the average bond length. The short-range order is considered for the bold lines, whereas completely random arrangement is assumed for the dash-dot lines.

be interpreted as follows: at the thermal equilibrium state, largely distorted bonds tend to decrease because such bond has large strain energy. For an example of x=0.5, A-C bond is distorted most largely when included in type-0 cell. Since type-0 cell has relatively large strain energy at x=0.5, it decreases from the value of the completely random case. Then, the distortion of A-C bond decreases on an average owing to the short-range order. The decrease in the average distortion of bonds results in the decrease in the total strain energy, as shown in Fig. 3-8. For $GaAs_{1-x}P_x$, for example, the effect of short-range order is almost negligible because the degree of order is low, as can be seen from Figs. 3-5.

3-4. DISCUSSIONS

The short-range order parameter can be estimated by X-ray diffuse scattering measurement.[9] However, the results of the measurement are not available for III-V alloys except for $Al_{1-x}Ga_xAs$[14] and $In_{1-x}Ga_xAs$[15]. For $Al_{1-x}Ga_xAs$, the atom arrangement was found to be completely random, and for $In_{1-x}Ga_xAs$, the short-range order parameter σ is evaluated to be -0.05. Those results are consistent with the results given here. However, further experimental data is needed to test the accuracy of the analysis.

Long-range order or superstructure has been observed by transmission electron microscope in some III-V ternary alloys.[16-20] The results for $GaSb_{1-x}As_x$ can be qualitatively explained from the results given here: Superstructures observed in the alloy of x=0.5 are monolayer structure along <100> axis and chalcopyrite structure.[16] They are, if perfect, composed of type-2 cell, which is shown to be energetically favorable by the present analysis. However, the experimental results for other alloys are not necessarily consistent with the present results. Long-range order in

$Al_{1-x}Ga_xAs$[17] cannot be explained by this analysis. For $In_{1-x}Ga_xAs$ ($x \simeq 0.5$), three different types of structures were observed: monolayer structure along <100>[18], famatinite structure[19], and monolayer structure along <111>[20]. The latter two are, if perfect, composed of type-1 and -3 cells, which are shown to be less favorable than type-2 cell in the analysis. In addition, the analysis on long-range order, described in Chap. VI, shows that the superstructure is unstable even for $GaSb_{1-x}As_x$ at temperatures of an usual crystal growth. Kinetic factors, e.g., surface reaction during the growth, would be necessary to consider in addition to the thermodynamic factors considered here.

The results of the analysis agree fairly well with the results from EXAFS in term of bond length. However, they must be compared with each other in term of dispersion of bond lengths, too. In EXAFS data analyses, length fluctuation including thermal vibration is taken into account as the Debye-Waller factor. The Debye-Waller factors experimentally determined for alloys do not significantly increase compared with those for binary compounds.[8,13] Thus, the dispersion of bond lengths predicted from the analysis has not been experimentally confirmed. As for the length dispersion, the theory is required to take into account the influence of local environment outside each tetrahedron, i.e., reexamin the assumption, and the EXAFS to improve the analysis for structurally disordered materials.[21]

In the analysis, it is assumed that the atoms on the mixed sublattice are on the VCA lattice sites. This assumption can be qualitatively justified by the discussion in Subsec.3-2-1, but it will cause some errors in the results. If the relaxation of the mixed sublattice is allowed, the strain energy of each cell will decrease further. Consequently, the total strain energy, i.e., H_m will also decrease, and then the difference between experimental and calculated interaction parameters will be reduced (see Fig.3-9). The energy decrease would be large for more largely

strained cell, and thus the energy difference among cells would decreases. This reduces the degree of the nonrandomness. The decrease in energy difference implies the decrease in the length difference of a certain bond among cells, i.e., the decrease in the dispersion of bond lengths. In reality, the dispersion might be so small that it cannot be detected by EXAFS measurements.

Recently, Sher et al. calculated the statistics of tetrahedra and the bond lengths for $In_{1-x}Ga_xAs$ taking account of the relaxation of the mixed sublattice.[22] Their results agree qualitatively with the present results, but, as expected, the energy difference among cells and the length dispersion are smaller than those given here. Further study is needed to include the relaxation of mixed sublattice into the present model.

In spite of the difference in estimation of enthalpy, the cell statistics obtained by Sher et al. quantitatively agree with the results given here. They use 16-bond cluster as a basic figure and use only 1/4 of the common element sites as cluster centers. Thus, for a certain number of alloy atoms, the number of basic figures is four times smaller in their analysis than in the present one, and consequently the decrease in S from the value of Eq.(3-4) is smaller in their analysis for a given degree of order. Then, higher degree of order will be concluded in their analysis even if the energies of cells are evaluated by the same way. Thus, their results are very similar to the present ones although energy difference among cells is smaller in their model.

The mixing enthalpy is considered to be the bond strain energy in this study. The interaction other than strain is customarily called chemical interaction and has been estimated by some researchers for III-V ternary alloys. According to the calculations by Sher et al.[22] and Ito[23], the chemical term is very small compared with the strain energy. On the other hand, the results of the calculation by Zunger et al. indicate that the chemical term is considerably large.[24,25] However, their cal-

culation is considered to overestimate the chemical interaction because of Brillouin zone effects in the pseudopotential calculation.[25] Therefore, the chemical interaction does not seem to greatly influence the atom arrangement in III-V ternary alloys.

3-5. SUMMARY

The statistics of tetrahedron cells and the average bond lengths have been calculated for 18 III-V ternary alloy semiconductors through a thermodynamic procedure. The results are summarized as follows:

i) In the atom arrangement of III-V ternary alloys, there is some degree of short-range order as well as randomness.

ii) The bond length deviation decreases on an average owing to the short-range order.

iii) The calculated average bond lengths agree fairly well with those obtained from EXAFS.

iv) The values of the interaction parameter obtained from the calculation of the strain energy agree qualitatively with the values determined from thermodynamic experiments. This supports the validity of the assumption that the mixing enthalpy is the bond strain energy.

v) For more accurate analysis, it is needed to take into account the relaxation of the mixed sublattice.

REFERENCES

1) As review, S. M. Sze, "Physics of Semiconductor Devices" 2nd ed. (John Wiley & Sons, New York, 1981), Chap. 12.

2) For example, Y. Takeda, A. Sasaki, Y. Imamura, and T. Takagi, J. Appl. Phys., 47 (1976) 5405.

3) T. Fukui, Jpn. J. Appl. Phys., 23 (1984) L208.

4) T. Onda, R. Ito, and N. Ogasawara, Jpn. J. Appl. Phys., 25 (1986) 82.

5) R. Kikuchi, Phys. Rev., 81 (1951) 988.

6) See Sec. A of Appendix. The same formula for entropy is obtained by different approaches in Ref. 22), and T. Onda and R. Ito, Jpn. J. Appl. Phys., 26 (1987) 967.

7) As review, R. A. Swalin, "Thermodynamics of Solids" 2nd Ed. (Wiley, New York, 1972).

8) J. C. Mikkelsen, Jr. and J. B. Boyce, Phys. Rev. B, 28 (1983) 7130.

9) J. M. Cowley, Phys. Rev. 77 (1950) 669, and J. Appl. Phys., 21 (1950) 24.

10) M. B. Panish and M. Ilegems, "Progress in Solid State Chemistry", edited by H. Reiss and J. O. McCaldin (Pergamon, New York, 1972), Vol.7, p. 39.

11) K. Osamura, K. Nakajima, and Y. Murakami, J. Jpn. Soc. Metall., 36 (1972) 744.

12) P. A. Fedders and M. W. Muller, J. Phys. Chem. Solids, 45 (1984) 685.

13) T. Sasaki, T. Onda, R. Ito, and N. Ogasawara, Jpn. J. Appl. Phys., 25 (1986) 231.

14) Y. Kashihara, N. Kashiwagura, M. Sakata, J. Harada, and T. Arii, Jpn. J. Appl. Phys., 23 (1984) L901.

15) K. Osamura, M. Sugahara, and K. Nakajima, Jpn. J. Appl. Phys., 26 (1987) L1746.

16) H. R. Jen, M. J. Cherng, and G. B. Stringfellow, Appl. Phys. Lett., 48 (1986) 1603.

17) T. S. Kuan, T. F. Kuech, W. I. Wang, and E. L. Wilkie, Phys. Rev. Lett., 54 (1985) 201.

18) T. S. Kuan, W. I. Wang, and E. L. Wilkie, Appl. Phys. Lett., 51 (1987) 51.

19) H. Nakayama and H. Fujita, "12th Int. Symp. GaAs and Related Compounds, Karuizawa, 1985, Inst. Phys. Conf. Ser. 79" (Adams Hilger, 1986), p.289.

20) M. A. Shahid, S. Mahajan, and D. E. Laughlin, Phys. Rev. Lett., 58 (1987) 2567.

21) P. A. Lee, P. H. Citrin, P. Eisenberger, and B. M. Kincaid, Rev. Mod. Phys., 53 (1981) 769.

22) A. Sher, M. Schilfgaarde, A. Chen, and W. Chen, Phys. Rev. B, 36 (1987) 4279.

23) T. Ito, Jpn. J. Appl. Phys., 26 (1987) 256.

24) A. A. Mbaye, L. G. Ferreira, and A. Zunger, Phys. Rev. Lett., 58 (1987) 49.

25) G. P. Srivastava, J. L. Martins, and A. Zunger, Phys. Rev. B, 31 (1985) 2561.

IV. ATOM ARRANGEMENT IN QUATERNARY ALLOY SEMICONDUCTORS OF (ABC)D TYPE

4-1. INTRODUCTION

III-V quaternary alloy systems have two independent variables to express their atomic composition, and thus two material parameters, e.g., band gap and lattice constant, can be independently selected within a certain range. This makes quaternary alloys indispensable for fabrication of closely lattice matched heterostructures. Quaternary alloys of (ABC)D type attract much attention as elements of various heterostructures,[1,2] and some of their band structures have been calculated on the basis of the coherent potential approximation.[3,4] In addition, by molecular beam epitaxial growth, an $(ABC)^{III}D^{V}$ alloy can in general be grown much easier than an $(AB)^{III}(CD)^{V}$ alloy and thus has began to be widely used.[5] A $D^{III}(ABC)^{V}$ alloy In(SbAsP) has been successfully grown by metalorganic vapour phase epitaxy.[6] Liquid-phase epitaxial growth of a $GaSb_{1-x-y}As_xP_y$ was also reported.[7]

In this chapter, the atom arrangement and the average bond length are discused for III-V quaternary alloy of (ABC)D type. In this type of quaternary alloys, mixing is restricted to one sublattice as in ternary alloys. Owing to this similarity, the approach is basically the same as for ternary alloys. The results of the analysis also have some similarities, but are different in some aspects; for example, clustering of like atoms never occurs in ternary alloys, but it can occur in a certain composition range in quaternary alloys of (ABC)D type.

4-2. ATOM ARRANGEMENT

4-2-1. Formalism of Free Energy

A. Basic figure and entropy

As for ternary alloys, a tetrahedron cell shown in Fig. 4-1 is taken as a basic figure of the thermodynamic analysis. While a ternary alloy is composed of five types of cells, an (ABC)D alloy is composed of 15 different types of cells. Their cell compositions are plotted by dark circles in the (ABC) composition plane in Fig. 4-1. The cell type is specified by the indices (i,j), where i and j are the number of B and C atoms in the cell, respectively. The relative number of each cell is represented by $g_{ij}q_{ij}$. Here, g_{ij} is the number of distinct configuration of atoms for the cell of type (i,j) and given by

$$g_{ij} = {}_4C_i \; {}_{4-i}C_j \quad , \tag{4-1}$$

where C denotes the computation of combination. q_{ij} is the probability of appearance of the cell of type (i,j) with a given atomic configuration. Since $g_{ij}q_{ij}$'s are relative numbers,

$$\sum g_{ij}q_{ij} = 1 \; . \tag{4-2}$$

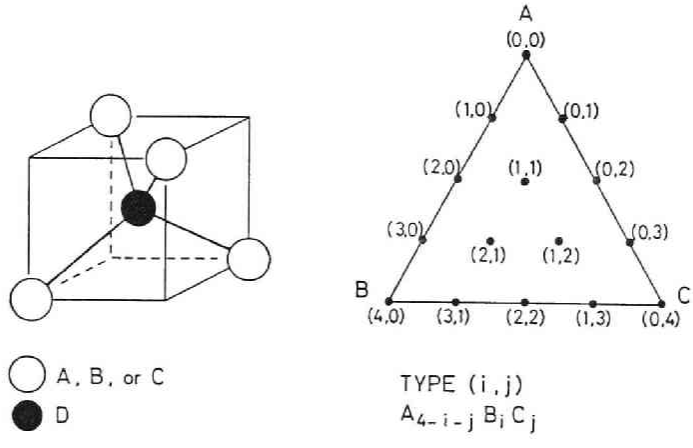

Fig. 4-1 Tetrahedron cell in an (ABC)D zincblende alloy. 15 different types of cells constitute an alloy, and their cell compositions are plotted by dark circles in (ABC) pseudoternary composition plane (right triangle).

Under a given composition, q_{ij}'s must satisfy the following conditions:

$$\sum_{i} \frac{i}{4} g_{ij} q_{ij} = x \quad , \tag{4-3}$$

$$\sum_{j} \frac{j}{4} g_{ij} q_{ij} = y \quad , \tag{4-4}$$

where x is the composition of element B and y that of element C.

The entropy S is derived by cluster variational method of Kikuchi[8] to be

$$S = -k_B N\{ \sum g_{ij} q_{ij} \ln q_{ij} - 3(x\ln x + y\ln y + z\ln z) \} \quad , \tag{4-5}$$

$(z=1-x-y)$

Equation (4-5) is basically the same as the entropy for a ternary alloy: if either x, y, or z is zero, it is reduced to Eq.(3-3).

If the atoms are distributed completely at random, then

$$q_{ij} = z^{4-i-j} x^i y^j \quad , \tag{4-6}$$

and

$$S = -k_B N(x\ln x + y\ln y + z\ln z) \quad . \tag{4-7}$$

This is the entropy of the regular solution model.

B. Enthalpy

In (ABC)D quaternary alloys, the relative numbers of bonds are uniquely determined from the atomic composition. Thus, the strain energy is thought to be the dominant portion of the mixing enthalpy as in ternary alloys. Then, the mixing enthalpy is given by

$$H_m = \sum g_{ij} q_{ij} \varepsilon_{ij} \quad , \tag{4-8}$$

where ε_{ij} is the strain energy of type (i,j) cell.

D atom is allowed to move from the central position of the cell for minimizing the strain energy of the cell, and then its

ε_{ij} is determined. However, atoms on the mixed sublattice, e.g., the group III atoms in (InGaAl)As, are assumed to be on the lattice sites of the virtual crystal approximation (VCA). This is the same assumption as that used for ternary alloys. As discussed in the last chapter for ternary alloys, an atom on the mixed sublattice is surrounded by four identical atoms (common element atoms), and thus it tends to remain at the central position among four atoms owing to the symmetry around it. On the other hand, a common element atom is surrounded by two (or more) different kinds of atoms. Thus the symmetry is broken and it moves largely from the central site. This discussion can be also applied to alloys of (ABC)D type, where the mixing is restricted to one sublattice. Therefore, the relaxation of the mixed sublattice is neglected. It should be noted that each ε_{ij} is a function of only the average lattice constant (VCA atomic spacing) owing to this assumption. The error caused by this assumption is discussed in the Sec.4-4.

C. Equilibrium state

The mixing free energy is given by

$$F_m = H_m - TS \quad , \tag{4-9}$$

q_{ij} at the thermal equilibrium state is obtained from the condition for a minimum free energy:

$$\sum \frac{\partial F_m}{\partial q_{ij}} \delta q_{ij} = 0 \quad , \tag{4-10}$$

$$\sum g_{ij} \delta q_{ij} = 0 \quad , \tag{4-11}$$

$$\sum \frac{i}{4} g_{ij} \delta q_{ij} = 0 \quad , \tag{4-12}$$

$$\sum \frac{j}{4} g_{ij} \delta q_{ij} = 0 \quad . \tag{4-13}$$

Equations (4-11), (4-12), and (4-13) are the derivative of Eqs. (4-2), (4-3), and (4-4), respectively. By using the Lagrange multipliers λ_0, λ_1, and λ_2, the above conditions are rewritten as

$$\frac{\partial F_m}{\partial q_{ij}} + \lambda_1 \frac{i}{4} g_{ij} + \lambda_2 \frac{j}{4} g_{ij} + \lambda_0 g_{ij} = 0 \qquad (4\text{-}14)$$

for i=0 to 4 and j=0 to 4-i. From Eqs.(4-3), (4-4), and (4-14), the following nonlinear simultaneous equations are obtained:

$$\sum \left(x - \frac{i}{4}\right) g_{ij} \exp\left(\frac{-\varepsilon_{ij}}{k_B T}\right) \Lambda_1^{\,i} \Lambda_2^{\,j} = 0 \qquad (4\text{-}15)$$

$$\sum \left(y - \frac{j}{4}\right) g_{ij} \exp\left(\frac{-\varepsilon_{ij}}{k_B T}\right) \Lambda_1^{\,i} \Lambda_2^{\,j} = 0 \qquad (4\text{-}16)$$

where $\Lambda_k = \exp(-\lambda_k / 4k_B T)$ (k=1,2). The equilibrium values q^o_{ij}'s are calculated by

$$q_{ij} = \Lambda_0 \exp\left(\frac{-\varepsilon_{ij}}{k_B T}\right) \Lambda_1^{\,i} \Lambda_2^{\,j} \qquad (4\text{-}17)$$

$$\Lambda_0 = \left[\sum g_{ij} \exp\left(\frac{-\varepsilon_{ij}}{k_B T}\right) \Lambda_1^{\,i} \Lambda_2^{\,j} \right]^{-1}$$

Equations (4-15) and (4-16) are solved by the Newton method.

D. Order parameter

The analysis here gives the relative numbers of the tetrahedron cells. However, it is not easy to deduce qualitative features in the atom arrangement directly from ratios of 15 different cells. Here, the short-range order parameters (SROP's) are used to represent relative numbers of the second-nearest pairs, e.g., A-A or A-B. For (ABC)D alloy system, the SROP's are defined by[9)]

$$\sigma_{pp} = \frac{(P_{pp} - x_p)}{(1 - x_p)} \quad , \qquad (4\text{-}18)$$

$$\sigma_{pq} = 1 - \frac{P_{pq}}{x_q} \quad , \tag{4-19}$$

where x_p is the composition of p element and P_{pq} the probability of a q atom occupying the second-nearest neighbour site of a p atom. For a completely random arrangement, all σ's become zero, and thus σ's represent the deviation from the random arrangement. In an (ABC)D system, there are six distinct SROP's: σ_{AA}, σ_{BB}, σ_{CC}, σ_{AB}, σ_{AC}, and σ_{BC}. However, for a three-component system, the number of linear-independent SROP's is three,[9] i.e., σ_{pp}'s can be calculated from σ_{pq}'s ($p \neq q$) by the equations such as

$$\sigma_{AA} = \frac{(x_B\sigma_{AB} + x_C\sigma_{AC})}{x_B + x_C} \quad . \tag{4-20}$$

However, all of six σ's are used for clarifying tendencies of atom arrangement.

In III-V ternary alloys, Eqs.(4-18) and (4-19) are reduced to the definition by Cowley[10], i.e., Eq.(3-13), and the number of independent SROP becomes unity: for example, in (AB)D system,

$$\sigma_{AA} = \sigma_{BB} = \sigma_{AB} \quad . \tag{4-21}$$

In the limit of $x_p \to 0$, σ_{pp} converges to zero, as can be seen from Eq.(4-18), but σ_{pq} does not necessarily converge to zero.

4-2-2. Numerical Results

A. $In_{1-x-y}Ga_xAl_yD^V$ (D^V=P,As,Sb) systems

Main features of atom arrangement are similar irrespective of species of D^V element, and thus the results for $In_{1-x-y}Ga_xAl_yAs$ are described in detail as an example. The results for other two alloys are also shown but not discussed in detail.

As noted in the last section, the strain energy of each cell is determined by the lattice constant of the alloy, a_Q. Figure

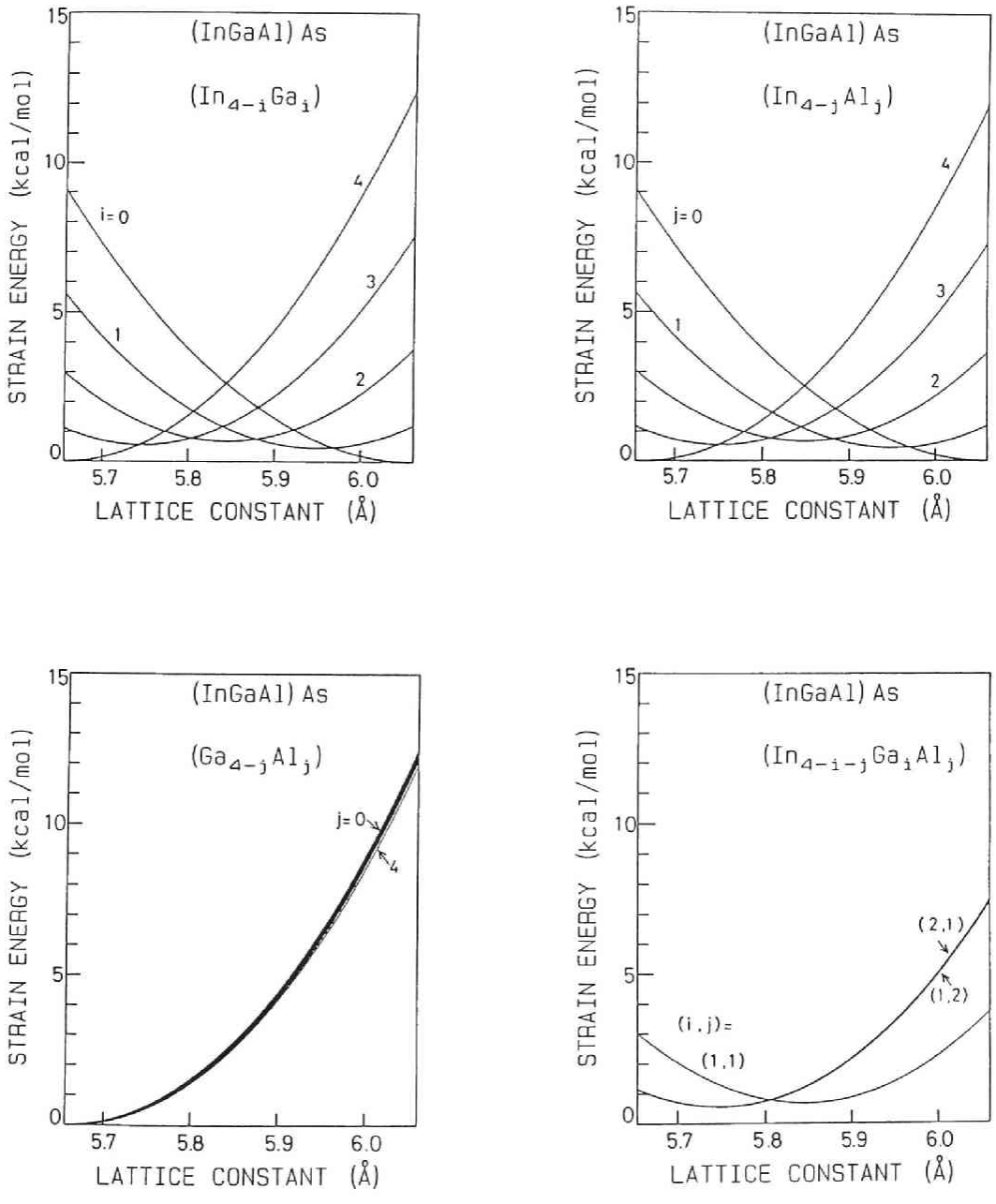

Fig. 4-2 Strain energies of tetrahedron cells in (InGaAl)As as functions of lattice constant of the alloy. The i and j are the numbers of Ga and Al atoms, respectively.

4-2 shows the ε_{ij}'s as functions of a_Q, where i and j are the numbers of Ga and Al atoms in the cell, respectively. In this system, a_Q is minimum for GaAs (5.6533Å) and maximum for InAs (6.0584Å), as shown in Fig. 4-3. Here, the lattice constant is approximated to follow the Vegard law. Each ε_{ij} becomes minimum when a_Q is nearly equal to the lattice constant at x=i/4, y=j/4. ε_{ij} is in general different for a different index i or j. In (InGaAl)D^V system, ε_{ij}'s with the same i+j are almost equal because Ga-D^V bond length is very close to the Al-D^V bond length.

Figures 4-4 are the contour charts of the SROP σ's. Negative σ indicates increase (decrease) for an unlike-pair (a like-pair) compared with the completely random arrangement. As can be seen from Figs. 4-4, all like-pairs decrease and In-Ga pair increases in the whole composition region. Ga-Al pair decreases, and In-Al pair increases at all compositions except in the vicinity of the line of x+y=1, where the opposite tendency appears for these two pairs. Those tendencies are all in accordance with the following simple rule: a pair composed of larger and smaller atoms is favorable, but a pair of two larger or two smaller atoms is unfavorable. Here whether an atom is larger or smaller is said relative to the average covalent radius of atoms being mixed in the alloy: A atom, for example, is larger atom when A-D bond length is larger than the bond length averaged in a whole alloy. It can be stated as a physical ground rule that the strain is reduced effectively by the shift of D atom (As atom in this case) when a large atom neighbours a small atom; on the contrary, a cluster of large or small atoms is unfavorable since it causes a large strain energy due to lattice-mismatch between the cluster and the surrounding alloy crystal. In $In_{1-x-y}Ga_xAl_yAs$ alloy, In-Ga and In-Al are larger-smaller pairs, In-In is a larger-larger pair, and Ga-Ga, Al-Al, and Ga-Al are smaller-smaller pairs except in the region of x+y≃1, where In-Al is a pair of larger atoms and Ga-Al is a smaller-larger pair. From these facts and the above

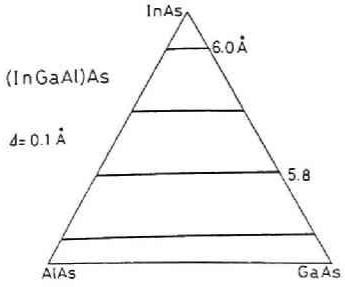

← Fig. 4-3 Contour chart of the lattice constant of (InGaAl)As alloy. The numerical values represent lattice constants in Å. Δ is difference in lattice constant between two contour lines.

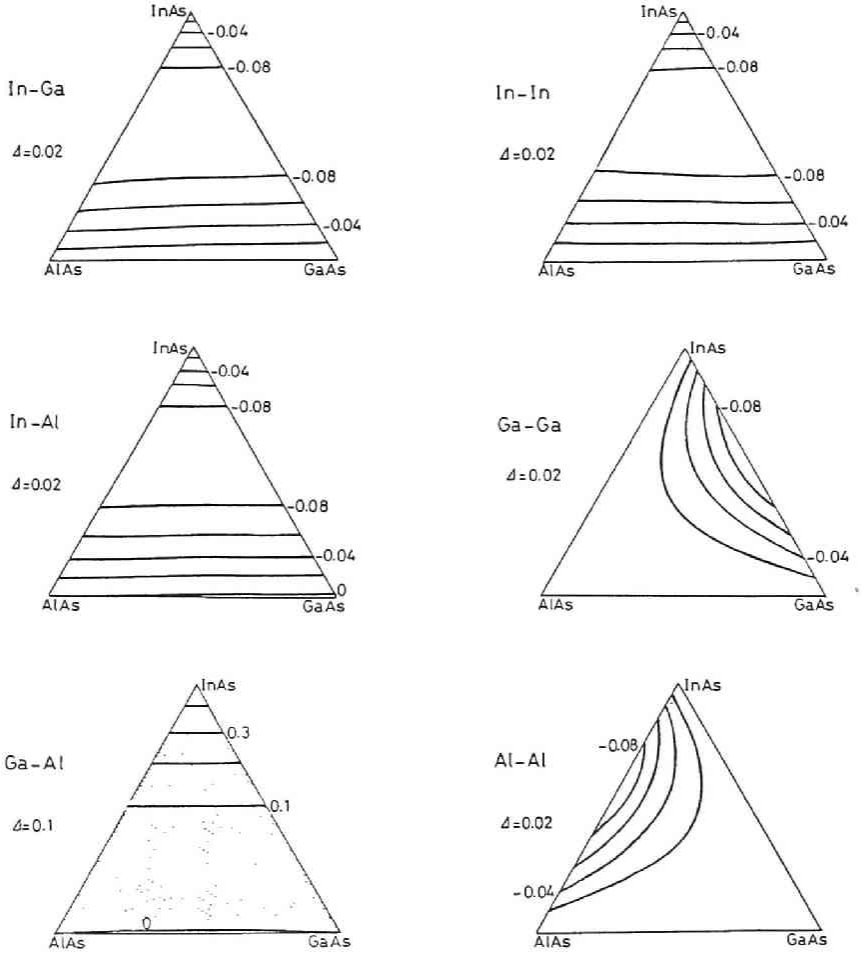

Fig. 4-4 Contour charts of the short-range order parameter σ's for (InGaAl)As alloy. The dotted areas indicate region with positive σ. Positive σ indicates increase (decrease) for a like- (an unlike-) pair. Δ is difference in σ between two contour lines.

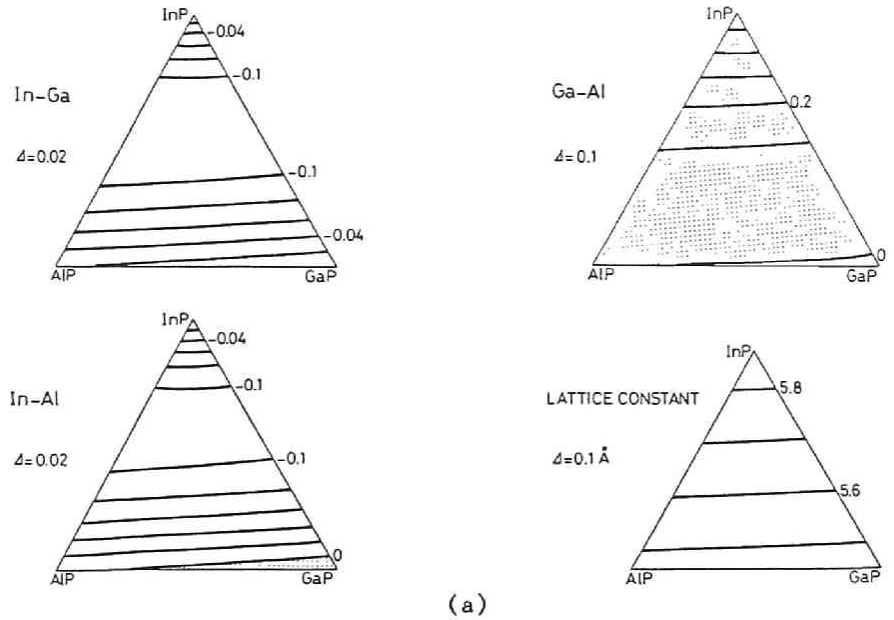

(a)

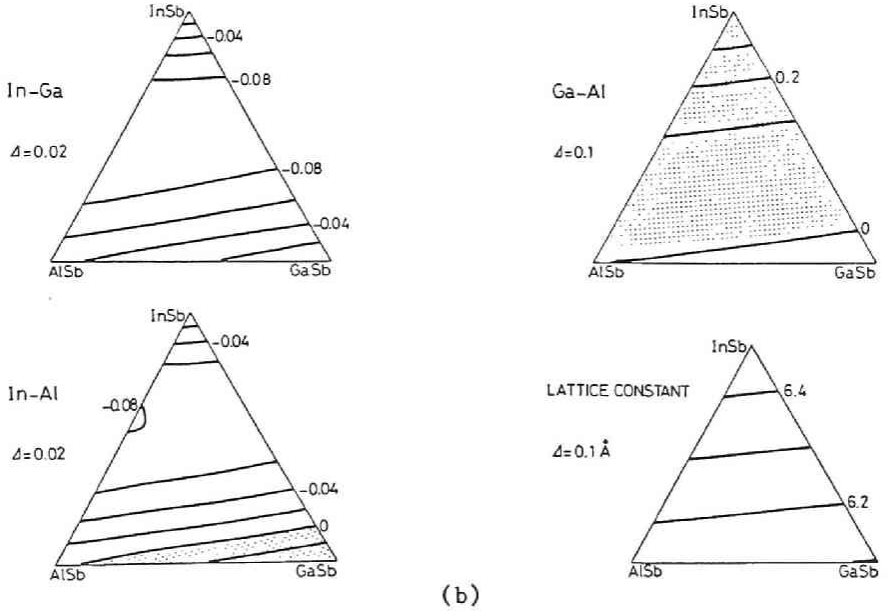

(b)

Fig. 4-5 Contour charts of short-range order parameter σ_{pq} a) for (InGaAl)P (T=1000K) and b) for (InGaAl)Sb (T=800K). Lattice constant at room temperature is also shown. σ_{pp}'s are not shown here but can be calculated by Eq.(4-20).

rule, one can predict the sign of σ correctly at any composition.

Figure 4-5 shows SROP's and lattice constant for (InGaAl)P and (InGaAl)Sb. Although the temperature is the same, each $|\sigma|$ is larger in (InGaAl)P than in (InGaAl)As, because the elastic constants and thus the strain energy are larger for (InGaAl)P. On the other hand, if at the same temperature, the elastic constants and thus $|\sigma|$'s will be smaller for (InGaAl)Sb, although 800K is adopted here because of low melting temperature of InSb. However, the sign of each σ is the same for all of the three systems, because it is determined from order of size among In, Ga, and Al atoms, i.e., In > Al $\simeq$ Ga.

B. $D^{III}Sb_{1-x-y}As_xP_y$ (D^{III}=Al,Ga,In) systems

Here, the results for $GaSb_{1-x-y}As_xP_y$ are described in detail, and then those for other two alloys are shown.

The strain energy ε_{ij}'s, lattice constant, and SROP σ's are shown in Figs. 4-6, 4-7, and 4-8, respectively. Here, i and j are the numbers of As and P atoms, respectively. Again, all of these tendencies in Fig. 4-8 can be interpreted on the basis of the rule. Sb-Sb and P-P pairs are always a pair of larger atoms and of smaller atoms, respectively, and thus both decrease ($\sigma<0$). Sb-P, being always a larger-smaller pair, increases ($\sigma>0$) in the whole composition. The signs of other σ's change depending on composition. For σ_{AsP} and σ_{SbAs}, the boundary between negative and positive sign nearly coincides with the composition line where the alloy lattice constant a_Q is equal to that of GaAs a_{GaAs} (see Fig.4-7). As atom is an atom larger than the average when $a_Q<a_{GaAs}$ but a smaller atom when $a_Q>a_{GaAs}$. Thus, when $a_Q<a_{GaAs}$, As-P pair is a larger-smaller pair and increases ($\sigma_{AsP}<0$), while it is a smaller-smaller pair and decreases ($\sigma_{AsP}>0$) when $a_Q>a_{GaAs}$. Similarly, Sb-As pair is a larger-larger pair and decreases when $a_Q<a_{GaAs}$, but it is a larger-smaller pair and increases when

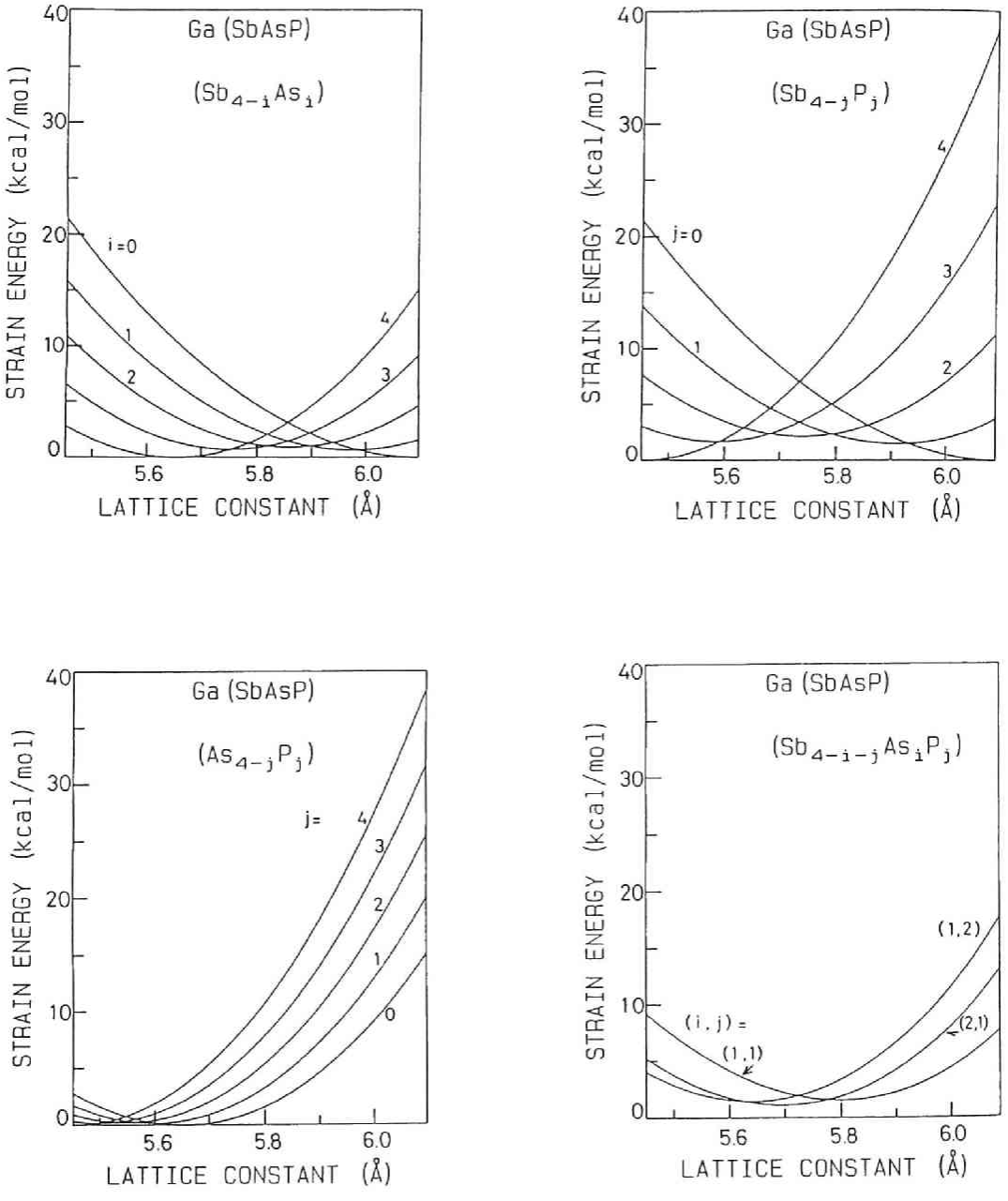

Fig. 4-6 Strain energies of tetrahedron cells in Ga(SbAsP) as functions of lattice constant of the alloy. The i and j are the numbers of As and P atoms, respectively.

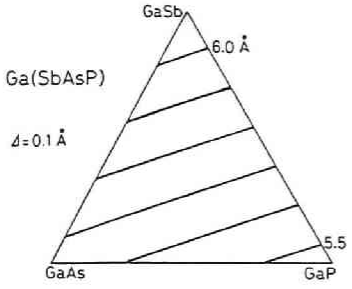

← Fig. 4-7 Contour chart of the lattice constant of Ga(SbAsP) alloy. The numerical values represent lattice constants in Å. Δ is difference in lattice constant between two contour lines.

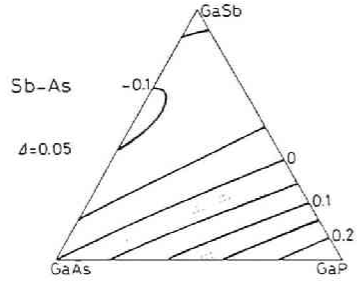

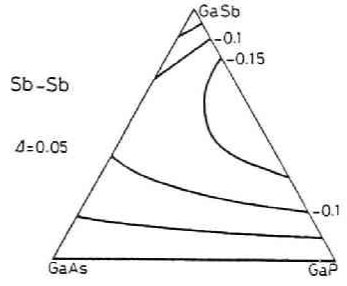

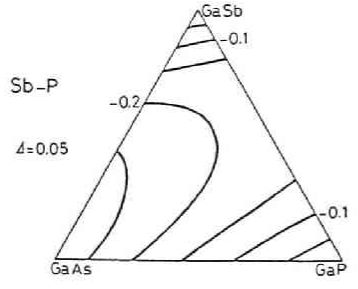

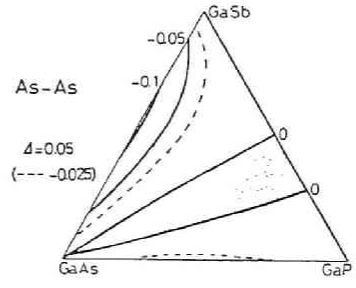

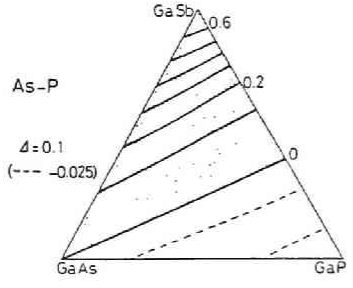

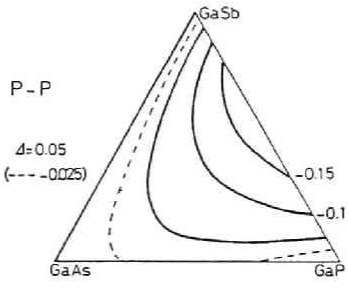

Fig. 4-8 Contour charts of the short-range order parameter σ's for Ga(SbAsP) alloy. The dotted areas indicate region with positive σ. Δ is difference in σ between two contour lines.

$a_Q > a_{GaAs}$.

As-As is a pair of smaller atoms in Sb rich region, while it is a pair of larger atoms in P rich region. Thus, it decreases in the both regions. However, in the region of $a_Q \simeq a_{GaAs}$, the cluster of As (GaAs) is closely lattice-matched to the surrounding crystal and thus has very small strain energy. Therefore, As 4 tetrahedron and thus As-As pair increase in that compositon region. In (InGaAl)As alloy, Al atom cluster becomes strain-free at the composition of $a_Q = a_{AlAs}$. However, since the size of Ga and Al atoms are very silimar, Ga-Al and Ga-Ga pairs are as favorable as Al-Al pair, and thus the tendency of Al clustering does not appear.

Figure 4-9 shows SROP's and lattice constant for Al(SbAsP) and In(SbAsP). 800 K is adopted for In(SbAsP) because of low melting point of InSb. Degree of nonrandomness in Al(SbAsP) is very similar to that in Ga(SbAsP) because of the similarity between AlD^V and GaD^V. On the other hand, at a certain temperature, In(SbAsP) is less nonrandom, since In based compounds have smaller elastic constant than Ga based ones.

4-3. AVERAGE BOND LENGTHS

The average bond lengths are calculated using equations similar to Eq.(3-16). Figures 4-10 and 4-11 show average bond lengths and VCA bond length for (InGaAl)As and Ga(SbAsP), respectively. The nonrandomnes in the atom arrangement at 1000 K is taken into account. Here, as an example, the results for Ga(SbAsP) are interpreted; from Fig. 4-11, the following features are summarized:

i) The change in bond length is largest in Ga-Sb bond and smallest in Ga-P bond.

ii) For all of three bonds, the spacing between contour lines become narrow when P composition is large, and thus bond length distortion increases on an average as P composition increases.

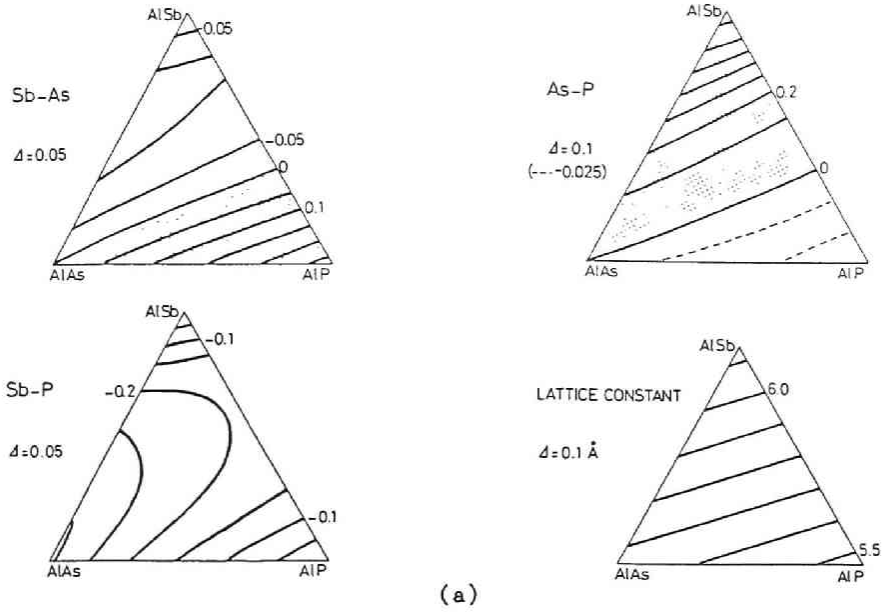

(a)

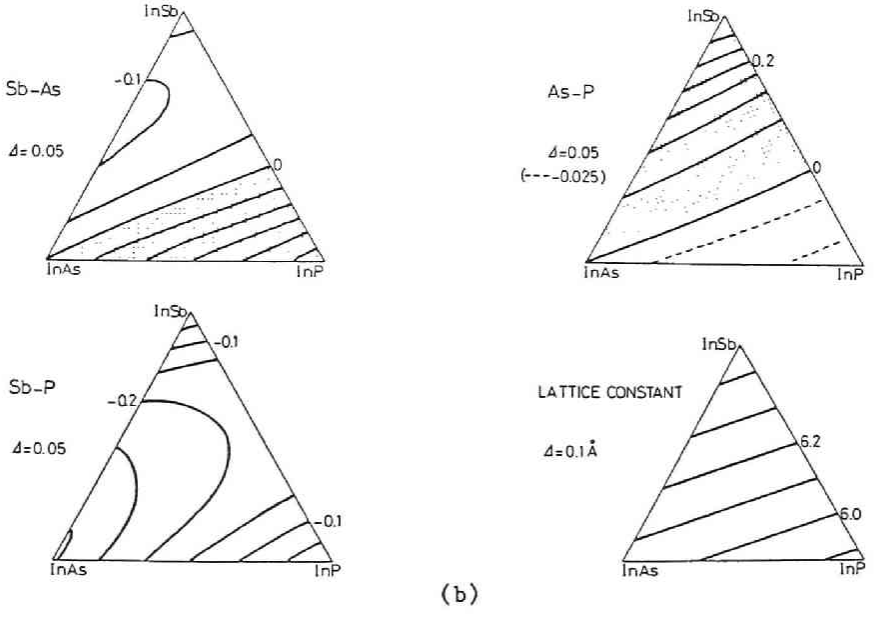

(b)

Fig. 4-9 Contour charts of short-range order parameter σ_{pq} a) for Al(SbAsP) (T=1000K) and b) for In(SbAsP) (T=800K). Lattice constant is also shown. σ_{pp}'s can be calculated by Eq.(4-20).

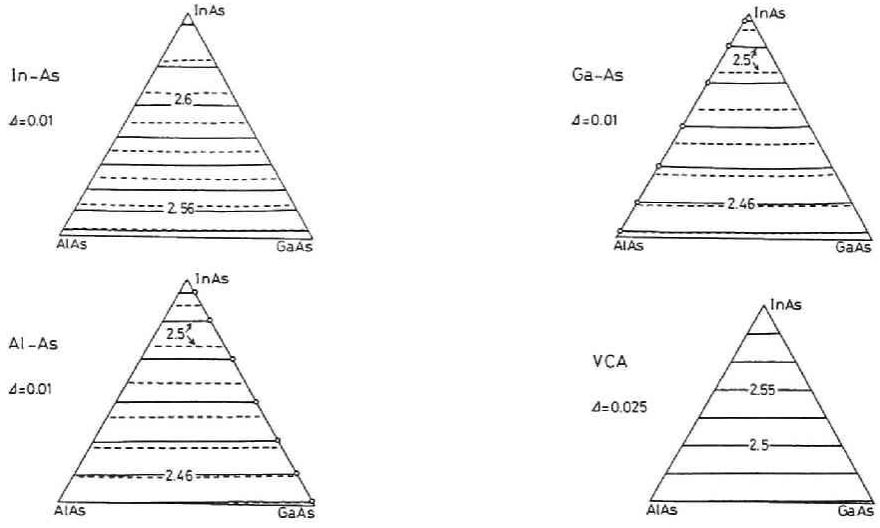

Fig. 4-10 Contour charts of average bond lengths in (InGaAl)As. Broken lines: completely random arrangement. Solid lines: equilibrium arrangement at 1000 K. Numerical values indicate bond length in Å. Δ is difference in length between two contour lines. VCA bond length is also shown.

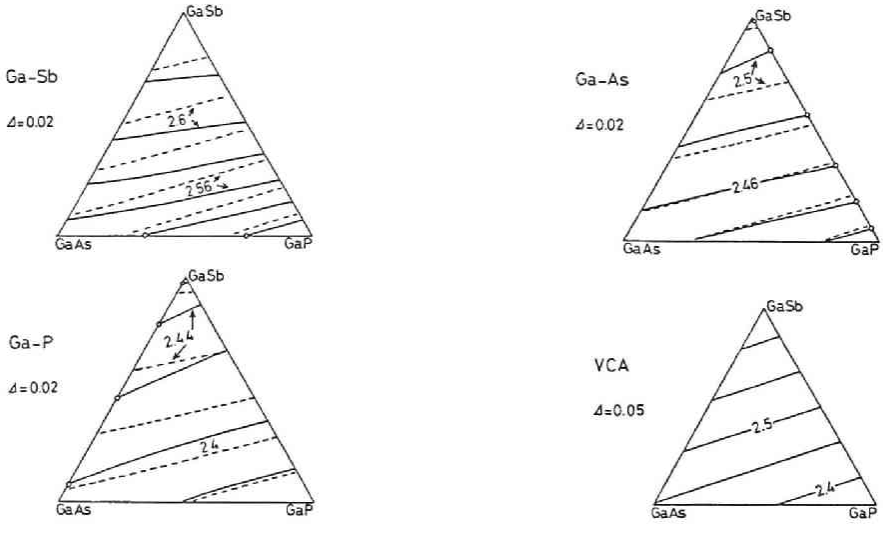

Fig. 4-11 Contour charts of average bond lengths in Ga(SbAsP). Broken lines: completely random arrangement. Solid lines: equilibrium arrangement at 1000 K. Numerical values indicate bond length in Å. VCA bond length is also shown.

iii) The contour lines of each bond length are nearly parallel to those of the VCA length, and thus the length of each bond barely depends on the composition if the lattice constant or the total average bond length is unchanged.

Feature i) is due to the difference in α. The Ga-P bond has the largest α among the three bonds and thus is difficult to distort, whereas Ga-Sb bond is the weakest and easy to distort. Feature ii) is attributed to the fact that GaP has a large elastic constant of angle distortion, β; in P-rich alloy, the angles of the crystal become stiff and difficult to distort. Then, length deviation becomes large, since the position of the common element atom in each tetrahedron is determined for equilibrium of angle and length distortions.

Feature iii) might seem due to the assumption that the cell sizes are determined from the lattice constant of the alloy. However, as composition changes, the relative numbers of tetrahedra also change. Since each bond length is different when involved in a different cell, it would have been possible to expect that each bond length changes with composition even if the lattice constant is unchanged. Thus, feature iii) cannot be directly deduced from the above assumption; it appears because length changes in various types of cells compensate each other.

For comparison, the average bond lengths for completely random arrangement are shown by broken contour lines. As in ternary alloys, the length deviation from the length in the binary compound is reduced by the nonrandomness in the atom arrangement. This tendency can be interpreted in the same way as for ternary alloys: at the thermal equilibrium state, the cell involving largely distorted bonds decreases, and thus the average length deviation decreases.

4-4. DISCUSSIONS

In this section, firstly, the results of statistic of tetrahedra are compared with those for ternary alloys, and then the accuracy of the analysis is examined.

As stated earlier, a pair of larger and smalller atoms is favorable for reducing the strain energy, since its strain can be effectively relaxed by the shift of the common element atom. For this reason, an unlike-pair increases and a like-pair decreases in ternary alloys; since the lattice constant of (AB)D is always an intermediate value between those of AD and BD, the unlike pair (A-B pair) is inevitably a pair of larger and smaller atoms and a like-pair a pair of larger or smaller atoms.

On the other hand, in quaternary alloys of (ABC)D type, certain unlike-pairs decrease ($\sigma_{pq}>0$), because an unlike-pair does not necessarily correspond to larger-smaller pair: the pair composed of largest and smallest atoms among three alloy atoms corresponds necessarily to a larger-smaller pair, but other unlike-pairs can be a pair of larger or smaller atoms at certain compositions.

The pair of largest (smallest) atoms, e.g., Sb-Sb (P-P) in Ga(SbAsP), is always a pair of two larger (smaller) atoms and decreases. However, like-pair of the mediate size atom, e.g., As in Ga(SbAsP) can increase at the compositions where the alloy is lattice-matched to the corresponding binary compound. This does not occur for ternary alloys, but for quaternary alloys. It may seem an exceptional case which occurs only in the limited compositions but is in fact very important, since the composition of a quaternary alloy is often selected so that the alloy is lattice-matched to a substrate of a binary compound. For example, $In_{1-x}Ga_xAs_{1-y}P_y$ is often grown on a InP substrate with lattice-matching, and then InP cluster in the alloy is a strain-free cluster, i.e., very favorable for reducing the strain energy. However, for $A^{III}_{1-x}B^{III}_xC^{V}_{1-y}D^{V}_y$ alloys, the change in the bond statistics must be considered, and thus one cannot immediately conclude the

tendency of clustering, as will be discussed in the next chapter. The analysis here predicts the tendency of clustering of As compound for D^{III}(SbAsP) alloy on D^{III}As substrate.

Since the approach described in this chapter is basically the same as that for ternary alloys, it involves similar shortcomings. The most important one is the neglect of relaxation of a mixed sublattice; it would result in overestimation of nonrandomness.

EXAFS experiment has not been carried out for quaternary alloys of (ABC)D type, and thus it is not possible to compare the calculated results with experimental ones.

4-5. SUMMARY

The atom arrangement and the bond lengths in III-V quaternary alloys of (ABC)D type have been investigated through the thermodynamic analysis. The results are summarized as follows:

i) The relative numbers of the second-nearest pairs are represented by short-range order parameters. A pair increases compared with the random arrangement case if it is composed of larger and smaller atoms than the average. Whereas, a pair of two larger or smaller atoms decreases.

ii) When the lattice constant of the alloy coincides with that of a constituent binary compound, there appears the preference for clustering of the compound.

iii) A proportional dependence is found between the average length of each bond and the VCA bond length.

iv) The length deviation from that of a binary compound is small if the elastic constant of length deviation is large and/or the average angle-distortion elastic constant is small.

v) The bond length deviation decreases on an average owing to the nonrandomness in the atom arrangement.

REFERENCES

1) A. Sasaki, M. Nishiuma, and Y. Takeda, Jpn. J. Appl. Phys., 19 (1980) 1695.

2) S. Adachi, J. Appl. Phys., 61 (1987) 4869.

3) F. Aymerich, Phys. Rev. B, 28 (1983) 6071.

4) J. R. Gregg, C. W. Myles, and Y. Shen, Phys. Rev. B, 35 (1987) 2532.

5) For example, D. Olego, T. Y. Chang, E. Silberg, E. A. Caridi, and Pinczuk, Appl. Phys. Lett., 41 (1982) 476.

6) T. Fukui and Y. Horikoshi, Jpn. J. Appl. Phys., 20, 587(1981).

7) A. Ya Vul', S. P. Vul', S. V. Kidalov, I. I. Saidashev, and Yu V. Shmartes, Sov. Tech. Phys. Lett., 11 (1985) 3.

8) R. Kikuchi, Phys. Rev. 81 (1951) 988 and Sec. A of Appendix.

9) D. de Fontaine, J. Appl. Cryst., 4 (1971) 15.

10) J. M. Cowley, Phys. Rev., 77 (1950) 669.

5-1. INTRODUCTION

In ternary alloys and quaternary alloys of (ABC)D type, the relative numbers of bonds are uniquely determined from the atomic composition. However, they cannot be uniquely determined in a quaternary alloy, $A^{III}_{1-x}B^{III}_{x}C^{V}_{1-y}D^{V}_{y}$:[1-3] two species of atoms are distributed on each of group III and group V sublattices, and thus the statistics of bonds, formed between group III and group V atoms, depend on the distribution of atoms in the sublattices. One can regard, for example, $In_{0.5}Ga_{0.5}As_{0.5}P_{0.5}$ alloy as a 1:1 mixture of either InP and GaAs or InAs and GaP: Various ratios of bonds yield the same atomic composition.

The strain energy is considered to be a dominant portion of the mixing enthalpy for quaternary alloys of (AB)(CD) type, too.[4] However, the cohesive energy change due to the change in the statistics of bonds also needs to be considered.[1] In this chapter, first, the factors which determine the statistics of bonds are qualitatively discussed, and then calculation procedure of the free energy including the mixing entropy and enthalpy is described in detail. Calculation results of statistics of bonds are given for nine quaternary alloy systems of (AB)(CD) type.

In calculating the strain energy, effects of local environment on the strain of bonds are taken into account as in the analyses of previous chapters: the length of a bond takes 16 different values depending on what bonds are its neighbours. The average bond length is calculated for $In_{1-x}Ga_{x}As_{1-y}P_{y}$, and its dependence on the bond statistics are discussed.

5-2. STATISTICS OF BONDS

5-2-1. Enthalpy of Quaternary Alloys of (AB)(CD) Type

Statistics of bonds must be consistent with the atomic composition. For example, the sum of the relative numbers of A-C and A-D bonds should not contradict the composition ratio of A atom in $A^{III}_{1-x}B^{III}_{x}C^{V}_{1-y}D^{V}_{y}$ alloy. Because of these constraints, the statistics of bonds are expressed by a single variable ξ which is defined in Subsec. 5-2-2. Here, it should be noted that A-C and B-D bonds simultaneously increase or decrease by the same amount, and so do A-D and B-C bonds.[1-3)]

For determining relative numbers of bonds, the following two factors should be taken into account: i) cohesive energy and ii) strain energy of each bond. The strain energy here corresponds to a change in the cohesive energy of bonds, as discussed in Chap. II. As the factor i), the cohesive energy in unstrained bonds is considered, and then the strain energy is included as the factor ii).

The effect of the factor i) on the statistics of bonds is easily understood: the number of bonds with large cohesive energy tends to increase at the thermal equilibrium. Since the numbers of two kinds of bonds increase or decrease simultaneouly, the sum of cohesive energy of these two bonds determines whether they will increase or decrease. For example, A-C bonds and thus B-D bonds increase if the sum of cohesive energy of them is larger than that of A-D and B-C bonds.

Next, we turn to the factor ii), i.e., the strain energy. In a ternary alloy, the coexistence of two or more different composition regions or the composition fluctuations in lattice-coherent semiconductors causes some excess strain energy, since different composition regions necessarily have different lattice constants. Such mechanism cannot always be applied to quaternary

alloys: Consider an alloy system $A^{III}_{1-x}B^{III}_{x}C^{V}_{1-y}D^{V}_{y}$ in which the lattice constant of binary compound AD is equal to that of BC but there is large difference in lattice constant between AC and BD. Although such alloy system is hypothetical, it is very similar to $In_{1-x}Ga_{x}Sb_{1-y}As_{y}$: the lattice mismatch between InAs and GaSb is 0.76%, while that between GaAs and InSb is 14%. If the atom arrangement is random, an alloy $A^{III}_{0.5}B^{III}_{0.5}C^{V}_{0.5}D^{V}_{0.5}$ is composed of four kinds of bonds. Then, large strain energy is stored in this alloy because of the difference in length among three of four bonds. Assume that it is decomposed into two regions AD and BC. Then, the crystal is composed of A-D and B-C bonds only. Since their lengths are the same, they do not strain each other. Thus the strain energy is decreased down to zero by such decomposition, even if the lattice coherency is retained between two regions.

Noting that bonds increase or decrease in pairs, the above effect can be generalized as follows: the strain energy would decrease with increasing the bond pair with smaller length difference, such as A-D and B-C bond pair in the above case. If, on the contrary, the pair of larger length difference increases, the strain energy would increase because these two bond largely strained each other. This tendency is confirmed by the calculation described in later subsections.

Therefore, in the analysis, following two factors are considered for determining the statistics of bonds: i) cohesive energy of bonds and ii) strain energy. In a general case, A-C bond and thus B-D bond may increase when i) the sum of cohesive energy of A-C and B-D bonds is larger than that of A-D and B-C bonds, and/or ii) the length difference between A-C and B-D bonds is smaller than that between A-D and B-C bonds. The effects of these two factors are investigated more quantitatively in the next two subsections.

5-2-2. Formalism of Free Energy

The free energy is expressed by

$$F = H_b + H_s - TS \qquad (5\text{-}1)$$

where H_b is the enthalpy due to the cohesive energy of bond, i.e., the factor i) in the last subsection, H_s the strain energy, i.e., the factor ii), and TS the product of the entropy S and the temperature T. The statistics of bonds at the thermal equilibrium state are obtained by minimizing F with respect to relative numbers of bonds.

A. Relative number of bond and the entropy

Not all of the relative numbers of bonds are independent variables for a given atomic composition. They are conveniently expressed by using a single variable ξ as follows:[3)]

$$X_{AC} = x_A x_C + \xi \ , \qquad X_{BC} = x_B x_C - \xi \ ,$$

$$X_{AD} = x_A x_D - \xi \ , \qquad X_{BD} = x_B x_D + \xi \ , \qquad (5\text{-}2)$$

where X_{pq} is the relative number of the p-q bond, and x_p is the composition of atom p and satisfies the relation $x_A + x_B = 1$ or $x_C + x_D = 1$. It is easy to see that the statistics of bonds given by Eq.(5-2) are always consistent with the atomic compositions. The ξ becomes zero if the atom arrangement is completely random.

The approximate entropy of mixing S was derived as follows:[1)]

$$S = Nk_B(-4 \sum_{pq} X_{pq} \ln X_{pq} + 3 \sum_{p} x_p \ln x_p) \ , \qquad (5\text{-}3)$$

where N is the number of group III (V) atoms.

B. Cohesive energy

The enthalpy due to the cohesion of bonds, H_b, is written as

$$H_b = 4N \sum X_{pq} h_{pq} \quad , \tag{5-4}$$

where h_{pq} is the enthalpy due to the cohesion of an unstrained p-q bond. As noted earlier, the strain energy is taken separately into account by the term H_s. The 4N is the total number of bonds. It should be noted that the bond is less stable with smaller value of $|h_{pq}|$ since h_{pq} is the enthalpy. The h_{pq} is a negative value, and its absolute value corresponds to the amount of the cohesive energy.

With the use of Eq.(5-2), H_b can be rewritten as follows:

$$\begin{aligned} H_b &= H_o + \omega_b \xi \\ H_o &= 4N \sum x_p x_q h_{pq} \\ \omega_b &= 4N\{(h_{AC}+h_{BD})-(h_{AD}+h_{BC})\} \quad . \end{aligned} \tag{5-5}$$

If the quaternary alloy system $A^{III}_{1-x}B^{III}_{x}C^{V}_{1-y}D^{V}_{y}$ is an ideal solution, there is no strain energy in the alloy and the atom arrangement is completely random. Then the total enthalpy becomes H_o. Since H_o is uniquely determined by the composition, only $\omega_b \xi$ is necessary to consider for the determination of statistics of bonds: the mixing enthalpy H_m is expressed by

$$H_m = H_s + \omega_b \xi \quad . \tag{5-6}$$

Since h_{pq} is defined as the enthalpy for the unstrained p-q bond, we can derive it from the thermodynamic properties of the binary compound pq, which consists of unstrained bonds. The entropy of mixing is zero for a binary compound, and the cohesion of the crystal is considered to be solely due to bonds in the model. Thus $4Nh_{pq}=\mu_{pq}$ corresponds to the free energy or the chemical potential of the binary compound pq. The ω_b can be calculated by

$$\omega_b = (\mu_{AC} + \mu_{BD}) - (\mu_{AD} + \mu_{BC}) \quad . \qquad (5\text{-}7)$$

The values of the equivalent of ω_b have already been obtained for nine III-V quaternary alloy systems in Ref. 5.

C. Strain energy

The strain of each bond is affected by what kinds of bonds surround it; for example, the bond tends to be greatly compressed when surrounded by bonds longer than the total average length. In the model, the strain energy of a bond is calculated in each tetrahedron cell. For ternary alloys, it is assumed that the strain of a bond is determined in various types of tetrahedra where a central site is occupied by a common element and surrounding sites by mixed elements as shown in Fig. 3-1. For quaternary alloys of (AB)(CD) type, one need consider both group III and group V tetrahedra; for example, the B-C bond represented by the double line in Fig. 5-1 is simultaneously contained in an A(3)B(1) (group III) tetrahedron and a C(2)D(2) (group V) tetrahedron. In general, a

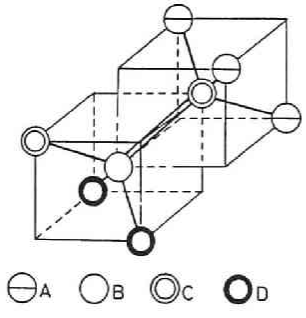

Fig.5-1 Tetrahedra in the quaternary alloy $A_{1-x}B_xC_{1-y}D_y$. The B-C bond represented by a double line is included in A(3)B(1) (group III) and C(2)D(2) (group V) tetrahedra.

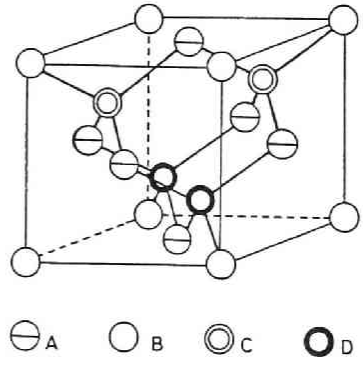

Fig.5-2 Zincblende-like unit cell which consists of A(3)B(1) and C(2)D(2) tetrahedra.

B-C bond can be contained in A(4-i)B(i) for i=1,2,3,4 and C(4-k)D(k) for k=0,1,2,3 tetrahedra. Note that tetrahedra without either B or C atom cannot contain B-C bond. Thus, there are 16 kinds of local environments for B-C bonds in an alloy, and the B-C bond can have 16 different amounts of strain energy, one for each local environment.

Another factor influencing the bond strain is the average lattice constant of the alloy crystal within which the tetrahedra are embedded; for example, a bond length in a certain type of tetrahedron would decrease when the lattice constant of the crystal decreases. Therefore, in this model, the strain energy of bonds is determined from a) the type of group III tetrahedron, b) the type of group V tetrahedron, and c) the lattice constant.

In calculating the strain energy in quaternary alloys, the unit cells such as shown in Fig. 5-2 is used. It should be noted that the crystal represented by this unit cell consists of only A(3)B(1) and C(2)D(2) tetrahedra. Thus the B-C bond (double line) in Fig. 5-1 and that in Fig. 5-2 are surrounded by the same tetrahedra. Although some other A(3)B(1) and C(2)D(2) unit cells are possible, they are all obtained by symmetric operations from the cell in Fig. 5-2, and thus all of them are equivalent. Let the size of the unit cell be equal to the lattice constant of the alloy in which the tetrahedra shown in Fig. 5-1 are embedded. Then, with respect to the above three factors a), b), and c), the environment around the B-C bond in Fig.5-1 is the same as that in Fig.5-2, and thus the strain energy is considered equal for both B-C bonds in the model. The lattice constant of the alloy is calculated from the atomic compositions by using the Vegard law.

The strain calculation in the unit cell was carried out by taking account of the deviation from VCA structure for both sublattices: the strain energy of the ordered alloy represented by a unit cell such as shown in Fig. 5-2 is minimized by moving all

atoms under a given lattice constant, and then the strain of each bond is determined. First, calculation was done for the case where the size of the unit cell is equal to the average lattice constant weighted by the composition of that cell. The amounts of angle distortion and/or length deviation of a certain kind of bond are quite different among unit cells. Then, strain energy is calculated for several unit cells by varying the size of the cell. The results show that the angles between bonds depend little on the size of the cell. This indicates that the angle distortion energy depends weakly on the size of the cell. Thus, it can be assumed that the change in the cell size does not much influence the angle distortion energy. It does influence the length deviation energy: if the size of the unit cell changes by Δa, each bond within it changes by $\sqrt{3}/4\Delta a$. The strain energy of, for example, a B-C bond in A(4-1)B(i)C(4-k)D(k) unit cell is expressed as

$$\varepsilon_{BC}(i,k) = \frac{1}{2}\,\varepsilon^{a}_{BC}(i,k) + \frac{3}{2}\,\alpha_{BC}\{d^{0}_{BC}-d_{BC}(i,k)\}^{2} \quad , \quad (5\text{-}8)$$

where $\varepsilon^{a}_{BC}(i,k)$ is the strain energy stored in the angles between B-C bond and its neighbors. The factor 1/2 appears because the strain energy of each angle will be counted twice when the strain energy for all bonds is summed up. The second term is the length deviation energy of the B-C bond. Here, d^{0}_{BC} and α_{BC} are the unstrained bond length and the elastic constant of length deviation of B-C bond, respectively, and $d_{BC}(i,k)$ is the length of B-C bond in A(4-i)B(i)C(4-k)D(k) unit cell. It was assumed that the size of a unit cell does not influence $\varepsilon^{a}_{BC}(i,k)$ but $d_{BC}(i,k)$, as discussed above.

The strain energy of all B-C bonds in an alloy is given by

$$H^{BC}_{s} = 4N\sum_{ik} P_{BC}(i,k,\xi)\varepsilon_{BC}(i,k) \quad , \quad (5\text{-}9)$$

where $P_{BC}(i,k,\xi)$ is the relative number of B-C bond contained in

A(4-i)B(i) and C(4-k)D(k) tetrahedra, and given by

$$P_{BC}(i,k,\xi)={}_3C_{i-1}\ {}_3C_k \frac{X_{AC}^{4-i}\ X_{BC}^{i+4-k}\ X_{BD}^{k}}{x_B^3\ x_C^3} \quad , \tag{5-10}$$

where ${}_3C_m$ is the combination number and defined as zero when m=0,4. For other bonds, i and 4-i (k and 4-k) are exchanged according to the exchange between A and B (C and D). The $P_{pq}(i,k,\xi)$ satisfies

$$\sum_{ik} P_{pq}(i,k,\xi) = X_{pq} \quad . \tag{5-11}$$

The total strain energy is expressed by

$$H_s = \sum_{pq} H_s^{pq} = 4N \sum_{pq} \sum_{ik} P_{pq}(i,k,\xi)\epsilon_{pq}(i,k) \quad . \tag{5-12}$$

5-2-3. Numerical Results

A. $In_{1-x}Ga_xAs_{1-y}P_y$

First, the results for $In_{1-x}Ga_xAs_{1-y}P_y$ system are shown, and it is discussed how each term influences the equilibrium value of ξ. Figure 5-3 shows H_s, $\omega_b\xi$, and TS as functions of ξ for the composition x=0.5 and y=0.5 at the temperature T=1000 K. The

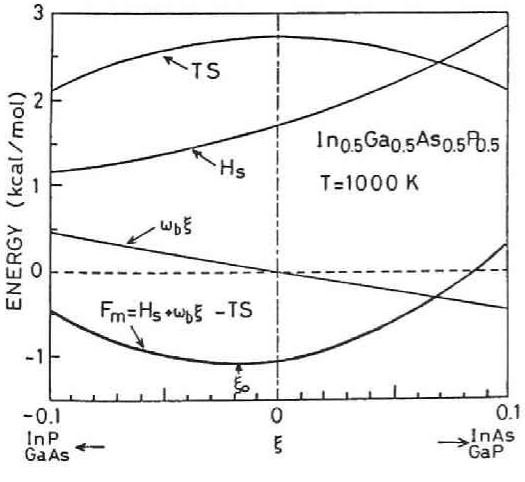

Fig.5-3 Strain energy H_s, cohesive energy term $\omega_b\xi$, entropy term TS, and the mixing free energy $F_m=H_s+\omega_b\xi-TS$ as functions of ξ for $In_{0.5}Ga_{0.5}As_{0.5}P_{0.5}$ at T=1000 K. Positive (negative) ξ indicates more In-As and Ga-P (Ga-As and In-P) bonds.

mixing free energy F_m is the sum of these three terms and differs from the total free energy F by H_o, which is independent of ξ. The ξ_o represents the equilibrium value of ξ at which F_m is minimum. As seen from Fig. 5-3, H_s increases with ξ, while $\omega_b\xi$ decreases. Thus, their effects compensate each other to some extent, and the ξ_o is close to zero because of TS being maximum at ξ=0. However, because the slope of H_s near ξ=0 is somewhat larger than that of $\omega_b\xi$, i.e., $|\omega_b|$, the ξ_o becomes negative (-0.018). The dependence of H_s on ξ is in accordance with the prediction that H_s will decrease if the pair of bonds with smaller length difference increases. In the $In_{1-x_o}Ga_xAs_{1-y}P_y$ system, $d_{InP}-d_{GaAs}$=0.093 Å and $d_{InAs}-d_{GaP}$=0.263 A.

Figure 5-4 shows the temperature dependence of ξ_o for x=0.5 and y=0.5. At low temperatures, TS is negligible, and thus $H_s+\omega_b\xi$ determines ξ_o. The result near T=0 K indicates that $H_s+\omega_b\xi$ is minimun at ξ=-0.09. As T increases, the entropy term begins to dominate, and ξ_o is close to zero at temperatures of usual crystal growth.

B. Other quaternary alloy systems

Next the results are shown for other eight quaternary alloy systems at x=0.5, y=0.5, and T=1000 K. When assigning the element to the symbol, A,B,C,or D, we put the heavier element to

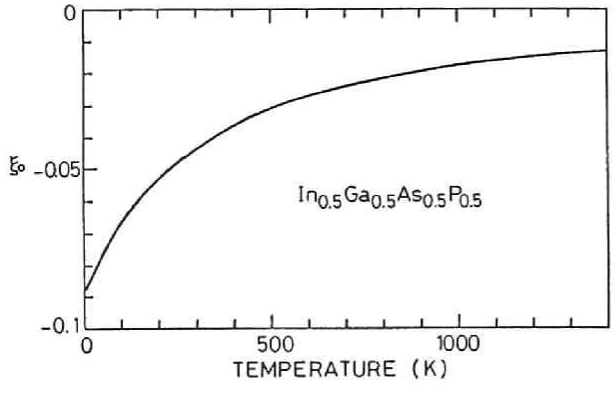

Fig.5-4 Temperature dependence of the equilibrium value of ξ for $In_{0.5}Ga_{0.5}As_{0.5}P_{0.5}$.

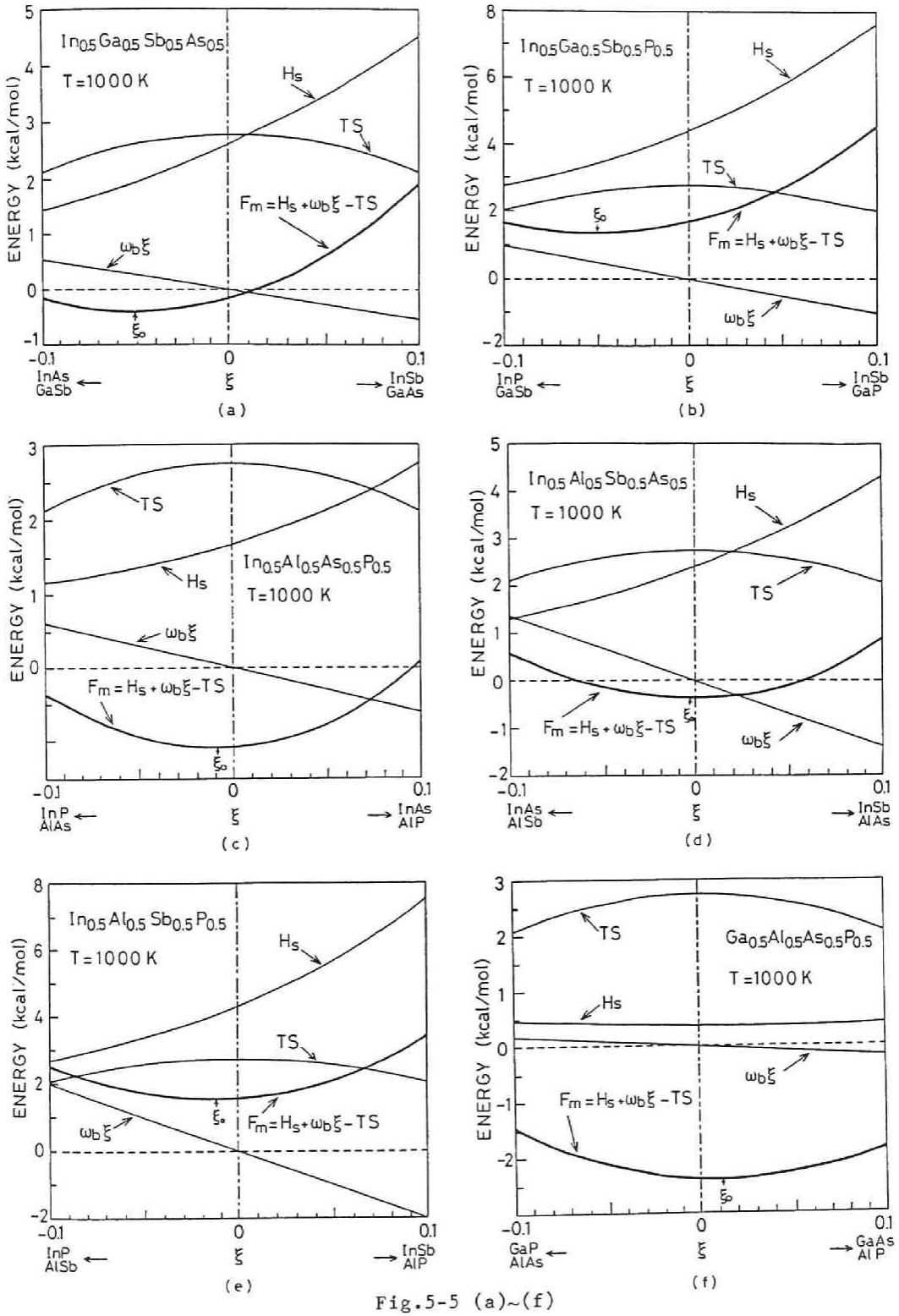
In0.5Ga0.5Sb0.5As0.5
T=1000 K
Hs
TS
Fm=Hs+ωbξ-TS
ωbξ
ξ0
ENERGY (kcal/mol)
InAs GaSb
InSb GaAs
(a)
In0.5Ga0.5Sb0.5P0.5
T=1000 K
InP GaSb
InSb GaP
(b)
In0.5Al0.5As0.5P0.5
T=1000 K
InP AlAs
InAs AlP
(c)
In0.5Al0.5Sb0.5As0.5
T=1000 K
InAs AlSb
InSb AlAs
(d)
In0.5Al0.5Sb0.5P0.5
T=1000 K
InP AlSb
InSb AlP
(e)
Ga0.5Al0.5As0.5P0.5
T=1000 K
GaP AlAs
GaAs AlP
(f)

Fig.5-5 (a)~(f)

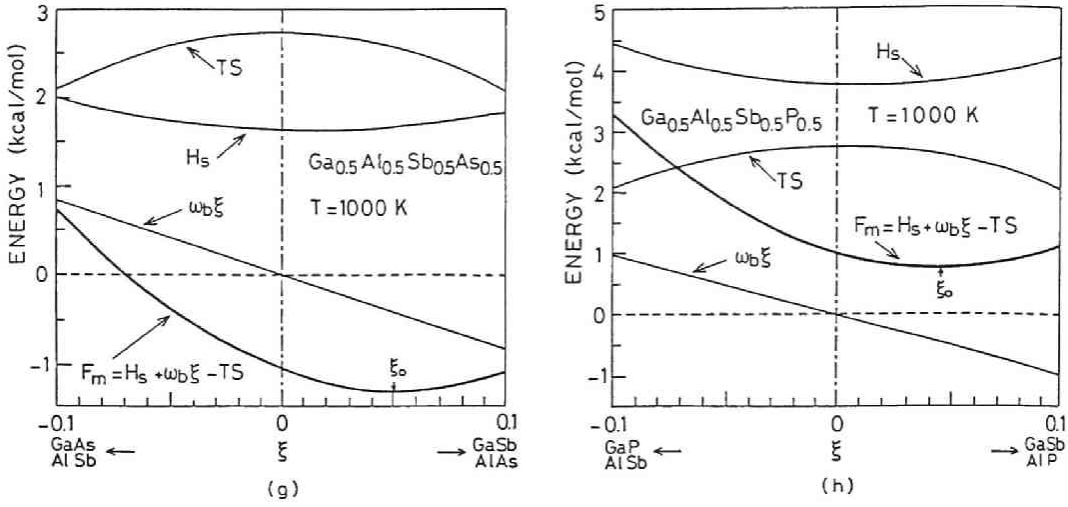

Fig.5-5 Figures similar to Fig.5-3 for quaternary alloys other than $In_{1-x}Ga_xAs_{1-y}P_y$ at x=0.5, y=0.5, and T=1000 K.

A(C), as in $In_{1-x}Ga_xAs_{1-y}P_y$.

The results are shown in Figs. 5-5. On the basis of qualitative features of the results, the nine alloy systems are classified into the following three groups.

1) $In_{1-x}Ga_xC^V_{1-y}D^V_y$ (C^V, D^V=Sb, As, P; Figs.5-3,-5 a,b): $\omega_b\xi$ decreases and H_s increases with ξ. However, the slope of H_s at ξ=0 is larger than $|\omega_b|$. Thus, ξ_o becomes negative. In the alloy of $In_{0.5}Ga_{0.5}Sb_{0.5}As_{0.5}$, H_s decreases down to a very small value, 0.03kcal/mol at the lower limit of ξ (ξ=-0.25) because the length difference between In-As and Ga-Sb is very small, as mentioned in Subsec. 5-2-1.

2)$In_{1-x}Al_xC^V_{1-y}D^V_y$ (Figs.5-5 c-e): the value of H_s is not much different from that in the corresponding $In_{1-x}Ga_xC^V_{1-y}D^V_y$ system, because the elastic properties of Ga-C^V and Al-C^V bonds are very similar. However, $|\omega_b|$ is larger than that in $In_{1-x}Ga_xC^V_{1-y}D^V_y$. Thus, though H_s dominates over $\omega_b\xi$ in $In_{1-x}Ga_xC^V_{1-y}D^V_y$, the variations of H_s and $\omega_b\xi$ compensate each other almost completely in $In_{1-x}Al_xC^V_{1-y}D^V_y$, and thus ξ_o is very close to zero.

3) $Ga_{1-x}Al_xC^V_{1-y}D^V_y$ (Figs.5-5 f-h): $\omega_b\xi$ decreases with ξ, while H_s weakly depends on ξ and is nearly symmetric with respect to the line of ξ=0. Thus, ξ_o is positive owing to the variation of $\omega_b\xi$. The even-function-like dependence of H_s on ξ is due to the fact that $d_{GaC^V}\simeq d_{AlC^V}$; for example, in $Ga_{1-x}Al_xAs_{1-y}P_y$, $d_{GaP}\simeq d_{AlP}$ and $d_{GaAs}\simeq d_{AlAs}$, and thus, as concerns the elastic properties, the increase of Ga-P and Al-As bonds is almost equivalent to the increase of Al-P and Ga-As bonds. On the other hand, the chemical properties of Ga-C^V and Al-C^V bonds are quite different. Thus ω_b can be a large negative value relative to the variation of H_s.

The composition dependence of ξ_o at 1000 K is shown in Fig. 5-6 for nine systems. The ω_b is independent of the composition as seen in Eq. (5-5). The value of H_s depends on the composition rather strongly, but the slope of H_s at ξ=0 depends weakly; for an example of $In_{1-x}Ga_xAs_{1-y}P_y$, the slope varies within ±15% from that at x=0.5 and y=0.5. For $In_{1-x}Al_xSb_{1-y}As_y$ and $In_{1-x}Al_xSb_{1-y}P_y$, in which two factors compensate each other, the sign of ξ_o changes owing to the small variation in slope of H_s. Except for these two systems, the dependence in Fig. 5-6 is mainly influenced by change in the entropy: a certain amount of deviation of ξ from zero causes larger decrease in S, as x or y approaches zero or unity. In addition, the variable range of ξ diminishes:

$$-\min\{(1-x)(1-y),xy\}< \xi <\min\{(1-x)y,x(1-y)\}, \qquad (5\text{-}13)$$

since $X_{pq}>0$. (Refer to Eq.(5-2)) For ternary alloys and binary compounds, there is no freedom in the statistics of bonds. Thus, ξ_o=0 at the sides of each rectangle.

5-2-4. Interpretation of the Results

The following features are commonly observed from the results for all quaternary alloy systems: ω_b is negative, and H_s increases

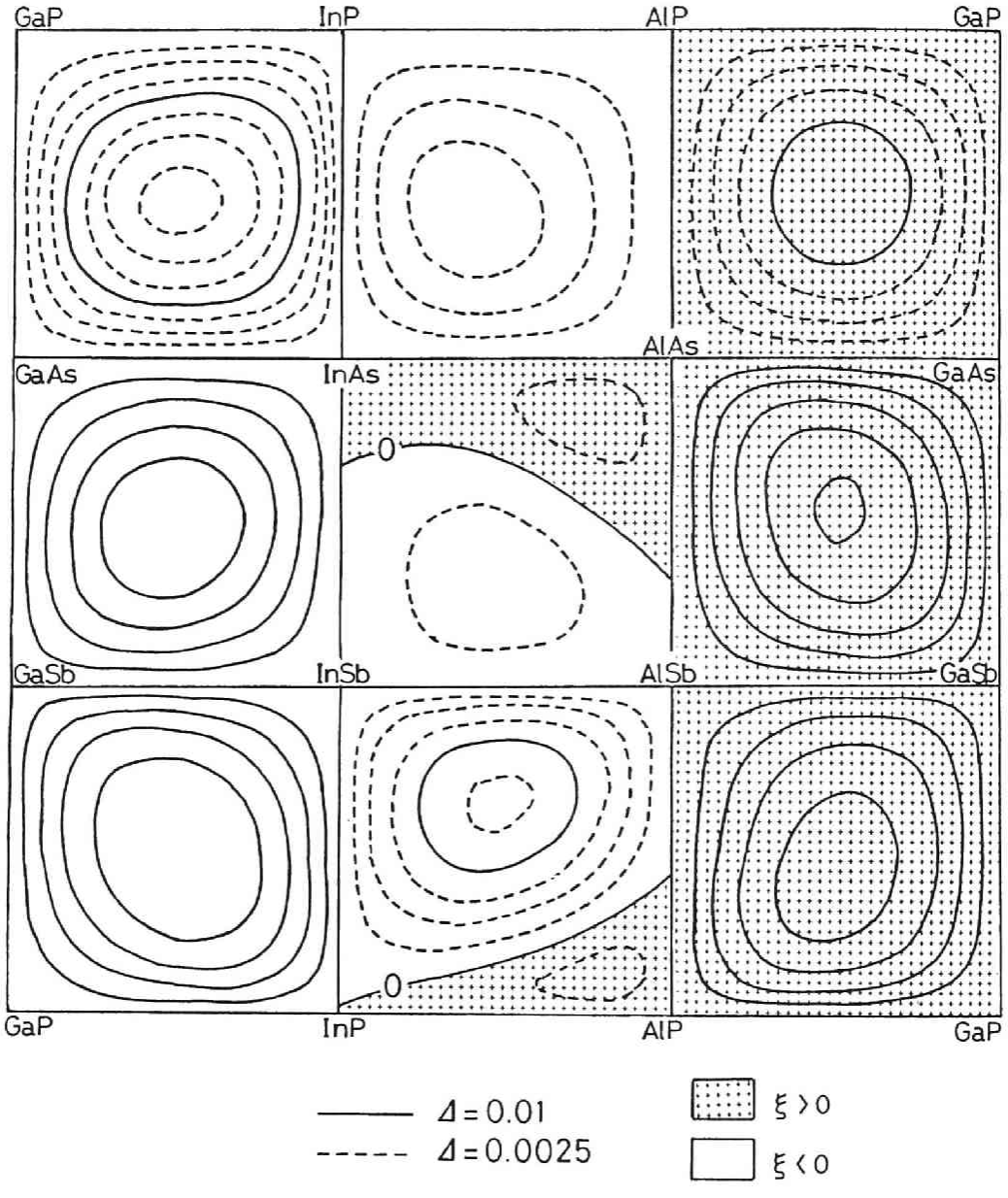

Fig.5-6 Composition dependence of the equilibrium value of ξ for nine quaternary alloy systems at T=1000 K. ξ=0 at sides of each rectangle. Δ is difference in ξ between two contour lines.

with ξ except for $Ga_{1-x}Al_xC^V_{1-y}D^V_y$ systems where H_s weakly depends on ξ. This is not accidental but can be interpreted as follows.

Consider the covalent radius r_p for each atom. The p-q bond length d_{pq} is approximately given by r_p+r_q (or the covalent radii are defined so that $r_p+r_q=d_{pq}$). If it is assumed that $r_A>r_B$ and $r_C>r_D$ for $A^{III}_{1-x}B^{III}_xC^V_{1-y}D^V_y$ system, then,

$$(r_A+r_C)-(r_B+r_D) > |(r_A+r_D)-(r_B+r_C)| . \qquad (5\text{-}14)$$

According to the consideration in Subsec. 5-2-1, H_s becomes large with the increase in the numbers of A-C and B-D bonds, because the pair of A-C and B-D strain each other more largely than A-D and B-C pair. Since the heavier atom usually has larger covalent radius and is assigned to A(C), the relations $r_A>r_B$, $r_C>r_D$ are satisfied except $Ga_{1-x}Al_xC^V_{1-y}D^V_y$ systems. Thus, H_s increases with more A-C and B-D bonds, i.e., with positive ξ for $In_{1-x}Ga_xC^V_{1-y}D^V_y$ and $In_{1-x}Al_xC^V_{1-y}D^V_y$ systems. We have $r_{Al}\simeq r_{Ga}$ for $Ga_{1-x}Al_xC^V_{1-y}D^V_y$, since $d_{AlC^V}\simeq d_{GaC^V}$ and thus

$$\begin{aligned}
&|(r_{Ga}+r_C)-(r_{Al}+r_D)|-|(r_{Ga}+r_D)-(r_{Al}+r_C)| \\
&=(r_{Ga}+r_C-r_{Al}-r_D)-(r_{Al}+r_C-r_{Ga}-r_D) \\
&=2(r_{Ga}-r_{Al}) \\
&\simeq 0 . \qquad (5\text{-}15)
\end{aligned}$$

Therefore, H_s depends weakly on ξ for $Ga_{1-x}Al_xC^V_{1-y}D^V_y$ system.

The sign of ω_b can also be understood by considering covalent radii. The negative ω_b indicates that the sum of cohesive energy of A-C and B-D bonds is larger than that of A-D and B-C bonds. The cohesive energy of the covalent crystal is considered to be approximately proportional to $d^{-2.5}$,[6] and under the conditions of $r_A>r_B$ and $r_C>r_D$, the following relation is satisfied:

$$(r_A+r_C)^{-2.5}+(r_B+r_D)^{-2.5} > (r_A+r_D)^{-2.5}+(r_B+r_C)^{-2.5}. \qquad (5\text{-}16)$$

This indicates that the sum of the cohesive energy of A-C and B-D bonds is larger than that of A-D and B-C bonds, i.e., $\omega_b<0$, under the above conditions. As mentioned earlier, these conditions are satisfied for all quaternary alloys except for $Ga_{1-x}Al_xC^V_{1-y}D^V_y$. For AlC^V compounds, the cohesive energy is larger than that expected from the $d^{-2.5}$ dependence; for example, although the bond lengths of AlAs and GaAs are almost the same, the melting point of AlAs is significantly higher than that of GaAs, which implies that the cohesive energy of Al-As is larger than that of Ga-As. Thus, one should regard d_{AlC^V} and thus r_{Al} as smaller than the crystallographic one when the $d^{-2.5}$ dependence of cohesive energy is assumed. Such effective bond length was found to be useful to predict some electronic properties of AlC^V, although its physical basis is not clear.[7] Then, as concerns the cohesive energy, we can expect that Eq. (5-16) is satisfied for all quaternary alloy systems discussed here. Thus ω_b is negative for all quaternary alloy systems.

As described in the last section, the qualitative features of the results depend on species of the group III elements. This is ascribed to the fact that the cohesive energy of $Al\text{-}C^V$ bond is larger than that expected from its crystallographic length: the effect of $\omega_b\xi$ becomes relatively large as compared with that of H_s when the alloy includes Al.

For binary or ternary $A_{1-x}B_xC$ alloy, the atom arrangement is described in term of order (preference for unlike neighbor pair) or cluster (preference for like neighbor pair). However, it is difficult to relate the value of ξ to order or cluster in quaternary alloys. For example, if ξ becomes positive, i.e., A-C bond increases, then the triplet A-C-A increases, but A-D-A decreases because of the decrease of A-D bond. Then, in general, one cannot conclude whether the like pair A-A increases or not. Rather, ξ is the measure for the uniformity in an alloy. If A-C and B-D

bonds increase, the region including both A and C atoms more than the average composition increases, and the region with more B and D atoms also increases. Thus, there would be two types of regions with different compositions in the alloy, i.e., the alloy would become nonuniform. The alloy is the most uniform at $\xi=0$, and the value of $|\xi_o|$ represents the degree of nonuniformity.

At $x=0.5$ and $y=0.5$, like pairs necessarily increase, i.e., clustering occurs with the increase of $|\xi|$, because $(0.25+\xi)^2+(0.25-\xi)^2 = 0.25+2\xi^2$, where the two terms in the left-hand side are the probabilities of appearance of two different triplets including the same like-pair, such as A-C-A and A-D-A. The increase in H_s at nonzero ξ in $Ga_{1-x}Al_xC^V_{1-y}D^V_y$ is due to the cluster; the strain energy tends to increase by the clustering as discussed in the previous chapters.

5-3. BOND LENGTHS

5-3-1. Bond Lengths in Unit Cells

The results given in this subsection are obtained on the basis of the assumption that an alloy is composed of a single type of unit cell such as shown in Fig. 5-2. This is not a realistic approach since an actual quaternary alloy is composed of various types of unit cells. In addition, the calculation is limited to an alloy with certain compositions, i.e., multiples of 0.25. However, the results give a basis for understanding how the lattice is relaxed in quaternary alloys of (AB)(CD) type. Here, the results for $In_{1-x}Ga_xAs_{1-y}P_y$ are given as an example, but they can be generalized for other quaternary alloys. The results for average bond lengths are given in the next subsection.

A. Equilibrium position of atoms

The equilibrium positions of atoms are determined by varying

all of the nearest- and second-nearest-neighbour distances and minimizing the strain energy of the unit cell. For all ternary alloys, the mixed sublattice, e.g., the sublattice for In and Ga in $In_{1-x}Ga_xAs$ is found to be an undistorted virtual crystal fcc lattice even after the minimization of the total strain energy. Figure 5-7 illustrates how different the relaxation of the mixed sublattice is from that of the common element sublattice, taking an $In_{0.5}Ga_{0.5}As$ as the example. In this alloy, an In atom or a Ga atom is surrounded by 4 identical atoms, i.e., 4 As atoms, whereas As atoms are surrounded by two kinds of atoms, e.g., 2 In atoms and 2 Ga atoms. Thus, the configuration around In or Ga atom is symmetric, whereas that around As atoms is asymmetric. This asymmetry causes As atom to move from the VCA lattice site. In a random alloy, this distortion of the As lattice breaks the symmetry around In and Ga atoms. However, such effect is of the second order and the distortion of the cation sublattice is expected to be small. In the approach based on the single unit cell model, the periodicity of the atom arrangement is assumed. Because of this assumed periodicity, a Ga atom or an In atom remains just at the center position among 4 As atoms.

These theoretical results qualitatively explain the EXAFS re-

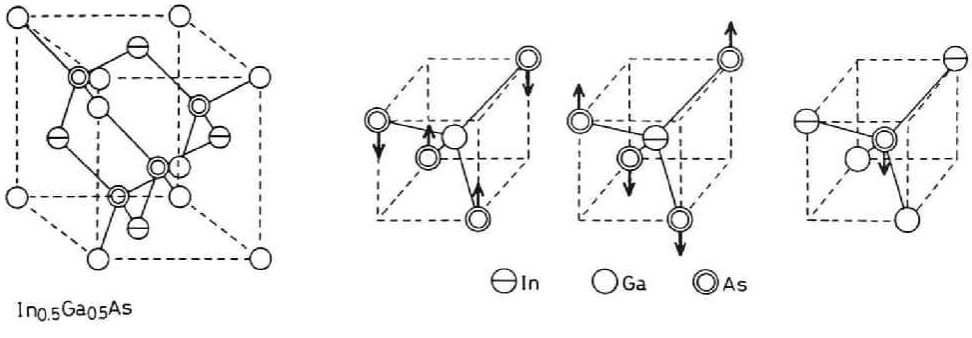

Fig.5-7 The displacement of As atoms in $In_{0.5}Ga_{0.5}As$ unit cell. The arrow schematically indicate the direction of this displacement. The symmetry is preserved around In and Ga atoms.

sults for $In_{1-x}Ga_xAs$ that the cation sublattice remains relatively undistorted compared with the anion sublattice[8] and support the validity of the assmption used for ternary alloys in Chap. III.

In an $In_{1-x}Ga_xAs_{1-y}P_y$ quaternary alloy, both sublattices obtained by the calculation are distorted from fcc lattice. It is because atoms of both sublattices are surrounded by two different kinds of atoms in quaternary alloys of (AB)(CD) type.

B. Bond length

Figure 5-8 shows the contour lines of bond lengths for four bonds in $In_{1-x}Ga_xAs_{1-y}P_y$ alloy. For the composition to which this approach may not be applied, the value of bond lengths are obtained by linear inter- or extra-polation. Although the shape of contour line would somewhat depend on the method of inter- and

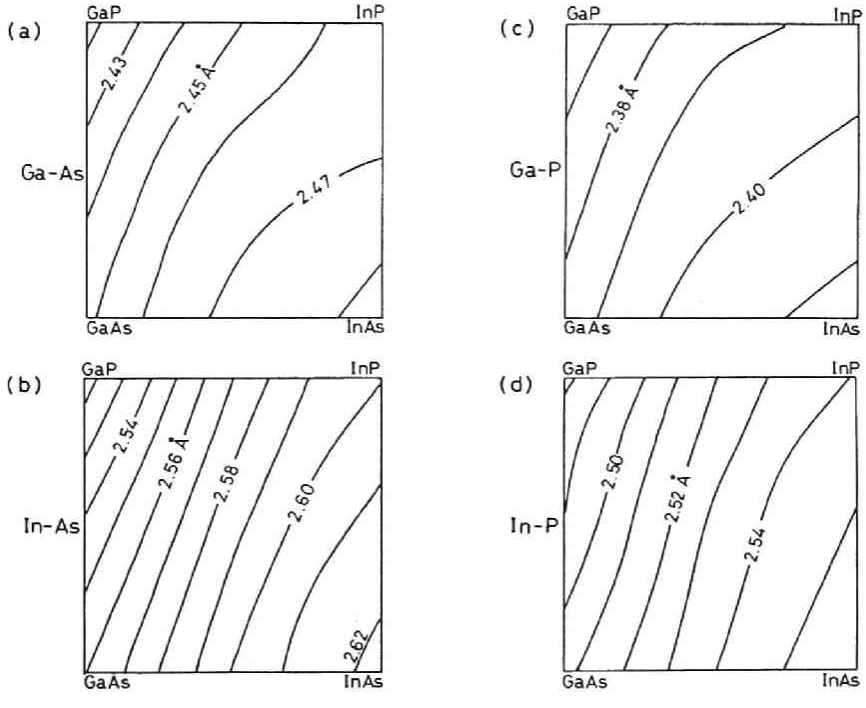

Fig.5-8 Contour charts of bond lengths calculated by the single unit cell model for $In_{1-x}Ga_xAs_{1-y}P_y$ alloy. a): Ga-As, b): In-As, c): Ga-P, d): In-P. The numerical values indicate bond lengths in Å.

extra-polation, the results would be good enough for qualitative discussion. The total average bond length or VCA bond length is shown in Fig. 5-9. As seen from these figures, some qualitative features can be summarized in the following:

i) The change in bond length is the largest in In-As bond and the smallest in Ga-P bond.

ii) For all of four bonds, the spacing between contour lines becomes narrow where Ga composition is large, and thus bond length distortion increases on an average as Ga composition increases.

iii) The contour lines in Fig. 5-8 are nearly parallel to those in Fig. 5-9, and thus the length of each bond barely depends on the composition, if the lattice constant or the average bond length is constant.

These features are similar to those obtained for (ABC)D type quaternary alloys and can be interpreted similarly. Feature i) is due to the difference in α. The Ga-P bond has the largest α among the four bonds and thus its distortion results in large strain energy, whereas In-As bond is the weakest and easy to distort. Feature ii) is attributed to the fact that Ga-based compounds have large β than In-based compounds; as Ga composition increases, the average β increases and therefore a bond-angle distortion is accompanied with more strain energy. Thus, in Ga-rich alloy, the strain energy becomes minimum at the state with more

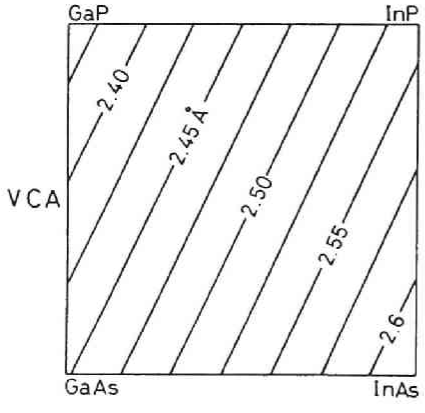

Fig.5-9 Contour chart of the VCA bond length in $In_{1-x}Ga_xAs_{1-y}P_y$. The Vegard law is assumed. The numerical values indicate bond lengths in Å.

Table 5-I. Comparison of the calculated values of the bond lengths in $In_{1-x}Ga_xAs_{1-y}P_y$ alloys with the experimental values obtained by EXAFS measurement.[9] The calculation is based on the single unit cell model. Bond lengths are given in Å.

COMPOSITION		Ga-As	In-As	Ga-P	In-P
x=0.47,y=0,	exp.	2.47	2.60	——	——
x=0.5, y=0	cal.	2.473	2.601	——	——
x=0.26,y=0.42	exp.	2.47	2.59	2.40	
x=0.25,y=0.5	cal.	2.468	2.604	2.400	2.543

bond length distortion and less bond angle distortion than in In-rich alloy. Feature iii) indicates that each bond length depends on the average properties of the lattice surrounding the bond.

Theoretical results are listed in Table 5-I for a comparison with EXAFS experimental data.[9] The experimental results are accidentally available for the crystal with composition close to those of unit cells. The theoretical results agree with them very well.

5-3-2. Average Bond Lengths

A. ξ-dependence

The average bond lengths, $\bar{d}_{pq}$'s, are calculated by the equation:

$$\bar{d}_{pq} = \frac{1}{X_{pq}} \sum P_{pq}(i,k,\xi)\, d_{pq}(i,k) \quad . \qquad (5\text{-}17)$$

As can be seen from this equation, each average bond length depends on ξ and atomic composition. Figures 5-10 show the average bond lengths as functions of ξ for $In_{1-x}Ga_xAs_{1-y}P_y$ at T=1000 K. At the composition x=0.5, y=0.5 (Fig.5-10 (a)), In-P and Ga-P bond lengths increase with ξ, whereas In-As and Ga-As lengths decrease. First these ξ-dependences are interpreted taking Ga-As bond as the

example. As mentioned earlier, the bond strain is influenced by what bonds are its neighbours. With a change in ξ, two kinds of replacements of bonds occur in the nearest-neighbourhood of a Ga-As bond, one around the Ga atom, and the other around the As atom. The probabilities of finding As and P atoms at the nearest neighbour site of Ga are X_{GaAs}/x and X_{GaP}/x, respectively; by using ξ, they are expressed by $\{x(1-y)-\xi\}/x$ and $\{xy+\xi\}/x$. If ξ increases by $\Delta\xi$, a certain portion ($\Delta\xi/0.5$) of As atoms are replaced by P atoms around Ga atoms, i.e., Ga-As bonds are replaced by Ga-P bonds. Similarly, $\Delta\xi/0.5$ of Ga-As bonds are replaced by In-As bonds around As atoms. The probabilities of these two replacements are equal, i.e., $\Delta\xi/0.5$. However, the replacement from Ga-As to In-As has larger influence than that from Ga-As to Ga-P; Ga-P is shorter than Ga-As by 0.088Å, while In-As is longer than Ga-As by 0.175Å. Thus, a Ga-As bond tends to be surrounded

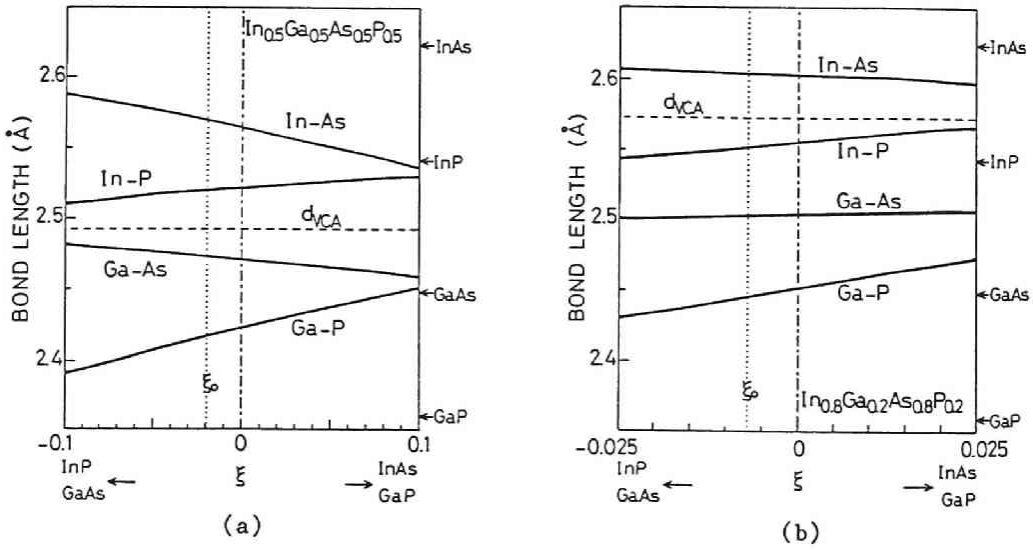

Fig.5-10 Average bond lengths (bold lines) as functions of ξ for (a) $In_{0.5}Ga_{0.5}As_{0.5}P_{0.5}$ and (b) $In_{0.8}Ga_{0.2}As_{0.8}P_{0.2}$. The VCA bond length is represented by a broken line. Arrows at the right side indicate bond lengths of binary compound. Equilibrium value of ξ at T=1000K is indicated by a vertical dotted line.

by longer bond with the increase in ξ. Then, a Ga-As bond becomes shorter on the average so that the volume of the tetrahedra including it remains matched to the average value of the surrounding crystal.

Next, we turn to In-As bond. With the increase in ξ, In-P bonds around In and Ga-As bonds around As are replaced both by In-As bonds in the nearest-neighbourhood of an In-As bond. By these replacements, the lengths of bonds surrounding the In-As bond increase on the average. Then, for matching to the average volume, the average In-As bond length decreases. The ξ-dependences of In-P and Ga-P lengths are interpreted similarly to those of Ga-As and In-As lengths, respectively.

The results at the composition x=0.2, y=0.2 are shown in Fig. 5-10 (b). Here, Ga-As bond length increases with ξ, in contrast to Fig. 5-10 (a). This is because around a Ga-As bond the replacement from Ga-As to Ga-P occurs four times as frequently as that from Ga-As to In-As with increase in ξ: the probability of the former replacement is $\Delta\xi/0.2$ whereas that of the latter is $\Delta\xi/0.8$. Then, a Ga-As bond tends to be surrounded by shorter bond with increase in ξ, and thus its average length becomes longer. The ξ-dependeces of other bond lengths are similar to those shown in Fig.5-10 (a) and can be interpreted similarly.

The total average bond length or the bond length of VCA, d_{VCA}, is shown by a broken line in Fig. 5-10. The bond lengths of the binary compounds or unstrained lengths d_{pq}^{0}'s are also indicated by arrows at the right side of the figure. The difference between d_{pq}^{0} and average bond length, $\bar{d}_{pq}$, corresponds to the average length deviation. For the example of x, y=0.5 (Fig. 5-10 (a)), the length deviation is large for In-As and Ga-P bonds, while it is relatively small for Ga-As and In-P bonds. This tendency can be easily interpreted from the fact that the difference between d_{VCA} and unstrained length is large for In-As and Ga-P, while small for Ga-As and In-P. A bond with large length

deviation has large strain energy. Thus, as shown in Fig. 5-3, the strain energy increases with the increase in ξ, i.e., with the increase of In-As and Ga-P bonds.

B. Composition dependence

The contours of the average bond lengths are shown in Fig. 5-11. The bond lengths represented by solid lines are calculated from the values of ξ_o obtained at T=1000K. The results are very similar to those given in the last subsection, and the discussions given there hold for the average bond lengths, too. However, the length deviations obtained here are larger than the previous results. In the last subsection, only the least distorted unit

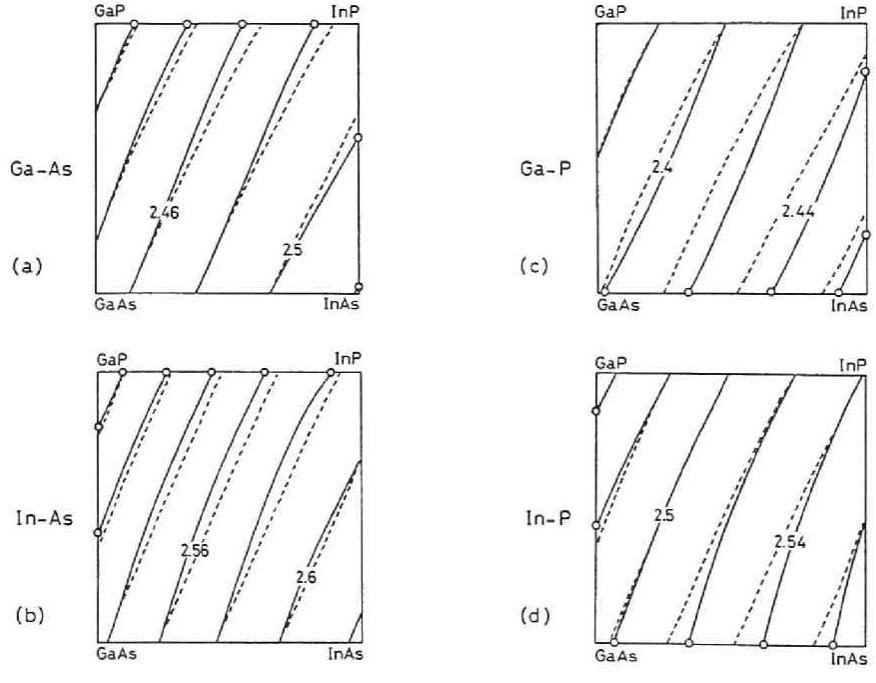

Fig.5-11 Contour charts of the average bond lengths for an $In_{1-x}Ga_xAs_{1-x}P_x$ alloy. a):Ga-As, b):In-As, c):Ga-P, d):In-P. The numerical values indicate bond lengths in Å. The bond lengths represented by solid lines are calculated from the equilibrium values of ξ while those represented by dashed lines by assuming ξ=0.

Table 5-II. Comparison of the calculated average bond lengths with the results of EXAFS measurements for $In_{1-x}Ga_xAs_{1-y}P_y$. The EXAFS data are from Ref.9. Bond lengths are given in A.

x , y	Ga-As exp.	Ga-As cal.	In-As exp.	In-As cal.	Ga-P exp.	Ga-P cal.	In-P cal.
0.47, 0	2.47	2.494	2.60	2.587			
0.40, 0.11	2.47	2.492	2.60	2.590	-	2.433	- 2.537
0.26, 0.42	2.47	2.491	2.59	2.592	2.40	2.433	- 2.540

cell among 25 cells is considered, e.g., In(3)Ga(1)As(2)P(2) cell for $In_{0.75}Ga_{0.25}As_{0.5}P_{0.5}$. In the present model, other cells, which are more largely strained, are included, and thus the bond length deviations become larger on the average.

The average bond lengths at $\xi=0$ are shown by broken lines in Fig. 5-11. As seen from Fig. 5-6 , $\xi_o<0$ for $In_{1-x}Ga_xAs_{1-y}P_y$ system. For Ga-P and In-As bonds, length deviation is smaller at $\xi=\xi_o$ than at $\xi=0$, i.e., both bond lengths approach to those in the respective binary compounds. This is because at any composition Ga-P becomes shorter and In-As becomes longer as ξ decreases, as shown in Fig. 5-10 for examples. On the other hand, Ga-As length decreases in the composition region of $x_{Ga}<x_{As}/2$ while increases when $x_{Ga}>x_{As}/2$ as compared with the case of $\xi=0$. We have already interpreted the fact that the sign of $\partial\bar{d}_{GaAs}/\partial\xi$ changes depending on composition by comparing Fig. 5-10 (a) and (b). $(\partial\bar{d}_{InP}/\partial\xi)\times\xi_o$ is negative when $x_{In}>x_P/2$ and positive when $x_{In}<x_P/2$.

C. Comparison with the EXAFS data

Table 5-II lists the results of the EXAFS measurements[9] with the calculated average bond lengths at the same compositions. The agreement between them is fairly good, but the calculated lengths tend to deviate from those in the corresponding binary compounds further than the experimental ones do. This discrepan-

cy would be mainly due to the assumption used here. Some error could not be avoided in the EXAFS measurements and data analyses.

5-4. DISCUSSIONS

The statistics of bonds could be experimentally determined from the lattice vibration spectra. For some alloys, there appear several phonon modes corresponding to bonds; for example, In-As, Ga-As, In-P, and Ga-P like phonon modes appear within a certain composition range for $In_{1-x}Ga_xAs_{1-y}P_y$, and the intensity of the signal of each mode is considered to represent the number of the oscillator, i.e., the corresponding bond. It have been reported that results of infrared reflectivity measurements on $In_{1-x}Ga_xAs_{1-y}P_y$ can be explained well by assuming $x_{pq}=x_px_q$, i.e., $\xi_o=0$.[10] This would be consistent with the results that ξ_o is close to zero for $In_{1-x}Ga_xAs_{1-y}P_y$. However, the accuracy of such experimental approach would not be good enough to estimate a small deviation from $\xi=0$. It seems that the experimental technique for determining the statistics of bonds is yet to be developed.

The pairwise interaction model (PIM) has been used for discussion about the atom arrangement of quaternary alloys and gives very different results from the present ones.[1] For example, according to PIM, enthalpy due to the second-nearest interaction decreases with ξ for $In_{1-x}Ga_xAs_{1-y}P_y$, and consequently ξ_o is relatively a large positive value. However, PIM seems inappropriate for III-V alloys since it neglects the strain energy, as discussed in Chap. II.

In the model proposed here, a bond is chosen as a basic figure of the thermodynamic analysis, and thus the correlation among atoms is considered only to the lowest order: single variable ξ is not enough to describe the atom arrangement of quaternary alloys. For example, the probability of the appearance of a tetrahedron in fact cannot be uniquely determined from the relative numbers of

bonds but should be treated as another independent variable; in deriving Eq.(5-10), it is assumed that there is no excess correlation among bonds. Equation (5-10) is reduced to a simple binomial distribution for tetrahedra in ternary alloys. (This does not mean that the arrangement of bond is completely random: the unphysical situations, such as A-D bond sharing an atom with B-C bond, are excluded in deriving the entropy.[1]) For a more accurate analysis, one need choose a tetrahedron as a basic figure, since the short-range order on a sublattice influeces the strain energy. However, this effect is rather small; for example, the decrease of the strain energy due to the short-range order is about 10 % for $In_{1-x}Ga_xAs$ at T=1000 K, as shown in Fig. 3-8. Thus, the qualitative features of the results given here will not be affected by neglect of the short-range order.

In calculating the strain of a bond within a certain atomic configuration, it is assumed that the strain depends on the nearest bonds, i.e., types of tetrahedra. However, the second or further bonds would also influence the bond strain. If the further bonds are included in the analysis, there appear the following differences in the results. i) In the present model, there are 16 distinct environments for each kind of bond in an alloy. If the further bonds are included, a greater number of distinct environments are possible and thus the number of different lengths becomes much more than 16 even for a single kind of bond. ii) The lattice relaxation of longer range can be taken into account. Then, in general, bonds tend to relax further, and $\bar{d}_{pq}$ will get closer to d^0_{pq}. It would result in a better agreement between the calculated and the experimental results.

5-5. SUMMARY

The relative numbers of bonds in III-V quaternary alloys of (AB)(CD) type have been derived by the thermodynamic analysis.

In calculating the strain energy, a given type of bond is considered to have 16 different amounts of strain, one for each distinct configuration of the surrounding bonds. The results are summarized as follows:

i) In $In_{1-x}Ga_xAs_{1-y}P_y$, Ga-As and In-P bonds slightly increase from the value of completely random atom arrangement to reduce the strain energy, although the sum of cohesive energy of Ga-P and In-As is larger than that of Ga-As and In-P. The same tendency is commonly observed for other $In_{1-x}Ga_xC^V_{1-y}D^V_y$ systems: when the heavier group V atom is assigned to C^V, $In\text{-}D^V$ and $Ga\text{-}C^V$ bonds increase compared with the random arrangement case.

ii) For $Ga_{1-x}Al_xC^V_{1-y}D^V_y$, the effect of the cohesive energy is predominant: $Ga\text{-}C^V$ and $Al\text{-}D^V$ bonds increase.

iii) The effects of both energies compensate each other almost completely for $In_{1-x}Al_xC^V_{1-y}D^V_y$ systems, and thus the bond statistics are nearly equal to those of the random arrangement case.

iv) On the basis of the above results, the average bond lengths in $In_{1-x}Ga_xAs_{1-y}P_y$ have been obtained, and their dependences on the bond statistics and composition have been discussed. The calculated average bond lengths agree fairly well with the EXAFS data.

REFERENCES

1) K. Onabe, J. Phys. Chem. Solids, 43 (1982) 1071.

2) H. Sonomura, H. Horinaka, and T. Miyauchi, Jpn. J. Appl. Phys., 22 (1983) L689.

3) T. Onda and R. Ito, Jpn. J. Appl. Phys., 26 (1987) 1241.

4) H. Sonomura, J. Appl. Phys., 59 (1986) 739.

5) K. Onabe, Jpn. J. Appl. Phys., 21 (1982) L323.

6) G. B. Stringfellow, J. Cryst. Growth, 27 (1974) 21.

7) S. Gonda, Solid-St. Commun., 60 (1986) 249.

8) J. C. Mikkelsen, Jr. and J. B. Boyce, Phys. Rev. B 28 (1983) 7130.

9) H. Oyanagi, Y. Takeda, T. Matsushita, T. Ishiguro, and A. Sasaki, Inst. Phys. Conf. Ser. No. 79, Proc. Int. Symp. GaAs and Related Compounds, 1985 (Adam Hilger, 1986), p.295.

10) C. Pickering, J. Electron. Mater., 10 (1981) 901.

VI. ATOM ARRANGEMENT AND MATERIAL PROPERTIES

6-1. INTRODUCTION

The atom arrangement affects various aspects of material properties. In this chapter, the following four subjects are discussed mainly in terms of relation with tendency in atom arrangement.

i) Stability of superstructures of ternary alloy systems.
ii) Alloy scattering of carriers in ternary alloys.
iii) Mechanical properties: solution hardening in ternary alloys.
iv) Lattice constant and band gap of quaternary alloys of (AB)(CD) type.

6-2. STABILITY OF ULTRATHIN SUPERLATTICES OF TERNARY ALLOY SYSTEMS

Properties of ultrathin superstructures (or superlattices) of III-V semiconductors are extensively investigated since they are free from various phenomena inherent in alloys, e.g., alloy scattering.[1,2] Owing to recent development of crystal growth technology, mono- and bi-layer superstructures become possible to grow.[3,4] However, if structural stability of a superstructure is far more inferior to that of a bulk or a single-layered alloy, a superlattice seems not to be suitable to device applications.

In the analysis, the free energies are derived for mono- and bi-layer superstructures of III-V ternary alloy systems of average composition $x=0.5$ as the function of order parameter or structural completeness. If the free energy is minimum at a certain degree of ordering, a partially ordered structure is stable and will not collapse further. Otherwise, it will collapse to a random atom arrangement. Thus, the derivation of free energy gives what orderings of atoms are stable in superstructures.

6-2-1. Equation for Free Energy of Superstructures

Two kinds of sites can be settled in the mixed sublattice of an alloy with long-range order as shown in Fig. 6-1. A and B atoms occupy α and β sites, respectively, in a completely ordered structure. For specifying the degree of ordering or completeness, the Bragg-Williams order parameter φ is employed; it is defined by

$$\varphi = 2r - 1 \quad , \tag{6-1}$$

where r is the probability of an α site occupied by an A atom which is equal to the probability of a β site occupied by a B atom.[5] φ=0 for a random alloy where r=0.5, whereas φ=1 for a completely ordered structure where r=1.

With the use of the Bragg-Williams approximation,[6] the entropy is expressed as

$$S = -\frac{Nk_B}{2}\left[(1+\varphi)\ln\left\{\frac{1+\varphi}{2}\right\}+(1-\varphi)\ln\left\{\frac{1-\varphi}{2}\right\}\right] \quad . \tag{6-2}$$

Enthalpy is calculated by the same approach as described in Chap. III, i.e., the strain energy is calculated for each type of tetrahedron, and the mixing enthalpy is obtained by summing up the energy for all tetrahedra. The strain energies of tetrahedra, ε_i's are shown in Fig. 3-2 and 3-3, and the values at x=0.5 are used in the analysis for the superstructure of average composition x=0.5. At composition x=0.5, $\varepsilon_2 < \varepsilon_1 \simeq \varepsilon_3 < \varepsilon_0, \varepsilon_4$, as can be seen in the figures.

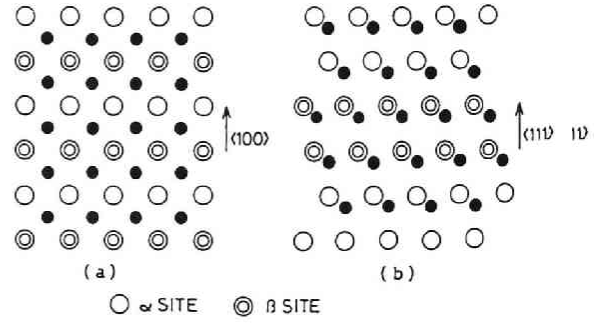

Fig.6-1 Atom sites a) in monolayer superstructure on (100) surface and b) in bilayer superstructure on (111) surface. The dark circle denotes the common element atom.

6-2-2. Free Energy and Equilibrium State

A. Monolayer superstructure

i) On (100) surface

In this structure, as shown in Fig. 6-2, two α sites and two β sites constitute a tetrahedron. From the definition of r given in the last subsection, the probabilities of an α site occupation by an A atom and by B atom are r and 1-r, respectively, and vice versa for a β site. Then, the relative numbers of cells, n_i's are expressed by using r as follows:

$$n_0 = n_4 = r^2(1-r)^2 \quad ,$$

$$n_1 = n_3 = 2r^3(1-r) + 2r(1-r)^3 \quad ,$$

$$n_2 = r^4 + 4r^2(1-r)^2 + (1-r)^4 \quad . \qquad (6\text{-}3)$$

From these and Eq. (6-1), n_i's are easily calculated as functions of φ.

The mixing free energy for the monolayer superlattice can be obtained by using Eqs. (6-1)~(6-3). It is

$$F_m = \frac{N}{16}\left[(\varepsilon_0+\varepsilon_4)(\varphi^4-2\varphi^2+1)+4(\varepsilon_1+\varepsilon_3)(-\varphi^4+1)+2\varepsilon_2(3\varphi^4+2\varphi^2+3)\right] - TS \qquad (6\text{-}4)$$

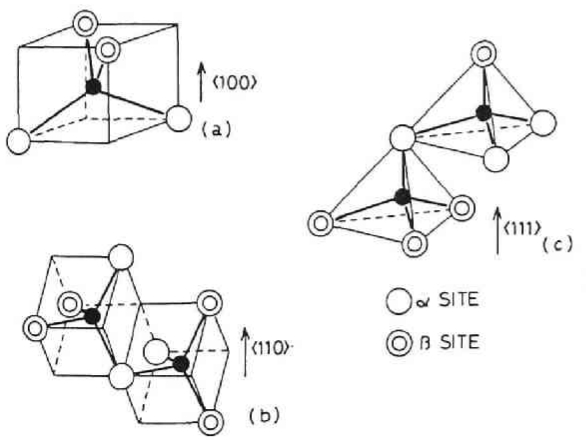

Fig.6-2 Tetrahedrons (groups of sites) in monolayer supersructures on a) (100), b) (110), and c) (111) surface.

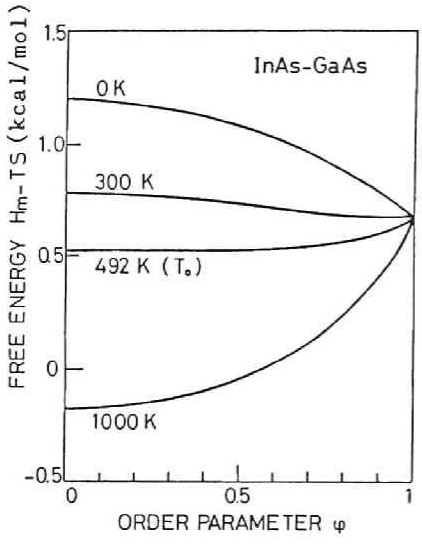

Fig.6-3 Mixing free energy of monolayer superstructure of (InGa)As system as a function of φ.

Table 6-I Upper limit temperature below which a partially ordered structure could be stable.

SYSTEM	T_o(K)
AlAs-GaAs	0.15
AlSb-GaSb	4.0
InP-GaP	627
InAs-GaAs	492
GaAs-GaP	139
InAs-InP	116
GaSb-GaAs	559
GaSb-GaP	1283

Figure 6-3 shows F_m as a function of φ at some temperatures. The equilibrium state of the atom arrangement is obtained by minimizing the free energy. Its value of φ, φ_0 is given by $\partial F/\partial\varphi=0$:

$$\varepsilon''\varphi_0^3 - \varepsilon'\varphi_0 + 2k_BT\ln\left\{\frac{1+\varphi_0}{1-\varphi_0}\right\} = 0 \quad , \tag{6-5}$$

$$\varepsilon'' = \varepsilon_0 + \varepsilon_4 - 4\varepsilon_1 - 4\varepsilon_3 + 6\varepsilon_2 \quad ,$$

$$\varepsilon' = \varepsilon_0 + \varepsilon_4 - 2\varepsilon_2 \quad .$$

From the results of Chap. III, $\varepsilon'>>\varepsilon''>0$. Equation (6-5) has nonzero value of solution when temperature is lower than T_o given by

$$T_o = \frac{\varepsilon_0 + \varepsilon_4 - 2\varepsilon_2}{4k_B} \quad . \tag{6-6}$$

The values of T_o for several ternary alloy systems are listed in Table 6-I. The dependence of φ on T/T_o for $In_{1-x}Ga_xAs$ is shown in Fig. 6-4. This dependency is not much different among materi-

als.

ii) On (110) surface

As shown in Fig. 6-2(b), 2 α sites and 2 β sites constitute a tetrahedron, which is the same as on (100) surface. Thus the expression of F_m and the equilibrium value of φ are the same as on (100) surface.

iii) On (111) surface

In this structure, the half of a whole number of tetrahedron cells are composed of 3 α sites and 1 β site, and the other half are composed of 1 α site and 3 β sites. Accounting a possible occupation by atom A and B in the tetrahedron as in the case of (100) surface, we obtain the free energy of the superstructure on (111) surface. The free energy is

$$F_m = \frac{N}{16}\left[(\varepsilon_0+\varepsilon_4)(-\varphi^4+1)+4(\varepsilon_3+\varepsilon_1)(\varphi^4+1)+6\varepsilon_2(-\varphi^4+1)\right] - TS \quad , \quad (6\text{-}7)$$

and the condition $\partial F/\partial\varphi=0$ is given by

$$-\varepsilon''\varphi_0^3 + 2k_BT\ln\left\{\frac{1+\varphi_0}{1-\varphi_0}\right\} = 0 \quad . \quad (6\text{-}8)$$

Since $\varepsilon''>0$, the nonzero value of φ_0 can exist under a certain temperature. It occurs only at extremely low temperatures because

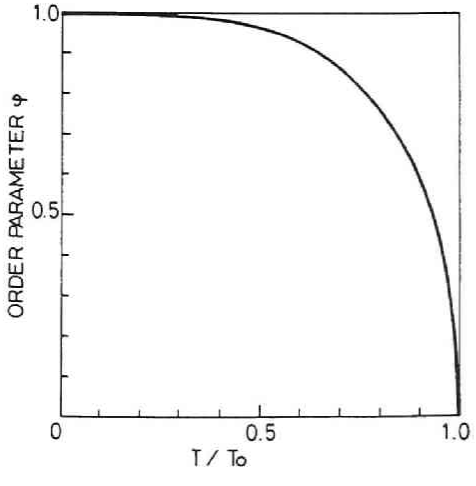

Fig.6-4 Equilibrium value of φ as a function of T/T_o for $In_{0.5}Ga_{0.5}As$ monolayer superstructure on (100) and (110) surface. This dependence of φ on T/T_o is almost the same for other materials. The T_o denotes the upper limit temperature listed in Table 6-I.

the values of ε'' are rather small. In addition, it can be easily proved that the value of F at $\varphi=0$ is always lower than the value at $\varphi>0$. Thus, on (111)-oriented surface, the completely disordered structure is always stabler than the monolayer superstructure of a certain degree of ordering.

B. Bilayer superstructure

The previous procedure can be applied for calculating the free energy of bilayer superstructures. For example, in a bilayer superstructure on (100) surface, the half of tetrahedron cells are composed of 2 α sites and 2 β sites and the other half are composed of 4 α sites or 4 β sites as shown in Fig. 6-5. From this configuration, one can calculate the probability of apperance, n_i. However, on (111) surface, the consecutive two α (β) site layers are not equivalent to each other. This corresponds to the difference between (111)A and (111)B surface. Here, it is assumed that the probabilities of finding atoms in these two layers are the same. This assumption is not necessary on (100) or (110) surface since such two layers are equivalent.

The free energies are written as follows:

$$F_m = \frac{N}{16}\left[(\varepsilon_0+\varepsilon_4)(\varphi^4+2\varphi^2+1)+4(\varepsilon_1+\varepsilon_3)(-\varphi^4+1)+2\varepsilon_4(3\varphi^4-2\varphi^2+3)\right] - TS \quad , \text{ for (100) surface.} \qquad (6\text{-}9)$$

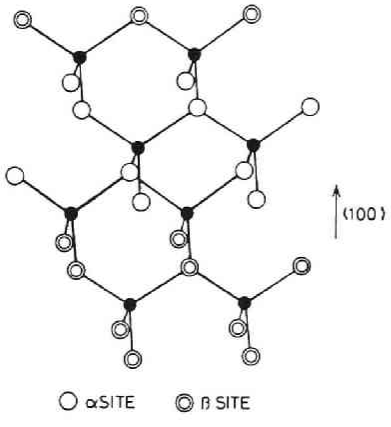

Fig.6-5 Tetrahedrons (group of sites) in bilayer superstructure on (100) surface.

Equation (6-7) , for (110) surface.

$$F_m = \frac{N}{16}[(\varepsilon_0+\varepsilon_4)(3\varphi^2+1)+4(\varepsilon_1+\varepsilon_3)+6\varepsilon_2(-\varphi^2+1)] - TS \quad ,$$

for (111) surface. (6-10)

All of these energies are minimum at $\varphi=0$ at any temperature. Thus, random arrangement is energetically preferable to bilayer superstructures.

6-2-3. Discussion

One result of the analysis is that the monolayer superstructures are energetically stabler than the bilayer structures. This result is attributed to the fact that tetrahedron cells other than type-2 cell increase in bilayer superstructures when ordering occurs. In a crystal of average composition $x=0.5$, the strain energy becomes minimum at the type-2 cell. The monolayer superstructure with a complete ordering on (100) surface is constructed with only type-2 cell. On the other hand, only the half of tetrahedron cells in a bilayer structure on (100) surface are type-2 cell, and the other half are type-0 or -4 cells, which have higher strain energy. Thus, a monolayer superstructure could have a lower enthalpy. The longer period superstructures (such as tri-, tetra-layers) are less stable because the numbers of type-0 and type-4 cells are increased.

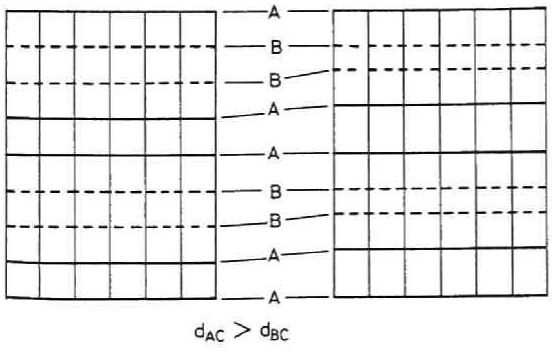

Fig.6-6 Lattice relaxation in a bilayer superstructure. It is assumed that the lattice constant of compound AC is larger than that of BC.

However, it should be considered that the lattices in long period superstructures could relax towards those of composite binary compounds, as shown in Fig. 6-6. The lattice relaxation appears along the growth direction, although the lattice along the direction parallel to the interface is bound to the average spacing. Taking the strain reduction due to such relaxation into account, the total strain energy is calculated for the bilayer superstructure of complete order. It results in higher strain energy than that of monolayer structure. Thus, the monolayer superstructure can be stabler than the bilayer superstructure, even though the relaxation is considered.

This result will be supported by the experiment by Fukui et al.[4] They reported that the monolayer superstructures of InAs and GaAs had better surface morphology and smaller linewidth of X-ray rocking curve than the bilayer superstructures.

Another result is that the superstructure on (100) or (110) surface is stabler than that on (111) surface. This dependence on surface orientation can be understood similarly, i.e., by counting the possible number of each cell. In the monolayer superstructure on (111) surface, there is no type-2 cell when the ordering is complete and therefore the superstructure is unstable.

It should be noted that a structure in which the free energy is not minimum can exist, because the atom arrangement cannot be altered at room temperature because of a small diffusivity of atom in a solid phase. It would take very long term for a crystal to approach the equilibrium state. Although the usual growth temperatures are higher than T_o's listed in Table 6-I for most of the alloy systems, the growth of superstructures with a higher free energy can be possible because of small diffusivity of atom.[3,4] One must take the diffusivity into account to discuss the stability of grown structures.

If an alloy of composition x=0.5 is grown below T_o, a monolayer superstructure tends to align with a certain degree of

ordering along <100> or <110>. However, the T_o is considerably lower than usual growth temperatures for most III-V ternary systems. Thus, the present analysis does not fully explain the unintentional formation of superstructures observed in some ternary alloys.[7-11] The energetical interaction other than strain might be responsible for the formation. However, the results of recent total energy calculations indicate that the monolayer structure of GaAs and AlAs is energetically unstable,[12,13] although its unintentional formation was observed.[8] Thus, kinetic factors, such as surface reactions, would be necessary to consider.[14]

6-3. ALLOY SCATTERING MOBILITY IN TERNARY ALLOYS WITH NONRANDOM ATOM ARRANGEMENT

Electrical properties of III-V alloy semiconductors, especially alloy scattering have been greatly investigated because of their importance to high speed devices.[15] However, in most of theoretical calculations of alloy scattering mobility, it has been assumed that atom arrangement is completely random. As discussed in the previous chapters, this assumption should be reconsidered: it is necessary to investigate the effects of order or cluster on alloy scattering. The aim of the analysis is to estimate alloy scattering mobility in III-V ternary alloys as a function of short-range order parameter.

6-3-1. Analytical Procedure

Multiple scatterings of electron would occur in alloys, but their influence is considered to be rather small on alloy scattering mobility in most III-V ternary alloys.[16] Thus, the theory developed by Asch and Hall is adopted, where multiple scatterings are neglected.[17] The square of the transition matrix element between the states $\psi(K)$ and $\psi(K')$ is given by[17]

$$|M(K,K')|^2=\sum_{\tau} \sigma(\tau)\ Nx(1-x)\exp(i\Delta K\cdot\tau)|m(K,K')|^2, \qquad (6\text{-}11)$$

$$m(K,K') = \int\psi(K)\ \Delta u(r)\ \psi(K')\ dr\ , \qquad (6\text{-}12)$$

where K and K' denote wave vectors and N is the number of atom on the mixed sublattice in the crystal of a unit volume, $\Delta u(r)$ the potential difference between an A atom and a B atom, i.e. the alloy scattering potential, and x the composition for B atom as in $A_{1-x}B_xC$. $\sigma(\tau)$ is the short-range order parameter defined by[18]

$$\sigma(\tau) = 1 - \frac{P_{AB}(\tau)}{x}\ , \qquad (6\text{-}13)$$

where $P_{AB}(\tau)$ is the probability that a B atom occupies the atom site with coordinate τ with respect to a given A atom. σ used in Chap. III is $\sigma(\tau)$ with τ corresponding to the second-nearest distance. In case of random arrangement, $\sigma(0)=1$ and $\sigma(\tau)=0$ $(\tau\neq 0)$. Because of the symmetry of the sublattice of zincblende structure, $\sigma(\tau)=\sigma(-\tau)$, and thus $\exp(i\Delta K\cdot\tau)$ can be replaced by $\cos(\Delta K\cdot\tau)$. According to Harrison and Hauser, Δu has been assumed to be constant within a volume v around an atom.[19] Then, $m(K,K')$ is independent of K and K', and can be written simply as $m=v\Delta u$. This is due to the fact that the product of lattice constant a and wave vector $|K|$ is much smaller than unity in direct band-gap semiconductors.[19]

In the following discussion, it is assumed that the degree of short-range order or cluster is low. Thus, $|\sigma(\tau)|$ decreases rapidly with increasing $|\tau|$ and becomes negligible for $|\tau|$ larger than several times of lattice constant. Then, the summation in Eq. (6-11) can be restricted within this range of τ. Since $|K|a<<1$, the relation $\Delta K\cdot\tau<<1$ and thus $\cos(\Delta K\cdot\tau)\simeq 1$ is satisfied for τ's concerned. Therefore, Eq. (6-11) becomes,

$$|M|^2 \simeq |M_0|^2 \sum \sigma(\tau)\ , \qquad (6\text{-}14)$$

where $|M_0|^2$ is the value of $|M|^2$ in case of random arrangement and written as $x(1-x)N(v\Delta u)^2$. The alloy scattering mobility μ is proportional to $1/|M|^2$, and thus $\mu=\mu_0/\{\sum\sigma(\tau)\}$ where μ_0 is the alloy scattering mobility for the random arrangement.

In the following discussion, the notation σ_i is used instead of $\sigma(\tau)$ for τ corresponding to the distance between the i-th nearest pair. Here, the order of neighbours is counted on the mixed sublattice. Thus, for example, 'the nearest neighbour' used here in fact corresponds to the second nearest neighbour in a zinc-blende structure. The value of σ_1 was obtained from the thermodynamic analysis given in Chap. III. However, for III-V alloys, any of the theories proposed so far cannot derive σ_i with i>1. Here, the approximate equation derived by Cowley is adopted:[18]

$$2\sum_j n_{ij}\sigma_j + k_B \frac{T}{V_1} \ln\left[\frac{\left\{ \frac{x}{1-x} +\sigma_i\right\}\left\{ \frac{1-x}{x} +\sigma_i\right\}}{(1-\sigma_i)^2} \right] = 0 , \qquad (6\text{-}15)$$

where k_B and T are the Boltzmann constant and temperature, respectively, n_{ij} the number of the j-th site among the 12 nearest neighbours of the i-th neighbour site, and V_1 the interaction potential between the nearest neighbour pair. Though in III-V ternary alloys there is no evidence that such pairwise interaction is dominant, this equation is used by considering V_1 as an effective potential which reproduces a given σ_1. Here, V_1 is not related to a specific physical quantity but it phenomenologically represents the strength of attractive or repulsive interaction among atoms.

As mentioned earlier, only a low degree of nonrandomness is considered: in calculating $\sigma(\tau)$, it is assumed that one can neglect σ_j with j greater than a certain integer, i_{max}. Then, Eq. (6-15) can be written for i=1 to i_{max}. By solving these simultaneous equations, we obtain the values of V_1/T, σ_2, $\sigma_3 \cdots \sigma_{i_{max}}$ for

a given σ_1. The choice of i_{max} could be justified by confirming that the value of $\sum\sigma(\tau)$ is little changed by increasing i_{max} further. Figure 6-7 shows the result of calculation of σ_i, where σ_i's with i up to 13 are considered. Figure 6-7(a) indicates the tendency of cluster , whereas (b) indicates that of order. If $|\sigma_1|<0.1$, 10 seems sufficient for i_{max}, because $\sum\sigma(\tau)$ for $i_{max}=10$ is little different from that for $i_{max}=13$.

6-3-2. Results and Discussions

Figure 6-8 shows the relation between the short-range order parameter σ_1 and $1/\{\sum\sigma(\tau)\}$ or μ/μ_0 obtained for $i_{max}=13$. At $x=0.5$, σ_1 can vary from -1/3 (complete order) to 1 (complete cluster), and thus the range of $-0.1<\sigma_1<0.2$ corresponds to rather low degree of order or cluster, to which this approach can be applied. The relation shown in Fig. 6-8 depends weakly on the composition within the composition range of $0.25<x<0.75$. However, as x approaches zero or unity, the lower limit of σ_1, σ_{min}, approaches zero:

$$\sigma_{min} = -\frac{x}{1-x} \qquad (0<x<0.25)$$

$$-\frac{1-x}{x} \qquad (0.75<x<1) \ . \qquad (6\text{-}16)$$

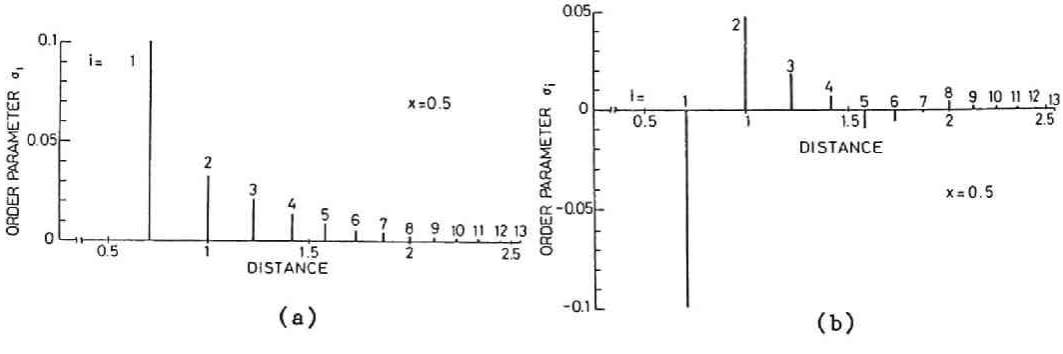

Fig.6-7 Short-range order parameter $\sigma(\tau)$ calculated using Eq.(6-16) for a given σ_1. (a): $\sigma_1=0.1$. (b): $\sigma_1=-0.1$. Distance is normalized by the lattice constant.

The result in Fig. 6-8 is valid only for σ_1 not near to its limit value, σ_{min}, because the calculation is valid only for a low degree of nonrandomness.

According to the thermodynamic calculation described in Chap. III, $\sigma_1 \simeq -0.1$ for $In_{0.5}Ga_{0.5}As$ grown at 1000 K (see Fig.3-6). As seen from Fig. 6-8, μ at this degree of order is 3 times larger than μ_0. Thus, if one estimates Δu from the measured alloy scattering mobility without considering atom arrangement, Δu will be underestimated by a factor of $\sqrt{3}$, because $\mu \propto 1/\{|\Delta u|^2 \sum \sigma(\tau)\}$.

Figure 6-9 shows examples of alloy scattering mobility influenced by nonrandom arrangement. Here, material properties of $In_{1-x}Ga_xAs$ are used, and the alloy scattering potential is assumed to be 0.53 eV[15] and σ_1 to be proportional to x(1-x) (see Fig.3-6).

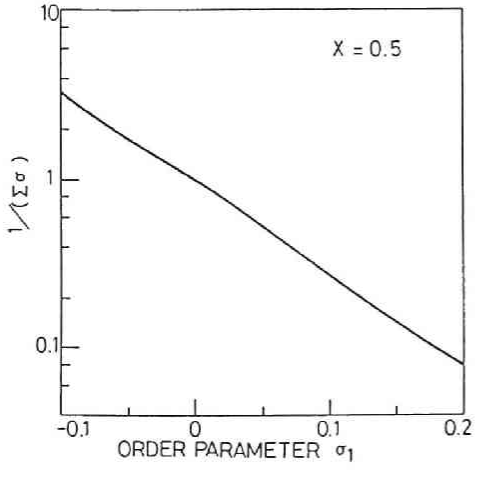

Fig.6-8 The relation between σ_1 and $1/\{\Sigma\sigma(\tau)\}$. Alloy scattering mobility is increased or decreased by a factor of $1/\{\Sigma\sigma(\tau)\}$, because of order ($\sigma_1<0$) or cluster ($\sigma_1>0$) in the atom arrangement.

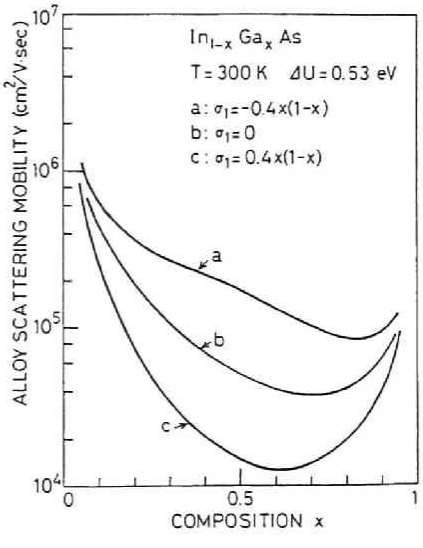

Fig.6-9 Examples of calculated alloy scattering mobilities. Material parameters for $In_{1-x}Ga_xAs$ are used. σ_1 is assumed to be proportional to x(1-x).

Oosaka calculated the alloy scattering incorporating cluster,[20] and long-range order was taken into account by Sasaki.[21] However, it is difficult to compare these results with each other because the different descriptions of atom arrangement were used. The results given here would be more general, because they include both order and cluster.

6-4. SOLUTION HARDENING DUE TO SHORT-RANGE ORDER IN TERNARY ALLOYS

Generation and motion of dislocations greatly affect performance and reliability of various semiconductor devices. For example, a dislocation manifests itself as a dark line defect in a light-emitting diode (LED) and a laser diode (LD).[22] The life time of these devices strongly depends on how easily dislocations move: it is considered that the life time of LD of (InGa)(AsP)/InP system is relatively long compared with that of (AlGa)As/GaAs system because the dislocations move more easily in (AlGa)As/GaAs than in (InGa)(AsP)/InP.[23] In this section, effects of atom arrangement on dislocation development is discussed.

6-4-1. Solution Hardening

In a semiconductor, there is a relatively strong intrinsic resistance against the dislocation movement. It originates from the Peierls potential, i.e., the periodic potential of the crystal. However, dislocations surmount the Peierls potential with the assistance of phonons at high temperatures. In addition, the motion of a dislocation becomes easy with large electric current injection or strong light irradiation. Thus, the generation and motion of dislocations become easy during the operation of devices.[22]

On the other hand, it is known that dislocations become more difficult to move in an alloy than in a pure crystal.[24] This

phenomenon is called solution hardening and have been extensively studied for metal alloys.[24] The solution hardening effect is expected for III-V alloys, too, and in fact the dislocation density of a GaAs bulk crystal is decreased by adding a small amount of In.[25] This is considered due to the dislocation pinning caused by the local strain field around In atoms:[26] it is due to the nonuniformity of strain in the crystal. This effect will be significant in a dilute alloy, but it does not seem clearly understood how strong the effect is in a concentrated alloy.

In a concentrated alloy, nonrandomness in the atom arrangement hardens the crystal.[27,24] As a dislocation moves, crystal atoms in the one side of the gliding plane are shifted relative to atoms in the other side of the plane. The shift vector corresponds to the Burgers vector of the dislocation. Then, if there is nonrandomness in atom arrangement, it is disturbed by the passage of a dislocation.[27] Since the nonrandomness in atom arrangement is induced for reduction in the internal energy of the crystal, the internal energy is increased if the nonrandomness is disturbed. Thus, the motion of the dislocation needs excess external force corresponding to the increment of the internal energy of the crystal. The resolved shear stress (RSS) needed to overcome the resistance due to the nonrandomness is expressed by[27]

$$\tau = \frac{\Delta\varepsilon}{|b|} \quad , \tag{6-17}$$

where $\Delta\varepsilon$ is the increment in the internal energy per unit area due to the passage of a dislocation, and b is the Burgers vector of the dislocation.

This hardening mechanism affects the glide motion of a dislocation. Although the climb motion of a dislocation also affects a device performance,[23] it is not discussed in this study.

In calculating $\Delta\varepsilon$, it is assumed that the nonrandomness disappears on the gliding plane after the passage of a dislocation.

This will be a reasonable assumption for short-range ordering (preference for unlike nearest pair): if the order is of short-range, it is largely disturbed by shifting atoms even by a small amount, e.g., b. On the other hand, the assumption involves relatively large error for large scale clustering or long-range ordering: the large scale cluster is not completely decomposed by the passage of a single dislocation. And in case of long-range ordering, dislocations are expected to regroup themselves and reduce $\Delta\varepsilon$.[27)]

$\Delta\varepsilon$ is calculated from the difference in the internal energy or the enthalpy between the ordered state and the random state:

$$\Delta\varepsilon = \frac{4}{\sqrt{3}\, a^2\, N} (H_r - H) \quad , \qquad (6\text{-}18)$$

where H_r and H are the enthalpy per N atoms in the random and the ordered states, respectively, and a the lattice constant. By multiplying the factor, H_r-H is converted to the energy difference per unit area of the gliding plane, i.e., {111} plane for a zincblende structure. The Burgers vector of the dislocation is a/2<110>. Although a dislocation is decomposed into two partial dislocations in a zincblende crystal,[28)] these two dislocations

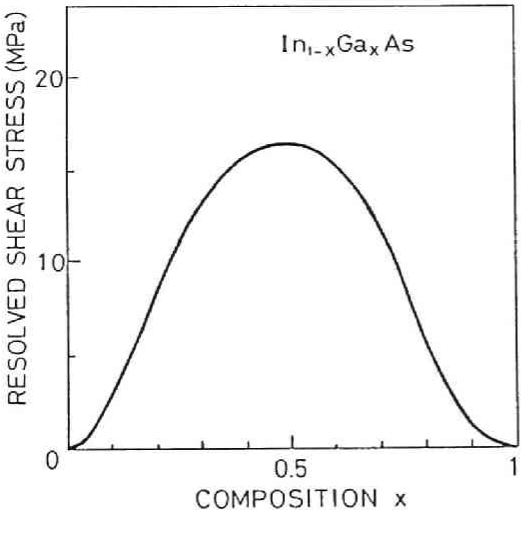

Fig.6-10 Resolved shear stress required for a dislocation to move against the resistance due to short-range order in the atom arrangement for $In_{1-x}Ga_xAs$. Short-range order at 1000 K is taken into account.

MATERIAL (x=0.5)	τ (MPa)	Δd/d (%)
(GaAl)As	0	0.13
(GaAl)Sb	0.001	0.64
(GaAl)P	0	0.2
(InGa)P	27.2	7.4
(InGa)As	16.1	6.9
(InGa)Sb	7.55	6.1
(InAl)As	15.0	6.7
Ga(AsP)	1.80	3.6
In(AsP)	1.04	3.2
Ga(SbAs)	20.7	7.5
In(SbAs)	12.5	6.7
Ga(SbP)	84.1	11.2
In(SbP)	59.0	9.9

Table 6-II. Resolved shear stress τ required for a dislocation to move against the resistance due to short-range order for various ternay alloys. Relative lattice mismatch between two constituent compound Δd/d is also shown. Composition is 0.5, and the short-range order at 1000 K is considered.

move in pair and the shift caused by the dislocation pair is equal to that caused by a single dislocation with the Burgers vector a/2<110>.

6-4-2. Results and Discussions

Figure 6-10 shows the RSS τ required for a dislocation to move against the resistance due to the short-range order in atom arrangement for $In_{1-x}Ga_xAs$ as a function of Ga composition x. The effect of the Peierls potential is not included in it. In calculating τ, the short-range order at 1000 K is considered. As shown in the figure, τ becomes maximum at x=0.5 and is very small value in a dilute alloy. Thus, the mechanism considered here will not contribute to the reduction in dislocation density in In-doped GaAs.

Table 6-II lists the values of τ for various III-V ternary alloys at the composition of 0.5. Again, the short-range ordering at 1000 K is considered. The table also lists the amount of the

lattice mismatch between two constituent binary compounds. Alloys with large lattice mismatch tend to have large τ, whereas τ is negligibly small for $(GaAl)C^V$ (C^V=As, Sb) alloy systems: in $(GaAl)C^V$ alloys, the atom arrangement is almost completely random and thus the hardening considered here is little.

The resolved shear stress required for a dislocation to move in undoped GaAs crystal is 20 MPa at 250 °C and 2 MPa at 550 °C.[29] As stated earlier, phonon helps dislocations surmount the Peierls potential, and thus the resistance due to the Peierls potential decreases rapidly with a raise in temperature. However, the resistance due to the short-range order is independent of temperature unless the nonrandomness itself disappears by the interdiffusion of atoms.[27]

Therefore, the solution hardening due to the nonrandomness can be significant at relatively high temperatures, where the resistance due to the Peierls potential becomes weak. In addition, it will be effective under the large current injection or strong optical excitation, too: Under these circumstances, the Peierls potential is easily surmounted; this is considered due to the phonon emission accompanying the nonradiative recombination at a dislocation.[30] Then, the nonrandomness in the atom arrangement could be one of the dominant factors determining the rate of the dislocation development during the operation of devices. Thus, for example, devices of (AlGa)As/GaAs system will be degraded more easily than those composed of (InGa)As alloy. In practice, devices of (AlGa)As/GaAs use the Al-composition less than 0.4, whereas those of (InGa)As/InP the In-composition of about 0.5. This will also cause difference in the strength of the hardening.

Although the analysis here can be applied only to ternary alloys, we can expect that τ for quaternary alloys of (AB)(CD) type is no less than those of the relevant ternary alloys; τ is large for alloys with large strain energy, and the strain energy of a

quaternary alloy is no less than those of the relevant ternary alloys.[31] Then, for example, τ for (InGa)(AsP) will be comparable to that for (InGa)C^V (C^V=As, P) or that for C^{III}(AsP) (C^{III}=Ga, In) and thus will be much larger than τ for (GaAl)As. This would be relevant to the fact that life time of a (InGa)(AsP)/InP LD is in general longer than that of a (GaAl)As/GaAs LD. However, for more rigorous discussion, we should consider various factors, e.g., climb motion of dislocation, misfit stress, and surface damage during a device processing.

6-5. EFFECTS OF BOND STATISTICS ON PROPERTIES OF QUATERNARY ALLOYS OF (AB)(CD) TYPE

The ambiguity in the statistics of bonds could cause difficulties in predicting various material parameters.[32] In an usual interpolation procedure, the properties of constituent binary compounds are averaged weighted by their respective ratios in the alloy, i.e., the properties are linearly interpolated, although a nonlinear term is added for some parameters.[33-35] The ratio of a compound is usually assumed to be the product of the compositions of its composite atoms: for example, the ratio of GaAs is assumed to be x(1-y) for $In_{1-x}Ga_xAs_{1-y}P_y$. A change in the bond statistics is considered as a change in the ratios of the constituent compounds, and an interpolation using a different set of weighting ratios can give a different value of a material properties. Thus, the interpolation procedures applied to quaternary alloys should be reexamined on the basis of the actual bond statistics.

In this section, the effects of bond statistics on material properties are evaluated using an interpolation technique.

6-5-1. Variation in Material Properties

A. Lattice constant

Lattice constant accurately follows the Vegard law: the lattice constant of $A^{III}_{1-x}B^{III}_{x}C^{V}_{1-y}D^{V}_{y}$, a_Q, is expressed by

$$a_Q = \sum X_{pq} a_{pq} \qquad (6\text{-}19)$$

where a_{pq} is the latice constant of binary compound pq. The above equation is usually used with the assumption $\xi=0$:

$$a^o_Q = \sum x_p x_q a_{pq} \quad . \qquad (6\text{-}20)$$

a_Q can be rewritten as

$$a_Q = a^o_Q + \xi\omega_a$$

$$\omega_a = a_{AC}+a_{BD}-a_{AD}-a_{BC} \quad . \qquad (6\text{-}21)$$

As can be seen from the equation, the variation in lattice constant due to ξ is expressed ξ times a factor which is independent of the composition. The values of the factor ω_a are listed in the second column of Table 6-III. ω_a is very small for all of nine alloy systems. This could be attributed to the fact that each bond length is approximately expressed as the sum of the covalent radii of the composite atoms. Let r_p denote the covalent radius of p atom. Then p-q bond length d_{pq} is approximately equal to r_p+r_q. Since $a_{pq}=4/\sqrt{3}\ d_{pq}$,

$$\omega_a = \frac{4}{\sqrt{3}} (d_{AC}+ d_{BD}- d_{AD}- d_{BC})$$

$$\simeq \frac{4}{\sqrt{3}} \{(r_A+r_C)+(r_B+r_D)-(r_A+r_D)-(r_B+r_C)\}$$

$$=0 \quad . \qquad (6\text{-}22)$$

As can be seen from Fig.5-6 and Table 6-III, $\omega_a\xi$ is less than 10^{-3} Å and thus could be neglected in calculating lattice constant.

Table 6-III. Parameter ω describing the effects of bond statistics on lattice constant (ω_{a_o}), direct (Γ) and indirect (X) band gap (ω_g). ω_a is given in A and ω_g in eV.

SYSTEM	ω_a	$\omega_g(\Gamma)$	$\omega_g(X)$
(InGa)(AsP)	-0.013	0.37	-0.1
(InGa)(SbAs)	-0.0210	0.52	0.24
(InGa)(SbP)	-0.0345	0.89	0.13
(InAl)(AsP)	-0.0086	-0.35	-0.2
(InAl)(SbAs)	-0.0544	0.57	-0.08
(InAl)(SbP)	-0.063	0.22	0.28
(GaAl)(AsP)	0.0049	-0.72	-0.1
(GaAl)(SbAs)	-0.0334	0.04	-0.31
(GaAl)(SbP)	-0.0285	-0.68	-0.41

B. Energy band gap

The band gap does not accurately follow the Vegard law, and there appears downward bowing in its composition dependence. However, the portion of nonlinear variation is relatively small compared with linear-variational part. Since the purpose of the present analysis is not to obtain values of the band gap but to estimate the effect of bond statistics, the change in the linear-variational part is considered: the band gap of an alloy, ε_Q, is expressed by

$$\varepsilon_Q = \varepsilon_Q^o + \xi\omega_g$$

$$\omega_g = \varepsilon_{AC} + \varepsilon_{BD} - \varepsilon_{AD} - \varepsilon_{BC} \quad , \tag{6-23}$$

where, ε_Q^o is the band gap of the alloy when ξ=0, and ε_{pq} the band gap of the compound pq. Here, as a first approximation, ξ-dependence of the nonlinear-variational part is neglected.

The values of the factor ω_g are listed in the third and forth columns in Table 6-III for direct and indirect (X) band gaps. They are rather small compared with differences among ε_{pq}'s of constituent compounds. For example, the difference between ε_{InAs} and ε_{GaAs} or between ε_{InAs} and ε_{InP} is about 1 eV, but $|\omega_g|$ for (InGa)(AsP) is less than 0.4 eV. This is because the following relation is satisfied when the heavier element is assigned to A or C.

$$\varepsilon_{AC} < \varepsilon_{AD} \ , \ \varepsilon_{BC} < \varepsilon_{BD} \qquad (6\text{-}24)$$

Thus, ω_g is the difference between the sum of the largest and the smallest ε_{pq}'s and the sum of the two intermediate ε_{pq}'s: the differences among ε_{pq}'s are canceled to some extent. The relation (6-24) is generally satisfied because ε_{pq} is always smaller for a heavier composite element. The sign of ω_g depends on but $|\omega_g|$ does not depend on how the elements are assigned to the symbols.

The value of $\xi\omega_g$ is less than 10 meV for most alloy systems, and thus other factors, e.g., ambiguity in bowing parameter, would cause larger error than the bond statistics in an interpolation procedure.

6-5-2. Discussions

As described in the last section, the effects of the bond statistics are small, because $|\xi_o|$ is not large and the factor ω is relatively small owing to cancel of differences in parameters among constituent compounds. Therefore, the error caused by the assumption that $\xi=0$ is not large for lattice constant and band gap. However, ξ_o used here is the equilibrium value at 1000 K. $|\xi_o|$ could be larger, if the alloy is grown at lower temperatures or through nonequilibrium processes. Then, the effect of ξ could be considerably large.

For calculating the factor ω, the properties of the binary

compounds need be known. Here, ω is not given for other properties, e.g., dielectric constant, since they are not determined accurately enough for some binary compounds.

In this study, the material properties are discussed on the basis of the linear interpolation. It is accurate for lattice constant, but a more sophisticated approach, such as the coherent-potential approximation, need be emplyed for the band gap in order to take account of the compositional disorder effect.[36] In addition, the strain of bonds is also considered to influence the band gap.[37] Since the strain energy depends on ξ, the energy variation due to bond strain will also depend on ξ. For further study, the band gap should be obtained as a function of ξ by considering the compositional and structural disorder effects.

6-6. SUMMARY

The relation between atom arrangement and material properties has been discussed. The results are summarized as follows:

i) For ternary systems of average composition x=0.5, monolayer structure on a (100) or (110) surface becomes stable below a certain temperature, but monolayer structure on (111) surface and longer-period structures are not stable.

ii) The alloy scattering mobility is greatly influenced by even low degree of the nonrandomness in the atom arrangement. Thus, it is necessary to take into account the nonrandomness in estimating alloy scattering potential from experimental data.

iii) The short-range order impedes glide motion of dislocations. It could play an important role during operation of a certain device and elongate the life time of the device.

iv) Lattice constants and band gaps of quaternary alloys of (AB)(CD) type are calculated from the bond statistics at the thermal equilibrium state. The results are a little different from those for the random arrangement case.

REFERENCES

1) As review for semiconductor superlattices, L. L. Chang, J. Vac. Sci. Technol. B, 1 (1983) 120.

2) T. Yao, Jpn. J. Appl. Phys. 22 (1983) L680.

3) As examples of the growth of GaAs and AlAs monolayer superstrucure, A. C. Gossard, P. M. Petroff, W. Weigmann, R. Dingle, and A. Savage, Appl. Phys. Lett. 29 (1976) 323 and N. Sano, H. Kato, M. Nakayama, S. Chika, and H. Terauchi, Jpn. J. Appl. Phys., 23 (1984) L640.

4) T. Fukui and H. Saito, Jpn. J. Appl. Phys., 23 (1984) L521.

5) W. L. Bragg and E. J. Williams, Proc. Roy. Soc. A145 (1934) 699.

6) As review, T. Muto and Y. Takagi, Solid State Physics, edited by F. Seitz and D. Turnbull (Academic, New York, 1955), Vol.1, pp.193.

7) H. R. Jen, M. J. Cherng, and G. B. Stringfellow, Appl. Phys. Lett., 48 (1986) 1603.

8) T. S. Kuan, T. F. Kuech, W. I. Wang, and E. L. Wilkie, Phys. Rev. Lett., 54 (1985) 201.

9) H. Nakayama and H. Fujita, "12th Int. Symp. GaAs and Related Compounds, Karuizawa, 1985, Inst. Phys. Conf. Ser. 79" (Adams Hilger, 1986), p.289.

10) M. A. Shahid, S. Mahajan, D. E. Laughlin, and H. M. Cox, Phys. Rev. Lett., 58 (1987) 2567.

11) T. S. Kuan, W. I. Wang, and E. L. Wilkie, Appl. Phys. Lett., 51 (1987) 51.

12) D. M. Bylander and L. Kleinman, Phys. Rev. B, 34 (1986) 5280.

13) D. M. Wood, S. -H. Wei, and A. Zunger, Phys. Rev. Lett., 58 (1987) 1123.

14) J. A. van Vechten, J. Cryst. Growth, 71 (1985) 326.

15) For example, Y. Takeda, "GaInAsP alloy semiconductors", edited by T. P. Pearsall (John Wiley & Sons, Chichester, 1982) Chap.9, and references therein.

16) T. Nishinaga and K. Hiramatsu, Jpn. J. Appl. Phys., 22 (1983) 113.

17) A. E. Asch and G. L.Hall, Phys. Rev., 132 (1963) 1047.

18) J. M. Cowley, Phys. Rev., 77 (1950) 669.

19) J. W. Harrison and J. R. Hauser, Phys. Rev. B, 9 (1976) 5347.

20) F. Oosaka, T. Sugano, Y. Okabe, and Y. Okada, Jpn. J. Appl. Phys., 15 (1976) 2371.

21) A. Sasaki, Proc. 9th Conf. Solid State Divices, Jpn. J. Appl. Phys. Suppl.17-1 (1978) 161.

22) As review, H. C. Casey, Jr. and M. B. Panish, "Heterostructure Lasers" (Academic, New York, 1978) Part B, Chap 8.

23) O. Ueda, S. Yamakoshi, T. Sanada, I. Umebu, and T. Kotani, J. Appl. Phys., 53 (1982) 9170.

24) As a review, N. F. Fiore and C. L. Bauer, Prog. Mater. Sci, 13 (1967) 85.

25) For example, G. Jacob, M. Duseaux, J. P. Farges, M. B. van den Boom, and P. J. Roksnoer, J. Cryst. Growth, 61 (1983) 417.

26) H. Ehrenreich and J. P. Hirth, Appl. Phys. Lett., 46 (1985) 668.

27) J. C. Fisher, Acta. Metall., 2 (1954) 9.

28) For example, D. J. H. Cockayne and A. Hons, J. de Phys. 40 (1979) C6-11.

29) V. Swaminathan and S. M. Copley, J. Am. Cer. Soc., 58 (1975) 482.

30) D. Weeks, J. C. Tully, and L. C. Kimerling, Phys. Rev. B, 12 (1975) 3286.

31) H. Sonomura, J. Appl. Phys., 59 (1986) 739.

32) H. Sonomura, H. Horinaka, and T. Miyauchi, Jpn. J. Appl. Phys., 22 (1983) L689.

33) T. H. Glisson, J. R. Hauser, M. A. Littlejohn, and C. K. Williams, J. Electron. Mater., 7 (1978) 1, and reference therein.

34) A. Sasaki, M. Nishiuma, and Y. Takeda, Jpn. J. Appl. Phys., 19 (1980) 1695.

35) S. Adachi, J. Appl. Phys., 53 (1982) 8775.

36) A.-B. Chen and A. Sher, Phys. Rev. B, 19, (1979) 3057.

37) Effects of the structural disorder are discussed for ternary alloys in A. Zunger and J. E. Jaffe, Phys. Rev. Lett., 51 (1983) 662 and K. C. Hess, R. J. Lempert, and H. Ehrenreich, Phys. Rev. Lett., 52 (1983) 77.

VII. CONCLUSIONS

In this study, atom arrangements in III-V alloy semiconductors have been theoretically investigated. The thermodynamic approach has been adopted, and internal energy of an alloy has been estimated from the energy of nearest-neighbour interaction or covalent bonding between group III and V atoms. For ternary alloys and quaternary alloys of (ABC)D type, the bond strain energy has been considered as a dominant interaction among constituent compounds, but the energy change depending on change in the relative numbers of bonds has also been considered for quaternary alloys of (AB)(CD) type. For calculating the strain energy, bond lengths and angles must be known; in this work, they have been evaluated on the basis of the valence-force-field model. In addition, the average bond length has been calculated, and its relation with the atom arrangement has been described. The influences of the atom arrangement have been quantitatively studied for some material properties.

In Chap. II, it has been explained why the strain energy must be considered as a dominant interaction. It has also been shown that coherency of a lattice should be taken into account for discussing the microscopic atom arrangement in a single phase alloy.

In Chap. III, the atom arrangement in III-V ternary alloy semiconductors has been studied. Five types of tetrahedra are used as basic figures of the analysis. In most of ternary alloys, there is a preference for ordering but not for clustering. This is in contrast to the results obtained by the pairwise interaction model. In calculating the strain energy, the strain of a bond is assumed to depend on type of tetrahedron. The average lengths have been calculated by averaging bond length in all types of tetrahedra weighted by their relative numbers. The results agree fairly well with the reported EXAFS data.

In Chap. IV, the atom arrangement in quaternary alloys of

(ABC)D type has been studied with the same approach as in Chap. III. The second-nearest pairs composed of a larger atom and a smaller atom than the average are favorable, but a pair of two larger or smaller atoms is not. The average bond lengths have also been calculated.

In ternary alloys and quaternary alloys of (ABC)D type, the relative numbers of bonds are uniquely determined from atomic composition, but they are not in quaternary alloys of (AB)(CD) type. In Chap. V, the relative numbers of bonds have been derived for (AB)(CD) alloy systems. When heavier group V atom is assigned to C^V, In-D^V and Ga-C^V bonds increase in $In_{1-x}Ga_xC^V_{1-y}D^V_y$, and Ga-$C^V$ and Al-D^V bonds increase in $Ga_{1-x}Al_xC^V_{1-y}D^V_y$ compared with the case of random atom arrangement. The bond statistics are nearly equal to those in the random case for $In_{1-x}Al_xC^V_{1-y}D^V_y$. In the analysis, bond length is assumed to depend on types of group III and group V tetrahedra. The average bond lengths have also been calculated, and they agree fairly well with EXAFS data.

In Chap. VI, the relation between the atom arrangement and some material properties has been studied. It has been shown for ternary alloys that the alloy scattering mobility and the hardness of the crystal are greatly influenced by the nonrandomness in the atom arrangement. By extending the thermodynamic analysis, the stability of a superlattice has been analyzed for ternary alloy systems of x=0.5. The monolayer structure on (100) or (110) surface can be stable but other structures are not at any temperature. The effects of bond statistics on material properties of (AB)(CD) alloys have been discussed.

Although this study would give a physical basis for understanding the atomic scale structure of III-V alloy semiconductors, further investigations are needed for higher accuracy of the analysis and for disclosing implications of the results. Possible extensions of this study are summarized as follows.

i) The assumption that the volume of a tetrahedron cell is equal

to the average value need be reconsidered. Another and possibly better approach is to connect the tetrahedron to a certain effective medium and allow it to relax. In this case, the strain energy stored in the medium should be considered as a part of the strain energy of the tetrahedron, since it is caused by that cell.

ii) The thermodynamic analysis proposed here can be extended to investigation of a phase diagram. The nonrandomness in atom arrangement is induced for reduction in the free energy, and the change in the free energy causes some changes in the macroscopic phase diagram.

iii) The atom arrangement in a bulk crystal is analyzed in this study. A surface is quite different from the bulk, and thus the most favorable arrangement on a surface could be different from that in a bulk. During some sort of epitaxial growth, a crystal grows layer by layer, and then the arrangement favorable on the surface would appear on the growth surface because atoms move rather fast on a surface. This arrangement might be retained in the bulk, since atoms move much slower in a bulk. Thus, it will be important task to investigate the atom arrangement on surfaces.

iv) It will be very interesting to investigate the effects of atom arrangement on band structures. The band structure of an alloy has been calculated by the coherent-potential-approximation (CPA) but usually with the assumption of random arrangement. It will be very difficult to take short-range order into the CPA calculation, but long-range order can be taken into account without further theoretical development of the CPA theory. From the CPA calculation one can estimate not only band gap but also alloy scattering mobility and electronic density of states. In addition, from the energy of electrons in valence bands, one can estimate electronic binding energy of the crystal as a function of degree of order in the atom arrangement. If this energy is taken into account in addition to the strain energy, the thermodynamic analysis will become more accurate.

APPENDIX

A. DERIVATION OF THE ENTROPY [Eq.(3-3) and (4-5)]

First, Kikuchi's approach for deriving entropy is briefly described for a fcc lattice, and then it is applied to a zinc-blende structure. (For a more detailed description, see R. Kikuchi, Phys. Rev. 81 (1951) 988.)

Consider a system composed of N alloy atoms and an ensemble which contains L systems. In a fcc lattice, the number of ways, G_L, of putting an atom on lattice site A in Fig. A-1 is calulated as follows

$$G_L = \frac{\{\text{Triangle feg}\}}{\{\text{Tetrahedron Afeg}\}} \times C_L \qquad \text{(A-1)}$$

$$C_L = \left[\frac{\{\text{Triangle CDf}\}}{\{\text{Tetrahedron ACDf}\}} \div \frac{\{\text{Point f}\}}{\{\text{Bond Af}\}}\right] \times \left[\frac{\{\text{Bond BC}\}}{\{\text{Triangle ABC}\}} \div \frac{\{\text{Point C}\}}{\{\text{Bond AC}\}}\right] \times \left[\frac{\{\text{Bond Be}\}}{\{\text{Triangle ABe}\}} \div \left(\frac{\{\text{Point C}\}}{\{\text{Bond AC}\}} \times \frac{\{\text{Point B}\}}{\{\text{Bond AB}\}} \div \frac{L!}{\{\text{Point A}\}}\right)\right]$$

Here,

$$\{\ (\text{figure p})\ \} = \prod \{n_i^p\ !\}^{g_i^p} \quad , \qquad \text{(A-2)}$$

where n_i^p is the number of type-i of figure p (p=Point, Pair, Triangle, Tetrahedra), and g_i^p its degeneracy factor. C_L is the

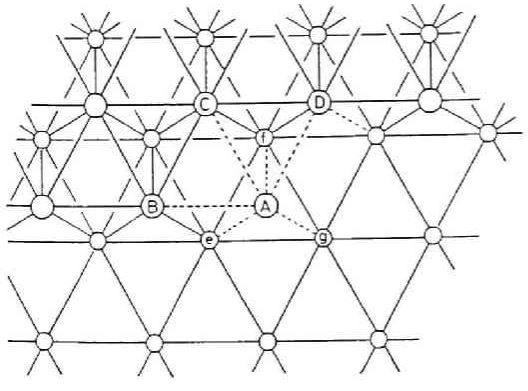

Fig.A-1 An intermediate stage of constructing a fcc lattice.

correction factor which makes relative numbers of the tetrahedra and the triangles containing A coincide with given values, n_i^p.

The entropy is calculated by

$$S = \frac{N}{L} k_B \ln(G_L) \qquad \text{(A-3)}$$

for N atom lattice.

A zincblende ternary alloy can be constructued by putting atoms of the other group at the central site of tetrahedra. In a zincblende type of semiconductor, there are two kinds of tetrahedra: one contains an atoms in it and the other does not. They are equal number in semiconductors; tetrahedra on a fcc lattice are twice as many as atoms. When the energy of bonds is considered, the statistics of the tetrahedra without any bonds can be neglected. Then the correction terms of the above equation can be reduced. For example,

$$C_L = \frac{\{\text{Bond CD}\}}{\{\text{Triangle ACD}\}} \div \frac{L!}{\{\text{Point A}\}} \times \frac{\{\text{Point B}\}}{\{\text{Bond AB}\}} \div \frac{L!}{\{\text{Point A}\}} \quad . \qquad \text{(A-4)}$$

In the next stage of the construction, Triangle ACD becomes an tetrahedron equivalent to Afeg, Bond AB a triangle equivalent to ACD. Then G_L is expressed by

$$G_L = \frac{\{\text{Triangle feg}\}}{\{\text{Tetrahedron Afeg}\}} \times C_L$$

$$= \frac{\{\text{Point }\}^3}{(L!)^2\{\text{Tetrahedron }\}} \qquad \text{(A-5)}$$

With the use of the Stirling formula, the above G_L gives the entropy expressed by Eq. (3-3) or Eq. (4-5) for a ternary alloy or a quaternary alloy of (ABC)D type, respectively.

B. CONTINUUM MODEL

The continuum model has been used for evaluating the strain field around an impurity atom in a metal. (See J. D. Eshelby,

"Solid State Physics", Academic, New York, 1956, Vol.3, p.79) Bond-length calculation based on this simplified model is described in this section.

In the continuum model, a crystal is considered as a plastic medium, and an impurity atom as a plastic ball. In the analysis, a space shared by a bond is regarded as a plastic ball inserted into a hole in the continuous medium. Then the volume change of the ball ΔV_i is

$$\Delta V_i = \frac{4\mu}{4\mu+3B_i}(V_h - V_i) \qquad \text{(A-6)}$$

where V_i and V_h are the volume of the unstrained ball and the unstrained hole, respectively, μ is the shear modulus of the medium, and B_i is the bulk modulus of the ball. The bond length may

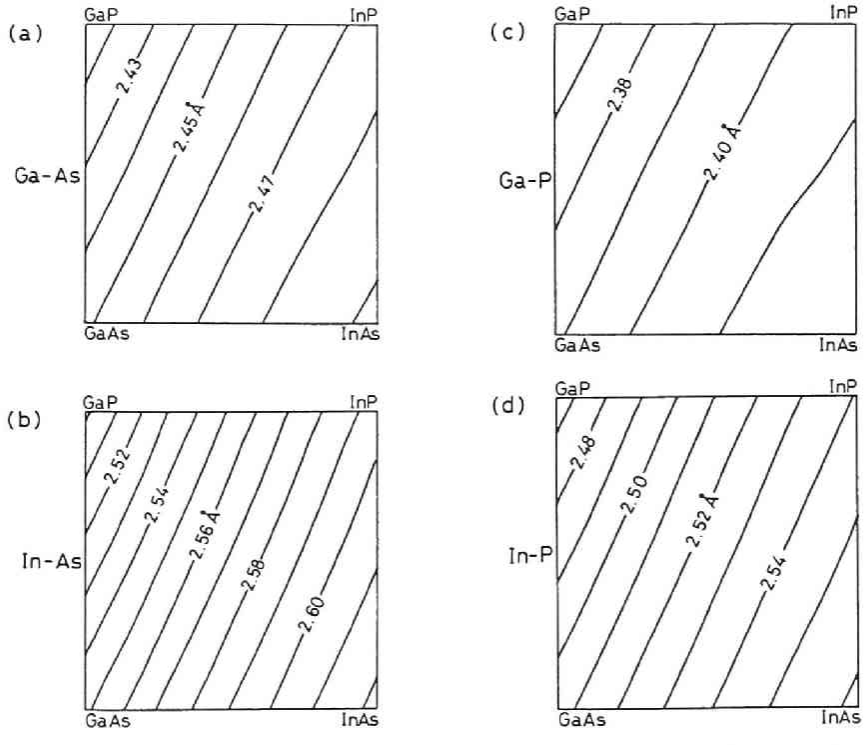

Fig.A-2 Contour charts of bond lengths calculated by the continuum model for $In_{1-x}Ga_xAs_{1-y}P_y$ alloy. The numerical values indicate bond lengths in A. The average bond length is assumed to follow the Vegard law.

Table A-I. Comparison of the calculated values of the bond lengths in $In_{1-x}Ga_xAs_{1-y}P_y$ alloys with the experimental values obtained by EXAFS measurement. The calculation is based on the continuum model. Bond lengths are given in Å.

Composition		Ga-As	In-As	Ga-P	In-P
x=0.47,y=0,	exp.	2.47	2.60	——	——
	cal.	2.477	2.593	——	——
x=0.4, y=0.11	exp.	2.47	2.60		
	cal.	2.477	2.59	2.410	2.542
x=0.26,y=0.42	exp.	2.47	2.59	2.40	
	cal.	2.477	2.594	2.409	2.541

correspond to the radius of the ball, and thus, the bond length d_i is, to a first approximation, given by

$$d_i = d_i^0 + \frac{4\mu}{4\mu+3B_i}(\bar{d} - d_i^0) \quad , \qquad \text{(A-7)}$$

where, d_i^0 is an unstrained bond length of the bond i and $\bar{d}$ the total average bond length of the alloy.

Figure A-2 shows composition dependence of bond lengths for $In_{1-x}Ga_xAs_{1-y}P_y$. The results are very similar to those described in Chap. V. The bond lengths obtained by Eq. (A-7) are listed in Table A-I with EXAFS results (H. Oyanagi, Y. Takeda, T. Matsushita, T. Ishiguro, and A. Sasaki, Inst. Phys. Conf. Ser. 79, Adams Hilger, 1986, p.295). The agreement is quite good.

Although the continuum model does not give us a realistic picture of a crystal lattice, the long-range relaxation of strain is taken into the model. Thus, it could be used for improving the strain calculation in this study.

C. VALIDITY OF THE VEGARD LAW FOR LATTICE CONSTANT

In this study, the Vegard law is assumed for lattice constant; lattice constant is assumed to vary linearly with composi-

tion. In this section, the validity of the assumption is discussed.

The lattice constant is determined so that the total energy of the crystal is minimum at that lattice constant. Figure A-3 shows the total strain energies as functions of lattice constant for two types of unit cells of $In_{1-x}Ga_xAs_{1-x}P_x$ system (see Fig. 5-2). The strain energies of other types of cells also become minimum when the lattice constant is slightly smaller (by 0.1 ~ 0.2 %) than the value of the Vegard law.

Lattice constant can be calculated by the continuum model, too. The total average bond length is given by

$$\bar{d} = \frac{\sum K_i d_i x_i}{\sum K_i x_i} \qquad \left(K_i = \frac{3B_i}{3B_i + 4\mu}\right) \quad . \qquad \text{(A-8)}$$

(See J. D. Eshelby, "Solid State Physics", Vol.3, p.79.) The lattice constant is $\bar{d}$ times $4/\sqrt{3}$.

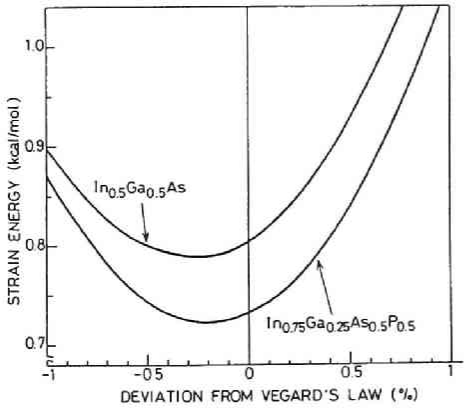

Fig.A-3 Calculated total strain energy as a function of the lattice constant. The values of the lattice constant are expressed as the deviation from the values obtained by the Vegard law.

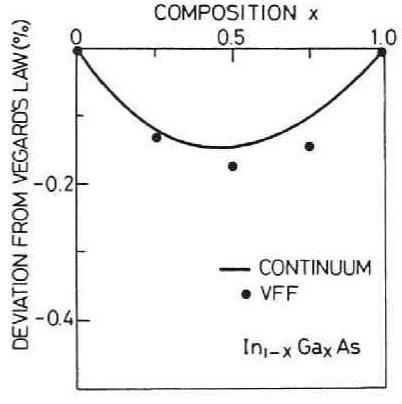

Fig.A-4 The difference between the calculated lattice constant and that obtained from the Vegard law for $In_{1-x}Ga_xAs$. Dark circle: calculated by the VFF model. Solid line: by the continuum model.

Figure A-4 shows the deviation of the equilibrium lattice constant from the Vegard law for $In_{1-x}Ga_xAs$; the solid line is obtained by Eq. (A-8) and dark circles are from unit cell calculation described above.

The deviation from the law is caused by a difference in the elastic constants; the lattice constant deviates from the Vegard law value and becomes close to that of a constituent compound with a large elastic constant (α or B) in order to reduce the strain of that compound. Since a compound with a large elastic constant tends to have a small lattice constant, negative deviation from the law is expected for most of III-V alloys. However, since the deviation is quite small, the use of the Vegard law will scarcely cause degradation in accuracy of the analysis. For observing the deviation experimentally, it will be necessary to prepare an uniform crystal and to accurately determine both of the lattice constant and the composition.

ADDENDUM

PUBLICATIONS

1) "Free Energies and Equilibrium States of Mono- and Bi-Layer Superstructures of III-V Ternary Alloy Semiconductors,"
M. Ichimura and A. Sasaki,
Jpn. J. Appl. Phys., 25 (1986) 976.

2) "Short-Range Order in III-V Ternary Alloy Semiconductors,"
M. Ichimura and A. Sasaki,
J. Appl. Phys., 60 (1986) 3850.

3) "Calculation of Bond Lengths in InGaAsP Quaternary Alloy Semiconductor,"
M. Ichimura and A. Sasaki,
Jpn. J. Appl. Phys., 26 (1987) 246.

4) "Statistics of Primitive Cells in InGaAs and AlGaAs Ternary Alloy Semiconductors,"
A. Sasaki and M. Ichimura,
Superlattices & Microstruct., 3 (1987) 127.

5) "Alloy Scattering Mobility in III-V Ternary Alloy Semiconductors with Nonrandom Atom Arrangement,"
M. Ichimura and A. Sasaki,
Jpn. J. Appl. Phys., 26 (1987) 776 (Short Note).

6) "Average Bond Lengths and Atom Arrangement in $In_{1-x}Ga_xAs$ and $GaAs_{1-x}P_x$ III-V Ternary Alloy Semiconductors,"
M. Ichimura and A. Sasaki,
Jpn. J. Appl. Phys., 26 (1987) 1296.

7) "Bond Lengths in III-V Ternary Alloy Semiconductors,"
A. Sasaki and M. Ichimura,
Jpn. J. Appl. Phys., 26 (1987) 2061.

8) "Bonds in III-V Quaternary Alloy Semiconductors of $A^{III}_{1-x}B^{III}_{x}C^{V}_{1-y}D^{V}_{y}$ Type,"
M. Ichimura and A. Sasaki,

Phys. Rev. B, 36 (1987) 9694.

9) "Atom Arrangement in III-V Quaternary Alloy Semiconductors of (ABC)D Type,"

M. Ichimura and A. Sasaki,

Jpn. J. Appl. Phys., 27 (1988) No.4, in press.

10) "Solution Hardening due to Nonrandom Atom Arrangement in III-V Ternary Alloy Semiconductors,"

M. Ichimura and A. Sasaki,

Jpn. J. Appl. Phys., 27 (1988) No.2, in press (Letter).

12) "Bond Statistics and Their Influences on Material Properties of III-V Quaternary Alloys of $(AB)^{III}(CD)^{V}$ Type,"

M. Ichimura and A. Sasaki,

submitted to J. Electron. Mater.

11) "Average Bond Lengths in InGaAsP Quaternary Alloy Semiconductors"

M. Ichimura and A. Sasaki,

in preparation for publication.

13) "Predicted Extremely High Mobilities of Two-Dimensional Electrons in AlGaSb/GaSb and AlInAsSb/InAs Single Heterostructures,"

Y. Takeda, M. Ichimura, and A. Sasaki,

Jpn. J. Appl. Phys., 24 (1985) L455 (Letter).

14) "AlGaSb Single, Double, and Multiple Heterostructures Grown by Liquid-Phase Epitaxy, and Their Photoluminescence Properties,"

M. Ichimura, Y. Takeda, and A. Sasaki,

submitted to Jpn. J. Appl. Phys.

ORAL PRESENTATIONS

Over-Sea Conference:

1) "Average Bond Lengths in $In_{1-x}Ga_xAs$ and $GaAs_{1-x}P_x$ III-V Ternary Alloy Semiconductors,"

M. Ichimura and A. Sasaki,

29th Electronic Materials Conference, Santa Barbara, June (1987)....

Domestic Meetings:

The Institute of Electronics, Information and Communication Engineers in Japan;

1) "Fabrication and Characterization of Liquid-Phase Epitaxial AlGaSb Multiple-Heterostructures,"

   Y. Takeda, M. Ichimura, and A. Sasaki,

   Rep. Tech. Group of Semiconductor and Semiconductor Devices, SSD84-165 (1984).

2) "Free Energies and Stable States of Mono- and Bi-Layer Superstructures of III-V Semiconductors,"

   M. Ichimura and A. Sasaki,

   Rep. Tech. Group of Electron Devices, ED85-108 (1985).

3) "Statistics of Bonds in $In_{1-x}Ga_xAs_{1-y}P_y$ Quaternary Alloy Semiconductor,"

   M. Ichimura and A. Sasaki

   Rep. Tech. Group of Electron Devices, ED86-105 (1986).

4) "Solution Hardening due to Nonrandom Atom Arrangement in III-V Ternary Alloy Semiconductors,"

   M. Ichimura and A. Sasaki,

   Rep. Tech. Group of Electron Devices, ED87-109 (1987).

The Japan Society of Applied Physics;

1) "Mobilities of Electrons in AlGaSb/GaSb and InAlAsSb/InAs Heterostructures,"

   M. Ichimura, Y. Takeda, and A. Sasaki,

   Okayama Univ., October, 1984, 14p-H-16.

2) "Characteristics of AlGaSb Multiple-Heterostructures Grown by Low-Temperature LPE,"

   M. Ichimura, Y. Takeda, and A. Sasaki,

   Aoyama Univ., March, 1985, 29p-Y-10.

3) "Free Energies and Stable States of Superstructures of III-V Semiconductors,"

   M. Ichimura and A. Sasaki,

   Kyoto Univ., October, 1985, 1p-Y-10.

4) "Electron Traps in Te-Doped GaSb and AlGaSb,"

Y. Takeda, M. Kasu, M. Ichimura, and A. Sasaki,

Kyoto Univ., October, 1985, 2a-A-7.

5) "Calculation of Bond Lengths in InGaAsP Alloy Semiconductor,"

M. Ichimura and A. Sasaki,

Nihon Univ., April, 1986, 4p-R-6.

6) "Short-Range Order in Atom Arrangement in III-V Ternary Alloys,"

M. Ichimura and A. Sasaki,

Nihon Univ., April, 1986, 4p-R-7.

7) "Determination of Alloy Composition and Composition Dependence of Electron Traps in AlGaSb on GaSb Substrate,"

Xiao Cheng Gong, Yu Zhu, Y. Takeda, M. Kasu, M. Ichimura, and A. Sasaki,

Nihon Univ., April, 1986, 2a-T-5.

8) "Calculation of Alloy Scattering Mobilities in III-V Ternary Alloys Taking Nonrandomness into Account,"

M. Ichimura and A. Sasaki,

Hokkaido Univ., September, 1986, 27p-C-5.

9) "Average Bond Lengths in III-V Ternary Alloy Semiconductors,"

A. Sasaki and M. Ichimura,

Hokkaido Univ., September, 1986, 27p-C-2.

10) "Relative Numbers of Bonds in InGaAsP Quaternary Alloy,"

M. Ichimura and A. Sasaki,

Waseda Univ., March, 1987, 30a-X-3.

11) "Relative Numbers of Bonds in III-V Quaternary Alloy Semiconductors of (AB)(CD) Type,"

M. Ichimura and A. Sasaki,

Nagoya Univ., October, 1987, 18p-ZB-2.

12) "Short-Range Order in III-V Quaternary Alloy Semiconductors of (ABC)D Type,"

M. Ichimura and A. Sasaki,

Nagoya Univ., October, 1987, 18p-ZB-3.